

The Gravitational-Wave Physics II: Progress

Ligong Bian,¹³ Rong-Gen Cai,^{1,5,8} Shuo Cao,² Zhoujian Cao,² He Gao,² Zong-Kuan Guo,^{1,5,8} Kejia Lee,^{4,3} Di Li,³ Jing Liu,^{8,5} Youjun Lu,^{3,6} Shi Pi,¹ Jian-Min Wang,^{7,6,3} Shao-Jiang Wang,¹ Yan Wang,⁹ Tao Yang,¹⁰ Xing-Yu Yang,^{1,5} Shenghua Yu,³ Xin Zhang^{11,12}

¹CAS Key Laboratory of Theoretical Physics, Institute of Theoretical Physics, Chinese Academy of Sciences, Beijing 100190, China

²Department of Astronomy, Beijing Normal University, Beijing 100875, China

³National Astronomical Observatories, Chinese Academy of Sciences, 20A Datun Road, Beijing 100101, China

⁴Kavli Institute for Astronomy and Astrophysics, Peking University, Beijing 100080, China

⁵School of Physical Sciences, University of Chinese Academy of Sciences, No.19A Yuquan Road, Beijing 100049, China

⁶School of Astronomy and Space Sciences, University of Chinese Academy of Sciences, 19A Yuquan Road, Beijing 100049, China

⁷Key Laboratory for Particle Astrophysics, Institute of High Energy Physics, Chinese Academy of Sciences, 19B Yuquan Road, Beijing, 100049, China

⁸School of Fundamental Physics and Mathematical Sciences, Hangzhou Institute for Advanced Study (HIAS), University of Chinese Academy of Sciences, Hangzhou 310024, China

⁹MOE Key Laboratory of Fundamental Physical Quantities Measurements, Hubei Key Laboratory of Gravitation and Quantum Physics, PGMF, Department of Astronomy and School of Physics, Huazhong University of Science and Technology, Wuhan 430074, China

¹⁰Asia Pacific Center for Theoretical Physics, Pohang 37673, Korea

¹¹Department of Physics, College of Sciences, Northeastern University, Shenyang 110819, China

¹²MOE Key Laboratory of Data Analytics and Optimization for Smart Industry, Northeastern University, Shenyang 110819, China

¹³Department of Physics, Chongqing University, Chongqing 401331, China

E-mail: lgbycl@cqu.edu.cn, cairg@itp.ac.cn, caoshuo@bnu.edu.cn, zjcao@bnu.edu.cn, gaohe@bnu.edu.cn, guozk@itp.ac.cn, kjlee@pku.edu.cn, dili@nao.cas.cn, liujing@ucas.ac.cn, luyj@nao.cas.cn, shi.pi@itp.ac.cn, wangjm@mail.ihep.ac.cn, schwang@itp.ac.cn, ywang12@hust.edu.cn, tao.yang@apctp.org, yangxingyu@itp.ac.cn, shenghuayu@bao.ac.cn, zhangxin@mail.neu.edu.cn

Abstract. It has been a half-decade since the first direct detection of gravitational waves, which signifies the coming of the era of the gravitational-wave astronomy and gravitational-wave cosmology. The increasing number of the detected gravitational-wave events has revealed the promising capability of constraining various aspects of cosmology, astronomy, and gravity. Due to the limited space in this review article, we will briefly summarize the recent progress over the past five years, but with a special focus on some of our own work for the Key Project “Physics associated with the gravitational waves” supported by the National Natural Science Foundation of China. In particular, (1) we have presented the mechanism of the gravitational-wave production during some physical processes of the early Universe, such as inflation, preheating and phase transition, and the cosmological implications of gravitational-wave measurements; (2) we have put constraints on the neutron star maximum mass according to GW170817 observations; (3) we have developed a numerical relativity algorithm based on the finite element method and a waveform model for the binary black hole coalescence along an eccentric orbit.

Contents

1	Introduction	1
2	Fundamental physics and GW cosmology	3
2.1	Cosmic first-order phase transition	3
2.2	Induced gravitational waves	9
2.3	GWs produced during preheating	14
2.4	Strongly lensed GW multimessenger	16
2.5	Standard siren cosmology	20
3	GW astrophysics	28
3.1	Orbital evolution of NS – Roche-Lobe filling WD binaries and their GWs	29
3.2	Constraints on the neutron star maximum mass from GW170817	30
3.3	Identifying supermassive binary black holes	33
3.4	GW background from stellar compact binaries	33
3.5	PTA probing solar system dynamics and constructing planet ephemeris	36
3.6	Detecting GWs using PTAs in the SKA era	38
3.7	Forecasting SKA-PTA detection of individual SMBBHs	39
4	Numerical relativity and gravitational waveform template	41
4.1	Finite element Numerical relativity	42
4.2	Gravitational waveform models for eccentric compact binaries	45
4.3	GW memory models for compact binaries	49
5	Conclusions	52

1 Introduction

Over the past half-decade, the direct detections of the gravitational wave (GW) events from the mergers of binary black holes (BBHs) [1] and binary neutron stars (BNSs) [2] have signified the coming of the era of the GW astronomy and GW cosmology, and ever since then, the increasing number of the detected GW events from Laser Interferometer Gravitational Wave Observatory (LIGO) first observing run (O1), O2 and O3 data [3, 4] has manifested its great potential to probe the unknown realms of the cosmology, astrophysics, and gravity. Due to the limited space of this paper, it is hardly feasible to give a thorough review for the numerous progress in this field, and we will only make a brief overview for the important progress over the past five years with a special focus on some of our own work. In the near future, the coming data from the Pulsar Timing Array (PTA), the Square Kilometre Array (SKA) and the Five-hundred-meter Aperture Spherical radio Telescope (FAST [5, 6]) will reveal the new era of radio astronomy. In the far future around the 2030s, the third generation of ground-based GW detectors [like the Einstein Telescope (ET) [7] and the Cosmic Explorer (CE) [8]] and space-borne GW detectors from the ongoing programs [like the Laser Interferometer Space Antenna (LISA) [9, 10], Taiji [11–13]¹ and TianQin [17–19]]

¹See [14, 15] for earlier proposal of the Advanced Laser Interferometer Antenna (ALIA) mission and [16] for its relation to the Taiji mission.

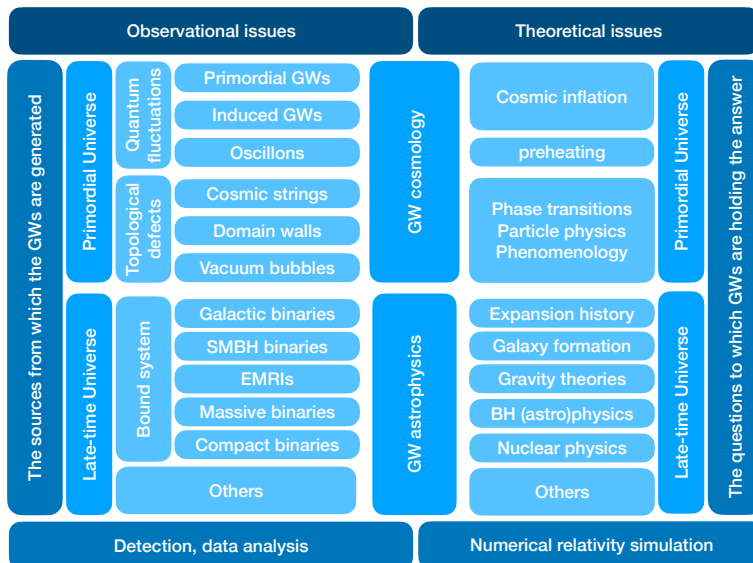


Figure 1. An overview for GW studies of observational and theoretical issues, the former contains the GW sources, detection and data analysis, while the latter contains the theoretical problems (GW cosmology/astrophysics) and numerical relativity simulation.

and planning proposals [like the DECi-hertz Interferometer Gravitational wave Observatory (DECIGO) [20, 21] and the Big Bang Observer (BBO) [22]] might be able to answer some important questions on the primordial Universe, multimessenger astronomy, and gravity tests.

The GW studies could be classified by either the sources from which the GWs are generated or the questions to which the GWs are holding the answer. In the former catalog, the GWs from the primordial Universe could be generated by the quantum fluctuations at large/small scales (primordial GWs, induced GWs, GWs from oscillons) and various topological defects (cosmic strings, domain walls, vacuum bubbles), while the GWs from the late Universe could be generated by the mergers of galactic binaries, supermassive binary black holes (SMBBHs), extreme-mass-ratio-inspirals (EMRIs), massive binaries, and compact binaries [solar-mass BHs, neutron stars (NSs), white dwarfs (WDs), pulsars, primordial black holes (PBHs), etc.]. In the latter catalog, GWs from the primordial Universe could be used to explore the fundamental physics of cosmic inflation, preheating, and cosmic phase transitions, while the GWs from the late Universe could be used to constrain the black hole (astro)physics, modified gravity theories, galaxy formation theories, late-time expansion history, nuclear physics, etc. The former catalog could be regarded as one end to the observational issues, which also include other issues like detection and data analysis. The latter catalog could be regarded as the other end to the theoretical issues, which also include other issues like numerical relativity simulations. This end-to-end picture is depicted in Fig. 1, which will be partially addressed in this short review as a sequential status report to our previous review [23].

For the recent progress on the GW observations, we make a brief review on the first BH-BH event [1], the first NS-NS event [2], the first two BH-NS events [24], and the recent NANOGrav 12.5-yr results [25]. The first BH-BH event (also known as the first direct detection of a GW event) was detected on 2015/09/14 (hereafter GW150914 [1]) by LIGO from

a transient GW signal matching the waveform of the binary stellar-mass black hole merger predicted by the numerical simulation of general relativity. Following up the detection of the GW150914 event, the test for general relativity [26] and the implications for astrophysics [27] and the stochastic GW background from BBH [28] are extensively discussed. The first NS-NS event (also known as the first multi-messenger GW event) was detected on 2017/08/17 (hereafter GW170817 [2]) by LIGO-Virgo from an unprecedented joint GW and electromagnetic wave observation matching the waveform of BNS inspiral and its transient counterparts [29, 30]. Following up the detection of the GW170817 event, the Hubble constant [31], the neutron star radii, and the neutron star equation of state [32] were first measured by GW. The test for general relativity [33] and the implication for stochastic GW background [34] are also discussed. The first two BH-NS events were detected on 2020/01/05 and 2020/01/15 (hereafter GW200105 and GW200115 [24]) by LIGO-Virgo, providing the first convincing observational evidence for the existence of neutron star-black hole (NSBH) systems. Although the spin measurement for GW200105 is insufficient to tell the isolated binary evolution from the dynamical interaction, the spin direction of BH in GW200115 seems to be opposite to the direction of the binary orbit. The recent search for an isotropic stochastic GW background in North American Nanohertz Observatory (NANOGrav) 12.5-yr data shows strong evidence for a common-spectrum stochastic process with power-law fitting over the red-noise processes in each pulsar [35]. The implications for inflation, cosmic strings, phase transitions, and PBHs are discussed extensively in the literature, some of which are reviewed in the context below.

The outline of this review is as follows: In section 2, we review the GW backgrounds from some topological defects like vacuum bubbles and domain walls in 2.1, scalar-induced GWs in 2.2, and GWs during preheating era in 2.3, as well as GW multimessenger from strong lensing time delay in 2.4 and standard siren in 2.5. In section 3, we review various aspects of GW astrophysics, for example, GWs from NS-WD binaries in 3.1, NS binaries in 3.2, SMBBHs in 3.3, and stellar compact binaries in 3.4 as well as PTA/SKA astronomy in 3.5, 3.6, and 3.7. In section 4, we review the numerical relativity and gravitational waveform template with related work from the finite element method in 4.1, gravitational waveform for eccentric compact binaries in 4.2, and GW memory model for compact binaries in 4.3.

2 Fundamental physics and GW cosmology

2.1 Cosmic first-order phase transition

The standard model (SM) of particle physics is known to be incomplete, either from the baryon asymmetry or the dark matter (DM), and our world is meant to be symmetry-broken, either with the electroweak symmetry or even the supersymmetry to be probed. Since the local searches for the new physics beyond the SM (BSM) have so far returned null results, either from particle acceleration colliders or DM detections, we therefore looked into the global Universe back to the early time, either from the electromagnetic waves or the GWs. The observations of electromagnetic waves (for example, the cosmic microwave background radiations and the large scale structures surveys) have established the boundaries for the new physics (for example, the upper bound on the inflationary scale, the lower bound on the reheating temperature, the upper bound on the new light degrees of freedom, the amount of DM fraction), the detailed structures of the new physics could only be depicted by the GWs that are transparent for the early Universe before the recombination. One of the GW backgrounds comes from the cosmic first-order phase transitions (see [36] for a comprehensive review and [37] for a pedagogical lecture on the cosmic first-order phase

transitions), which was proposed for detection [38, 39] in the European LISA (eLISA) and the European New Gravitational Wave Observatory (NGO) missions [40] and summarized by the eLISA working group in [41] and updated recently in [42] by the rejoined LISA working group [10]. See also [23, 43] for a brief review. In this short review, we will not devote ourselves to the historical developments and particle-physics model buildings but only to overview the important progress in the recent five years within the following four catalogs and highlight three of our work [44–46] for future perspective.

Phase transition dynamics on bubble nucleations and percolations

The cosmic first-order phase transition proceeds with the stochastic nucleations [47–50] of true-vacuum bubbles in the false-vacuum background with an exponentially varying probability [51] linear [50, 52] or quadratic [53, 54] in time elapse around the percolation time [52, 55–58], the later of which usually leads to a very strong first-order phase transition in a supercooled Universe that would have been slow [59, 60] but strongly constrained by a necessary condition [56, 61, 62] for the phase transition to be completed properly. The constraints on such a temporarily short duration of false vacuum domination of supercooled slow phase transition might be relaxed if the PBHs production channels are considered [63–65]. Note that the gravitational effect [66] might plays a role for the phase transitions realized in the usual particle physics models [67], and other phase transition models from inflationary era [68–71], matter-dominated eras [72, 73] and non-standard cosmology [74] are also studied in addition to the usual phase transition models during radiation-dominated era. In particular, for the phase transition completed during inflation, a unique GW signal could be produced with an oscillatory feature at large wave numbers [71].

Microscopic/Macroscopic dynamics on bubble expansion

The macroscopic dynamics of the bubble expansion in the thermal fluid could be captured essentially by the hydrodynamics with the bubble wall velocity as an input free parameter to solve for the fluid velocity profile, which in turn gives rise to the energy budget [44, 73, 75, 76] of the total released vacuum energy into the kinetic energies of the expanding bubble wall [44, 73, 76] and thermal fluid motions [73, 75, 76] as well as the thermal energy dissipation. Realistic description for the bubble expansion requires going beyond the flat spacetime background [77] (see [78] for earlier trial) and the simple bag model of equation-of-state [79–82].

The microscopic dynamics of the bubble expansion is governed by the Boltzmann equation [83–89] with an out-of-equilibrium term characterizing the wall-plasma interactions against the driving force from the released vacuum energy, from which the bubble wall velocity could be obtained for some simple BSM models [90–100] with the help of the planar wall approximation and flow ansatz for the particle distribution function. See also [101, 102] for recent attempts to infer the bubble wall velocity from the holographic point of view. However, a phenomenological approach [75, 87, 103–110] is usually adopted in general to conveniently parameterize the out-of-equilibrium term so as to reproduce the scaling behavior [109, 111–115] of the friction term in terms of the Lorentz factor of the bubble wall velocity. Therefore, an effective picture [44, 73, 76] is obtained for the bubble expansion as we will highlight shortly below:

- The numerical simulations for the first-order phase transition aim at solving the com-

bined equations of motion for the scalar field and thermal plasma,

$$\square\phi - \frac{\partial V_{\text{eff}}}{\partial\phi} = \delta f; \quad (2.1)$$

$$\partial_\mu T_p^{\mu\nu} + \partial^\nu\phi \frac{\partial V_T}{\partial\phi} = -\partial^\nu\phi \cdot \delta f, \quad (2.2)$$

respectively, where the out-of-equilibrium term δf is defined by

$$\delta f = \sum_{i=B,F} g_i \frac{dm_i^2}{d\phi} \int \frac{d^3\vec{k}}{(2\pi)^3} \frac{\delta f_i}{2E_i(\vec{k})} \quad (2.3)$$

in terms of the deviation of the particle distribution function from equilibrium, $f_i = f_i^{\text{eq}} + \delta f_i$. Usually it is hard to compute δf_i directly from a concrete particle physics model, hence a phenomenological parameterization is adopted in a model-independent manner by $\delta f = \eta_T u^\mu \partial_\mu \phi$, where η_T is some dimensionless function of the scalar ϕ , temperature T and fluid velocity u^μ . This parameterization is specifically chosen so that the effective equation-of-motion for the position $R(t)$ of the bubble wall,

$$\sigma\gamma^3 \ddot{R} + \frac{2\sigma\gamma}{R} = \Delta p_{\text{dr}} - \Delta p_{\text{fr}}, \quad (2.4)$$

from integrating the scalar equation-of-motion in the vicinity of bubble wall could reproduce the scaling behavior of the friction term $\Delta p_{\text{fr}} \propto \gamma$ with respect to the Lorentz factor $\gamma = 1/\sqrt{1 - \dot{R}^2}$ that roughly matches the microscopic estimations $\Delta p_{\text{fr}} = P_{1\rightarrow 1} + P_{1\rightarrow 2}$ consisting of the particle transmission/reflection $P_{1\rightarrow 1} \approx \Delta p_{\text{LO}}$ at the leading-order [111] and transition splitting $P_{1\rightarrow 2} \approx \gamma \Delta p_{\text{NLO}}$ at the next-to-leading-order [112]. Recent estimation to all orders reveals a friction of form $\Delta p_{\text{fr}} \approx \Delta p_{\text{LO}} + \gamma^2 \Delta p_{\text{NLO}}$ [114] or $\Delta p_{\text{fr}} = (\gamma^2 - 1)T\Delta s$ from thermodynamic considerations [113], which could be reproduced from a different parameterization [44],

$$\delta f = -\tilde{\eta}_T (u^\mu \partial_\mu \phi)^2, \quad (2.5)$$

with function $\tilde{\eta}_T$ of mass dimension 3. Numerical simulations using this parameterization should be feasible in future. To see immediately the impact from a general form of friction term $\Delta p_{\text{fr}} = \Delta p_{\text{LO}} + h(\gamma)\Delta p_{\text{NLO}}$ on the energy budget of the phase transition, note that the effective equation-of-motion (EOM) of the bubble wall should be modified as [44]

$$\left(\sigma + \frac{R}{3} \frac{d\Delta p_{\text{fr}}}{d\gamma} \right) \gamma^3 \ddot{R} + \frac{2\sigma\gamma}{R} = \Delta p_{\text{dr}} - \Delta p_{\text{fr}} \quad (2.6)$$

to respect the conservation law of the total energy $E = 4\pi R^2 \sigma \gamma - \frac{4}{3}\pi R^3 (\Delta p_{\text{dr}} - \Delta p_{\text{fr}})$, which could be solved directly as [44]

$$\frac{h(\gamma) - h(1)}{h(\gamma_{\text{eq}}) - h(1)} + \frac{3\gamma}{2R} = 1 + \frac{1}{2R^3} \quad (2.7)$$

with R already normalized with respect to the initial bubble size R_0 and γ_{eq} defined by $h(\gamma_{\text{eq}}) = (\Delta p_{\text{dr}} - \Delta p_{\text{LO}})/\Delta p_{\text{NLO}}$. Then the efficiency factor for the bubble collisions could be calculated directly from [44]

$$\kappa_{\text{col}} = \left(1 - \frac{\alpha_\infty}{\alpha} \right) \int_1^{R_{\text{col}}} \left(\frac{dR}{R_{\text{col}}} \right) \left[1 - \frac{h(\gamma(R))}{h(\gamma_{\text{eq}})} \right] \quad (2.8)$$

where R_{col} is the bubble radius at collisions, $\alpha = \Delta p_{\text{dr}}/\rho_{\text{rad}} = (\Delta V_{\text{eff}}(\phi_+) - \Delta V_{\text{eff}}(\phi_-))/\rho_{\text{rad}}$ is the strength factor of the total released vacuum energy with respect to the background radiation, γ_{eq} is the asymptotic Lorentz factor that balances the driving pressure with the friction force $\Delta p_{\text{dr}} = \Delta p_{\text{fr}}$, and $\alpha_{\infty} = \Delta p_{\text{LO}}/\rho_{\text{rad}}$. The new term in (2.6) defines a transition radius,

$$R_{\sigma} = \frac{3}{2} \frac{h(\gamma_{\text{eq}}) - h(1)}{h'(\gamma(R_{\sigma}))} R_0, \quad (2.9)$$

when the bubble wall slows down its acceleration and starts to approach a terminal velocity. Although our modified EOM (2.6) reproduces previous estimations [73, 76] in the limit of a large collision radius $R_{\text{col}} \gg R_{\sigma}$, the difference in the efficiency factor κ_{col} could be announced if the bubbles collide at a radius $R_{\text{col}} < 100R_{\sigma}$, which is important for the strong first-order phase transition where the bubbles collide with each other when they are still rapidly accelerating ever before having approached the terminal velocity. Numerical simulations should be carried out for checking this effective picture.

Numerical simulations and analytic auxiliary modeling on bubble collisions

Numerical simulations on bubble collisions in vacuum background [116–118] and thermal fluid [119, 120] have taken advantage of the envelope approximation, which was abandoned later in [121–124] with the discovery of sound waves [125] as the dominated contribution [51, 126] over the bubble collisions [127] to the stochastic background of GWs from the cosmic first-order phase transition if the bubble wall velocity could terminate at some constant velocity as opposed to the runaway expansion. See also [128] for checking the thin-wall approximation and [129, 130] for a new oscillating feature and inclusion of a complex scalar field. The last gravitational-wave source comes from the magneto-hydrodynamic (MHD) turbulence [119, 127], whose numerical simulation only made possible until very recent time [131–134]. See also [135–144] for the helical MHD turbulence.

On the other hand, the extraction of the energy-density spectrum from the numerical simulation results requires some analytic auxiliary models to generate some well-motivated parameterization formulas. Earlier analytic calculations [145, 146] on bubble wall collisions have been renewed in [147] with the aid of thin-wall and envelope approximations, the latter of which was further abandoned in [148]. The analytic treatments from the sound shell model [149, 150][77], bulk flow model [148, 151] and hybrid model [152–154] have depicted the lifetime evolution of the sound waves before the formation of the MHD turbulence [155–160]. See also [45] for a numerical simulation with inclusion of a gauge field for the generation of primordial magnetic field as we will highlight shortly below:

- In literatures, it was proposed that magnetic field (MF) that may seed the observed cosmic scale MF [161–164]. To verify if the MF and GW can be generated together during the first-order phase transition, Ref. [45] performed the lattice simulation of the magnetic field and GW production from bubble collisions and oscillations stages during the phase transition by considering the evolution of gauge fields and Higgs field on three-dimensional lattice. It was shown that the Higgs gradient effect not only dominates the GW production, its effects on the magnetic field production are also significant as seen from Fig.2 in Ref. [45]. The study further show that the observations of cosmic MF and GW are complementary to probe new physics admitting first-order phase transition, after taking into account the affects of MHD on the generated MF. For the GW calculation, Ref. [45] adopted the straightforward

procedure from Ref. [165] rather than the envelope approximation. The EOM of tensor perturbations h_{ij} reads

$$\ddot{h}_{ij} - \nabla^2 h_{ij} = 16\pi G T_{ij}^{\text{TT}}, \quad (2.10)$$

where the superscript TT denotes the transverse trace-less projection, and the energy-momentum tensor (right hand side) is given by

$$T_{\mu\nu} = \partial_\mu \Phi^\dagger \partial_\nu \Phi - g_{\mu\nu} \frac{1}{2} \text{Re}[(\partial_i \Phi^\dagger \partial^i \Phi)]. \quad (2.11)$$

Here Φ is the Higgs field, and the subdominant gauge field contributions are neglected. Nevertheless, the contribution from the magnetic fields still affects the evolution of the Higgs field through the combined EOMs

$$\partial_0^2 \Phi = D_i D_i \Phi - \frac{dV(\Phi)}{d\Phi}, \quad (2.12)$$

$$\partial_0^2 B_i = -\partial_j B_{ij} + g' \text{Im}[\Phi^\dagger D_i \Phi], \quad (2.13)$$

$$\partial_0^2 W_i^a = -\partial_k W_{ik}^a - g \epsilon^{abc} W_k^b W_{ik}^c + g \text{Im}[\Phi^\dagger \sigma^a D_i \Phi], \quad (2.14)$$

with the solutions subjected to Gauss constraints,

$$\partial_0 \partial_j B_j - g' \text{Im}[\Phi^\dagger \partial_0 \Phi] = 0, \quad (2.15)$$

$$\partial_0 \partial_j W_j^a + g \epsilon^{abc} W_j^b \partial_0 W_j^c - g \text{Im}[\Phi^\dagger \sigma^a \partial_0 \Phi] = 0, \quad (2.16)$$

where the temporal gauge $W_0^a = B_0 = 0$ is used. The energy spectrum of GW from the bubble collision and oscillation stage can be extracted from

$$\begin{aligned} \Omega_{\text{GW}} &= \frac{1}{\rho_c} \frac{d\rho_{\text{GW}}(k)}{d \ln k} \\ &= \frac{k^3}{32\pi G L^3 \rho_c} \int d\Omega \Lambda_{ij,lm}(\hat{k}) \dot{u}_{ij}(t, k) \dot{u}_{lm}(t, k), \end{aligned} \quad (2.17)$$

where $h_{ij}(t, k) = \Lambda_{ij,lm}(\hat{k}) u_{ij}(t, \mathbf{k})$, with $\Lambda_{ij,lm} = P_{il}(\hat{k}) P_{jm}(\hat{k}) - \frac{1}{2} P_{ij}(\hat{k}) P_{lm}(\hat{k})$ and the spatial projection operator $P_{ij} = \delta_{ij} - \hat{k}_i \hat{k}_j$ ($\hat{k}_i = k_i/k$). Here G is the Newtonian gravitational constant, ρ_c is the critical density, and L is lattice spacing in the simulation. The GW production are shown to be affected by bubble wall thickness and bubble wall velocity.

Particle physics phenomenology on the phase transition models

There are an immense amount of particle physics models with cosmic first-order phase transitions, most of which have been summarized in [41, 42] for their phenomenological detection. We will not review here a completed list of these BSM models with higher operators extensions, scalar extensions, supersymmetric extensions, warp extra dimensions, composite Higgs, and dark/hidden sector, but only to mention some phenomenological considerations on model selection.

Since the phenomenological predictions could be largely affected by some theoretical uncertainties from the renormalization group running [60], renormalization scale dependence [166, 167], the gauge dependence and infrared divergences [168] as well as careful treatments on phase transition dynamics and macroscopic thermal parameters [169], a non-perturbative approach to phase transition description using dimensional reduction has been developed

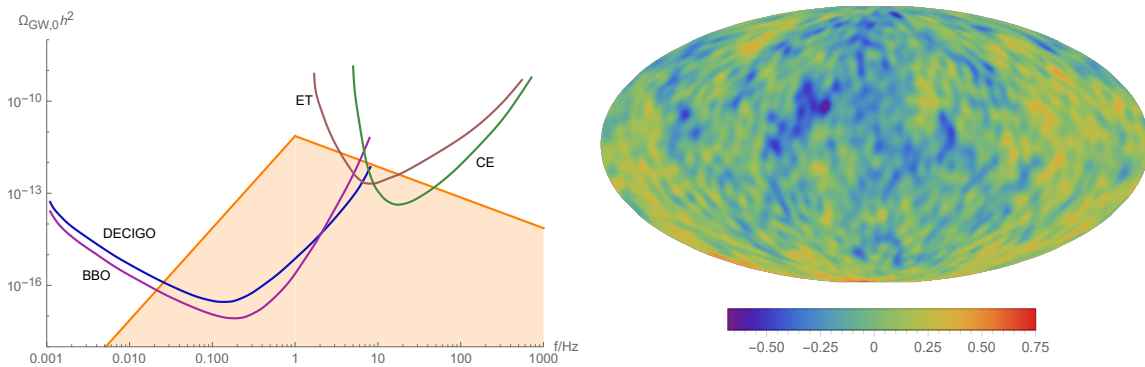


Figure 2. In the left panel, the orange line presents an example of the present energy spectrum of GWs from domain walls, $\Omega_{\text{GW},0} h^2$, using the approximation method in Ref. [201], where the tension and annihilation temperature of domain walls are $(5 \times 10^{10} \text{GeV})^3$ and 10^7GeV . This SGWB can be observed by DECIGO [21], BBO [207], ET [7] and CE [208]. The right panel shows a random realization of the SGWB using the first 50 l -modes, where the angular power spectrum is $l(l+1)C_l = 0.085$, predicted by models with $\phi_i \sim H_{\text{inf}}$. Copied from Ref. [46] with permission.

for some BSM models [170–183]. On the other hand, the observational perspectives on gravitational-waves signals extraction have been tested for some particle physics models [184–186] with LISA sensitivity curves. Recently, the model selections and comparisons have been confronted with the real data from the NANOGrav 12.5-yr data [187–193] and LIGO [194, 195]. To better extract BSM physics from the phase transition models, more theoretical understandings are needed for the possible features of anisotropies [196] and the non-Gaussianity [197] beyond the simple power-law shapes of the energy density spectrum. See also [46] for GW anisotropies from domain walls as we will highlight shortly below:

- Along with the spontaneous symmetry breaking during phase transitions, topological defects will finally form, as an important consequence of phase transitions [198]. For example, cosmic strings/domain walls are one/two-dimensional topological defects that can form in case of the continuous/discrete symmetry is spontaneously broken [199]. Since the energy density is highly concentrated, the motion of topological defects driven by their tension results in continuous GW productions. Different from the transitory GW production from bubbles and sound waves, GWs are continuously produced as long as the topological defects do not annihilate. The characteristic GW energy spectrums of cosmic strings and domain walls are reviewed in Refs. [200, 201], and through GWs one can detect or give more strict constraints on their tension [202, 203]. Moreover, GWs from topological defects can successfully explain the common-spectrum process observed by NANOGrav [190, 204, 205] (Note that an inflationary interpretation of the NANOGrav signal is not excluded for a sufficiently low reheating scale [206].).

Instead of the energy spectrum of GWs from topological defects, we also find the anisotropies of those stochastic GW backgrounds carry unique information about inflation. The anisotropies in stochastic GW backgrounds could be generated by the sources [196, 209–211] and the processes during propagation [212–215], which in most cases are still challenging to observe [216–221]. We explore the SGWB produced from unstable cosmic domain walls, which annihilates before dominating the Universe [222, 223]. The discrete symmetry is spontaneously broken before inflation, and the formation of DWs is realized because ϕ could cross the potential barrier due of quantum fluctuations. The corresponding probability that

ϕ crosses the barrier reads [224]

$$P(t) = \frac{1}{2} \operatorname{erfc} \left(\frac{\sqrt{2}\pi\phi_i}{H_{\text{inf}}\sqrt{N(t)}} \right), \quad (2.18)$$

where ϕ_i is the initial value of the inflaton, and we assume $\phi_i > 0$ without losing generality. H_{inf} is the Hubble parameter during inflation and $N(t) \equiv H_{\text{inf}}(t - t_i)$ where t_i is the horizon-crossing time of the CMB scale. After inflation the Hubble parameter H decreases with time, and once H becomes smaller than the effective mass of ϕ , then ϕ settles down in different vacua and DWs form. Large scale perturbations of ϕ remain constant at superhorizon scales, and then result in perturbations of the energy density of DWs, so that anisotropies in SGWBs arise. The angular spectrum of GWs is defined by

$$l(l+1)C_l = \frac{\pi}{2} \langle \delta\Omega_{\text{GW}}^2 \rangle, \quad (2.19)$$

where $\delta\Omega_{\text{GW}}(\mathbf{x}) \equiv (\Omega_{\text{GW}}(\mathbf{x}) - \overline{\Omega_{\text{GW}}})/\overline{\Omega_{\text{GW}}}$ denotes fluctuations of the GW energy spectrum. The GW energy spectrum, is proportional to quantum fluctuations of ϕ ,

$$\delta\Omega_{\text{GW}}(\mathbf{x}) = c_1 \delta\phi(\mathbf{x}), \quad (2.20)$$

where c_1 can be obtained from the derivative of Eq. 2.18 with respect to ϕ . During inflation quantum fluctuations of ϕ leads to $\langle \delta\phi^2 \rangle = H_{\text{inf}}^2/(4\pi^2)$, then the angular power spectrum could be obtained as [46]

$$l(l+1)C_l \approx \begin{cases} \frac{\pi}{N_{\text{peak}}} \alpha_{\text{peak}}^2, & \alpha_{\text{peak}} \gg 1, \\ \frac{1}{N_{\text{peak}}}, & \alpha_{\text{peak}} \ll 1, \end{cases} \quad (2.21)$$

where $\alpha_{\text{peak}} \equiv \frac{\sqrt{2}\pi\phi_i}{H_{\text{inf}}\sqrt{N_{\text{peak}}}}$, $N_{\text{peak}} = \ln(f_{\text{peak}}/H_0)$ and f_{peak} is the peak frequency of GWs from domain walls. Since the e -folding number of inflation is expected to be 50-60, the angular power spectrum is at least 10^{-2} at the CMB scales, see Fig. 2 as an example of random realization of a SGWB with $l(l+1)C_l = 0.085$, which could be used as a probe of the inflationary energy scale. Since primordial GWs are too weak to be detected for low-scale inflation, observing such anisotropies in stochastic GW backgrounds provides a novel method to detect the inflationary energy scale even it is orders of magnitude lower than the grand unified theory scale [46].

2.2 Induced gravitational waves

The perturbations of the metric in general relativity (GR) can be decomposed into scalar and tensor types. In an appropriate gauge, the spatial part of the flat FLRW metric can be written as $dl^2 = a^2((1+2\mathcal{R})\delta_{ij} + h_{ij})$, where \mathcal{R} is the scalar-type curvature perturbation and h_{ij} is the tensor perturbation². At the linear order, there are no interactions between these different types of perturbations, which evolve independently. By the recent observation of CMB [241], the curvature perturbation is measured to be $\mathcal{R} \sim 10^{-5}$ to very high accuracy, while there

²We will not enter the topic of gauge choice in this subsection. We recommend the interested readers to read Refs. [225–240] for details.

is still no evidence for the detection of the tensor-type primordial perturbation, which puts an upper bound of $\Omega_{\text{GW}} \lesssim 10^{-16}$ to the energy density spectrum of the primordial GWs for frequencies higher than 10^{-15} Hz. Another form of GW is the secondary wave induced by the scalar-scalar-tensor type interaction present in the non-linear order of the perturbed action, which are called induced GWs or secondary GWs [242–249]. If the curvature perturbations are as small as their values at the CMB scales, the induced GWs are much smaller than the first-order primordial GWs ($\Omega_{\text{GW}}^{(\text{ind})} \sim 10^{-24}$) and are completely negligible. However, in some inflation models, the curvature perturbation gets enhanced at scales much smaller than 1 Mpc, which can induce detectable GWs as well as substantial PBHs. For instance, in Ref. [250] we considered a non-minimally coupled scalar field with a flat concave potential in Starobinsky R^2 -gravity. The scalaron potential dominates in the early stage of inflation which makes the predictions of tensor-to-scalar ratio r and spectral tilt n_s on large scales favorable by Planck constraint, while on small scales the field roll down to the valley of the scalaron and starts to slowly roll in the other direction, which induces a huge enhancement of the power spectrum of the curvature perturbation that can generate abundant PBHs. Another example is to realize the parametric resonance in a single-field inflationary model with a small periodic structure upon the potential, of which the equation of the curvature perturbation has the form of the Mathieu equation, and the power spectrum of the curvature perturbation is enhanced thereby in the instability tongues of the parameter space [251].

The PBHs are generated by the gravitational collapse of the high- σ peaks of the curvature perturbation at its horizon reentry before recombination [252–257]. For recent discussions on the PBH formation, see for instance [258–266]. The masses of PBHs are roughly the horizon mass when the peak wavelength of the curvature perturbation reenters the Hubble horizon, which depends on the concrete inflation models that generates them [250, 251, 267–329]. The peak wavelength in turn, determines the frequency of the induced GWs, which is connected to the PBH mass by $M_{\text{PBH}}/M_{\odot} = (f/10^{-8}\text{Hz})^{-2}$. The cross check of the energy density spectrum of the induced GWs and the PBH abundance under such a mass-frequency relation is very important, especially considering the possibility that the PBHs can circumvent the measurement of baryonic matter on the CMB thus might contribute a substantial amount or all of the fraction of cold DM (CDM).

Due to Hawking radiation, light PBHs with $M_{\text{PBH}} \lesssim 10^{16}$ g have already evaporated completely during the current cosmic age, which leaves strong constraints on big bang nucleosynthesis and intergalactic γ -rays. Besides, the current observational constraints do not exclude the existence of a substantial amount of PBHs in several interesting “mass windows” [330–345], which can yield fruitful phenomena. For instance, the LIGO O3a data set of LIGO/Virgo implies that there might be two populations of black holes [346], which can be explained by the combination of the astrophysical black holes and PBHs of ~ 20 solar mass [347–349]. PBHs might be the supermassive or stupendously large BHs which seed the galaxy or even structure formation [350–356]. The planetary-mass PBHs could be the lensing objects of the microlensing events observed by the Optical Gravitational Lensing Experiment (OGLE) [357–360], or even the Planet 9 [361]. The formation of solar-mass PBHs is greatly enhanced due to the softening of the equation-of-state parameter during the QCD phase transition [362, 363], and can provide the hotspots for baryogenesis [364, 365]. The PBH abundance can not exceed that of CDM, and is further constrained by some additional observations according to the PBH masses [334, 366–369]. The PBH mass function, f_{PBH} , is defined as the PBH energy density normalized by the DM density. According to the observational constraints, especially the observations on the microlensing events in the halo of

our galaxy [370], the only window that affords $f_{\text{PBH}} \approx 1$, i.e. PBHs can serve as all the DM, is $10^{16} \text{ g} < M_{\text{PBH}} < 10^{22} \text{ g}$, the so-called asteroid-mass PBHs. Because of the finite-size effect and wave effect, it is impossible to observe the lensing events by visible lights when the asteroid-mass PBHs are the lensing objects [370–377]. Therefore the indirect constraints from the induced GWs associated with the asteroid-mass PBHs, which accidentally lie in the millihertz band of the space-based interferometers, becomes almost the only tool to detect the PBH-as-DM scenario.

As the PBH formation depends on the high- σ peaks of the probability distribution function (PDF) of the curvature perturbation, it crucially depends on the shape of the PDF. A typical deviation of the usually presumed Gaussian PDF is the quadratic local non-Gaussianity, which can be written as $\mathcal{R} = \mathcal{R}_g + F_{\text{NL}} (\mathcal{R}_g^2 - \langle \mathcal{R}_g^2 \rangle)$ [378–384]. It is shown that for positive local non-Gaussianity ($F_{\text{NL}} > 0$), the PBH abundance will be greatly enhanced, while for negative value it will be suppressed [385]. In Ref. [386], we discussed the PBH abundance with quadratic local non-Gaussianity, and calculated the GWs induced by such non-Gaussian scalar perturbations. We found that after taking into account the local non-Gaussianity with positive nonlinear parameter F_{NL} , the induced GWs are also enhanced, but not as much as that of the PBHs.

In the asteroid-mass window, if PBHs can be all the DM ($f_{\text{PBH}} = 1$), the required amplitude of the power spectrum of the curvature perturbation should be $\mathcal{O}(10^{-2})$. If there is positive non-Gaussianity, the PBH formation will be greatly enhanced and in turn, the curvature perturbation we require will be smaller than the Gaussian case as the PBH abundance is fixed. When considering the energy density spectrum Ω_{GW} of the induced GWs at millihertz, we found that when $F_{\text{NL}} > 0$ with a fixed f_{PBH} , the suppression of Ω_{GW} from the suppression of the curvature perturbation can not be fully compensated by the enhancement from the non-Gaussian part, which means that increasing the non-linear parameter F_{NL} will suppress the induced GW, if the PBH abundance is fixed. See Figure 3 for details.

An important implication of our result shown above is that the energy density spectrum of the induced GWs is bounded from below when F_{NL} is very large, and this lower bound is still higher than the sensitivity curve of the space interferometers like LISA [9, 10, 39, 40, 387], Taiji [11–13] and TianQin [17–19]. Therefore, our result actually reaches an important conclusion, that if DM consists mainly of PBHs, which is only possible for the asteroid-mass window, the corresponding millihertz induced GWs must be detectable by the space interferometers, regardless of the quadratic local non-Gaussianities [386]. On the contrary, the non-detection of such induced GWs in the space interferometers will close the only window of PBH-as-DM scenario [388–391]. Based on our conclusion, the indirect detection of the asteroid-mass PBH abundance by the millihertz induced GW becomes a very important scientific goal for the space-based interferometers [392–395] as shown in Figure 4.

To identify the physical origin of the stochastic GWs, the study of their spectral shapes are very important. In Ref. [397] we studied the infrared behavior of the stochastic GWs, and found that on scales much larger than any scales of the GW source, the stochastic GWs behave like a white noise with an infrared scaling of $\Omega_{\text{GW}} \sim f^3$, if the tensor mode reenter the Hubble horizon in the radiation dominated era. This implies the infrared scaling of any stochastic GW spectrum can be used to probe the thermal history of the universe, as a deviation from $\Omega_{\text{GW}} \sim f^3$ implies a deviation from $w = 1/3$ [398, 399]. On the other hand, the induced GW has some characteristic spectral shape near its peak, which depends crucially on the width of the power spectrum of the curvature perturbation that induces it [400]. The infrared scaling reduces to $\Omega_{\text{GW}} \sim f^2$ if the curvature perturbation power

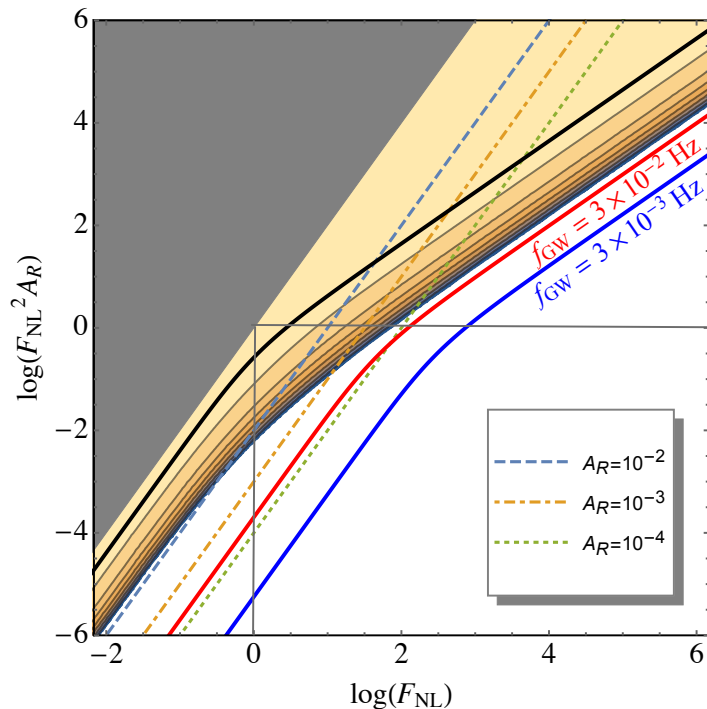


Figure 3. The PBH abundance as a function of F_{NL} and $F_{\text{NL}}^2 \mathcal{A}_{\mathcal{R}}$, where $\mathcal{A}_{\mathcal{R}}$ is the amplitude of the power spectrum of the curvature perturbation in the Newtonian gauge. The border between the colored and white regions corresponds to $f_{\text{PBH}} = 1$, i.e. PBHs are all the DM. The dashed lines are for $\mathcal{A}_{\mathcal{R}} = 10^{-2}$, 10^{-3} , and 10^{-4} from left to right, while the shaded area is unphysical since $\mathcal{A}_{\mathcal{R}} > 1$. The thick black curve is the absolute constraint that the GW energy density is smaller than the current density of radiation, while the red and blue curves are the sensitivity bound of LISA at $f_{\text{GW}} = 3 \times 10^{-2}$ Hz and 3×10^{-3} Hz, respectively; they correspond to PBH masses $M_{\text{PBH}} = 10^{20}$ g and 10^{22} g. Copied from Ref. [386] with permission.

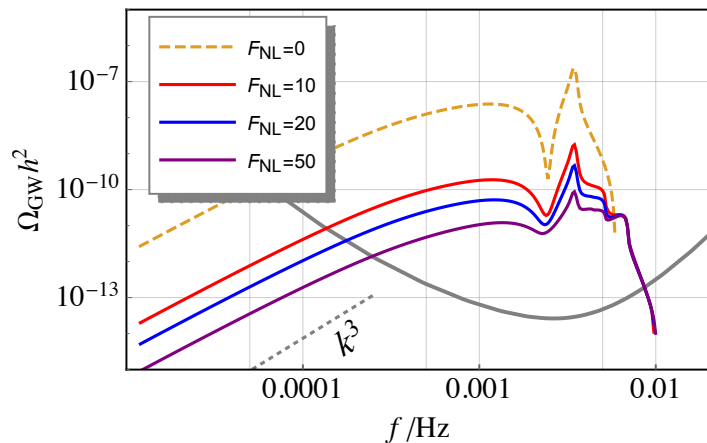


Figure 4. Typical energy density spectrum of the GWs induced by a non-Gaussian curvature perturbation at second order with $F_{\text{NL}} > 0$. The width of peak is fixed at 10^{-4} Hz. The abundance of the PBHs is fixed to be $f_{\text{PBH}} = 1$ for $M_{\text{PBH}} = 10^{22}$ g. We draw the induced GW energy density spectrum $\Omega_{\text{GW}} h^2$ for $F_{\text{NL}} = 0$ (orange dashed), 10 (red), 20 (blue), and 50 (purple). The gray curve is the sensitivity bound of LISA from Ref. [396]. A reference line of the k^3 slope is also drawn for comparison. Copied from Ref. [386] with permission.

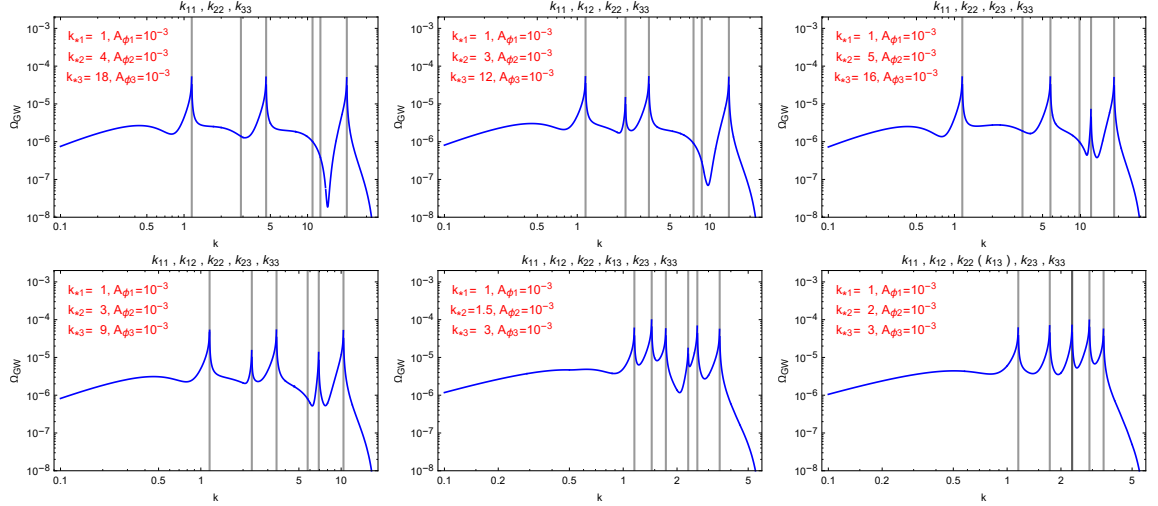


Figure 5. The energy density spectrum of induced GWs from curvature perturbations with triple δ -peaks at $k_{*1} < k_{*2} < k_{*3}$. The gray lines denote the positions of those would-be peaks at k_{ij} with $i, j = 1, 2, 3$. Copied from Ref. [408] with permission.

spectrum is a δ -function peak [401]. For a narrow peak, there is a breaking frequency f_b below which the power goes from 2 to 3. f_b moves towards the peak frequency f_p when the width increases, and disappears when the width is of order 1. For a broad peak in the power spectrum of the curvature perturbation with a lognormal shape, we derived an analytical formula for Ω_{GW} which fits the numerical integral well. This result can be used to speed up the signal searching of the stochastic GWs in the future.

The combination of a series of spectral peaks in the power spectrum of the curvature perturbation may bring a more distinctive feature in the energy density spectrum of the induced GWs: the resonance peaks. In some inflationary models, the spectrum of curvature perturbations has multiple sharp peaks [402–407]. Such peaks usually indicate the excitation of extra degree(s) of freedom during inflation whose effective mass is larger than the Hubble parameter. When the spectrum of the curvature perturbations has only one narrow peak, one can find that there is also a narrow peak in the spectrum of GWs as shown in Figure 6. One may naively guess that in the multiple-peak case, the numbers of peaks in the spectrum of induced GWs and curvature perturbation are equal. Unfortunately, it is not always true, and there may be more peaks in Ω_{GW} . In Ref. [408], a multiple-peak structure in the energy density spectrum of induced GWs is analytically identified, which exhibits at most C_{n+1}^2 and at least n peaks at wave-vectors $k_{ij} \equiv (k_{*i} + k_{*j})/\sqrt{3}$ due to resonant amplification and momentum conservation, when there are n narrow peaks located at k_{*i} in the power spectrum of the curvature perturbation. An example of 3 δ -peaks is shown in Figure 5, where at least 3 peaks and at most $C_4^2 = 6$ peaks are apparently observed, depending on the positions of the peak wavenumbers k_{*i} . It is straightforward to apply our result to the models with an oscillatory modulation in the power spectrum of the curvature perturbation, which is a typical feature in the multi-field inflation models with a curved field space proposed recently in Refs. [293, 294] to enhance the power spectrum and generate PBHs. The resonance peaks in the energy density spectrum of induced GWs studied in our paper [408] are verified in such models in Refs. [409–412].

It is possible that the binary black holes observed by LIGO/Virgo are of the primordial

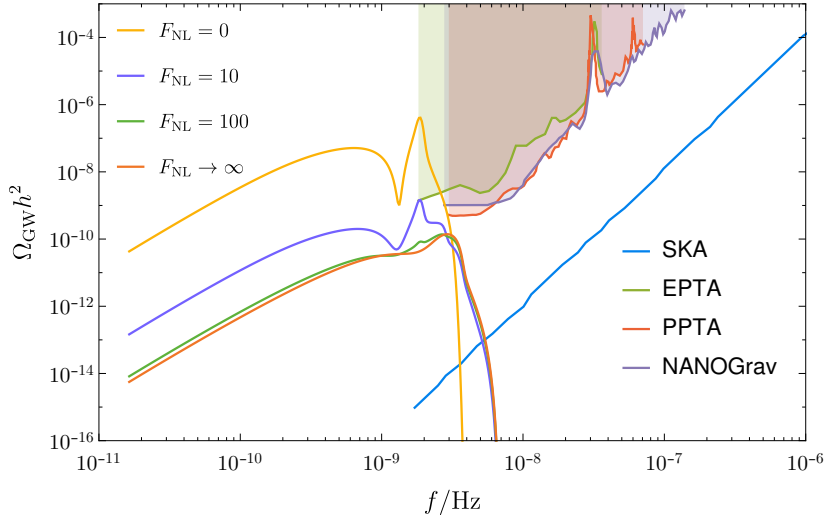


Figure 6. The GW spectrum with $F_{\text{NL}} = 0, 10, 100$ and $F_{\text{NL}} \rightarrow \infty$ fit from LIGO detections with respect to the sensitivities of current/future PTA projects. The current constraints (shaded) are given by EPTA [419], PPTA [420], NANOGrav[421], and the future sensitivity curve of SKA is depicted following [422]. The recent result from NANOGrav 12.5-yr data is not shown [25]. Copied from Ref. [415] with permission.

origin [413, 414]. If these black holes are primordial, the enhanced curvature perturbation on small scales can induce nanohertz GWs, which is sensitive for PTAs. The origin of the black holes observed by LIGO/VIRGO is the key issue to tackle this problem. In Ref. [415], it is shown that by assuming all the LIGO O1 and O2 events are from primordial origins, the power spectrum of the curvature perturbation can be reconstructed by the merger rate derived from the event rate. The induced GWs however, would be in seemingly mild tension with current constraints from PTA, if the curvature perturbation is Gaussian. Introducing local non-Gaussianity of the curvature perturbation with a non-linear parameter $f_{\text{NL}} \gtrsim \mathcal{O}(10)$ can relieve the tension. Nevertheless, even the non-Gaussianity is very large, such induced GWs must be detectable by the SKA in a decade or less, as is shown in Figure 6. Recent analysis on the LIGO GWTC-2 catalog implies that only 3% to 55% of the black holes can be primordial, with $f_{\text{PBH}} \sim 10^{-3}$ at $18M_{\odot}$ [348, 416]. As we anticipated, the induced GWs associate with such PBHs are inconsistent with the renewed nanohertz GW result from NANOGrav 12.5-yr data [25], unless there is a positive local non-Gaussianity of $f_{\text{NL}} \gtrsim 2.1$ [417]. Of course, as the abundance of the PBHs depends crucially on the spectral shape, statistics, formation process, etc., it is also possible for the NANOGrav signal to be consistent with the LIGO/VIRGO events without invoking non-Gaussianity, when a modified Gaussian window function and a broader width is chosen [418].

2.3 GWs produced during preheating

Preheating is a violent process next to inflation, and the amplified energy density perturbations during preheating produce considerable GWs. To set the initial conditions of the hot Big-Bang Universe, the vacuum energy transfers into radiation and reheats the universe after inflation, which is referred to as reheating [423, 424]. Many inflationary models predict the existence of preheating process at the beginning of reheating. In the preheating scenario [425], the inflaton field begins to oscillate around the minimum of its potential after inflation

and ultimately decays into elementary particles in the standard model of particle physics. Ref. [426] thoroughly investigates the case the inflaton ϕ is coupled to a scalar field χ by the coupling $\frac{1}{2}g^2\phi^2\chi^2$ (see also [427] for an intermediate decay via vector particles). Ref. [428] considers tachyonic preheating after hybrid inflation. Refs. [429–431] consider the case of the coupling between the gauge fields and the inflaton. The parametric resonance induced by non-minimal coupling is studied in Refs. [432–434]. During preheating, the Fourier modes of a scalar matter field coupled to the inflaton field grow exponentially via parametric resonance [435]. The modes are quickly pumped up to a large amplitude. Such highly pumped modes correspond to large, time-dependent density inhomogeneities in configuration space, which can source significant GWs [436].

Preheating is the first process after inflation, happening at the energy scale much higher than the colliders could reach [437–439], so this period of history is very unclear and model-dependent. The uncertain equation of state of the Universe during preheating affects the model prediction of the e -folding numbers of inflation, the amplitude of the power spectrum of scalar perturbations, and the scalar spectral index, so that the CMB constraints on inflationary models also depends on preheating [440, 441]. The complex dynamics of preheating also results in other interesting consequences, for example, the production of topological defects [442, 443], primordial magnetic fields [444, 445] and PBHs [446–450]. Then, from GWs generated during the preheating we now have a new opportunity to explore new physics and the history of the very early Universe.

In case of the resonance strength being strong enough, the present peak frequency of such a GW signal is proportional to the energy scale of inflation while the present peak amplitude is independent of the energy scale of inflation [451–453]. In the single-field model, in general the peak frequency of GWs is so high that it is hard to be detected by interferometers. In hybrid inflation, since the energy scale ranges from the grand unification theory (GUT) scale to the TeV scale, GWs produced during preheating for low-scale inflationary models is expected to be detected by future ground-based or even space-based interferometers [165, 454].

When the scalar potential satisfies the “opening up” condition [455], oscillons, localized nontopological quasisolitons, can be generated during preheating, which lead to a stochastic GW background. This case is referred to as oscillon preheating and studied in symmetric smooth potentials [456] as well as asymmetric potentials [457–460].

We find oscillons naturally arise in such a cuspy potential,

$$V(\phi) = \lambda M_{\text{pl}}^{4-p} |\phi|^p \quad (2.22)$$

with $p = 1, 2/3, 2/5$ and $M_{\text{pl}} = (8\pi G)^{-1/2}$, the nonsmooth oscillations can trigger the amplification of fluctuations of the inflaton field itself at the moment when $\phi(t) = 0$, so that oscillons copiously form during oscillations of the inflaton field, which sources a significant stochastic GW background [461]. Interestingly, these cuspy potentials lead to a characteristic energy spectrum of GWs with double peaks (see Fig. 7), which can be distinguished from other potentials by measuring the shape of the energy spectrum of GWs. Actually, the cuspy potentials can be mimicked by the following more general form of potential in the asymptotically smooth limit,

$$V(\phi) = \frac{m^2 M^2}{p} \left[\left(1 + \frac{\phi^2}{M^2} \right)^{p/2} - 1 \right]. \quad (2.23)$$

When ϕ/M is large, the potentials can be approximated by Eq. (2.22), while when ϕ/M is small, the potential becomes smooth near the minimum. We find that the smoothness

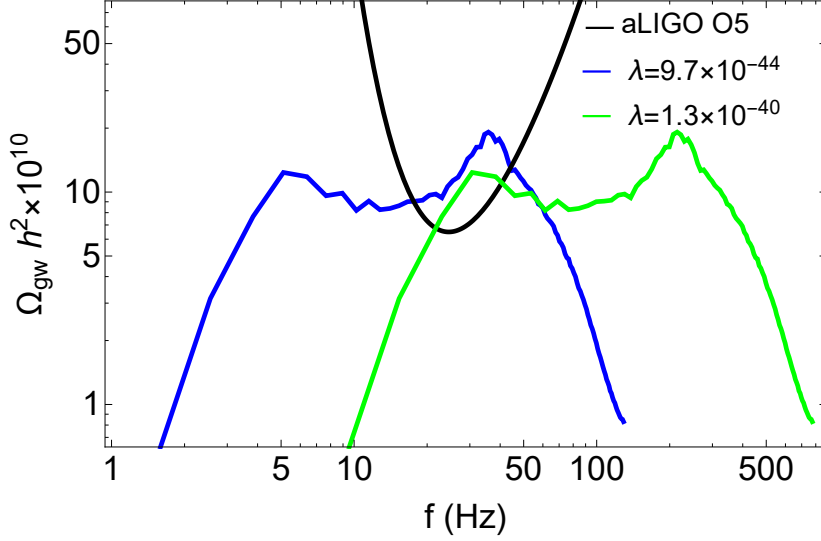


Figure 7. Energy spectra of GWs today, predicted by the linear potential with $\lambda = 9.7 \times 10^{-44}$ (blue) and $\lambda = 1.3 \times 10^{-40}$ (green). The black curve is the expected sensitivity curve of the fifth observing run (O5) of the aLIGO-Virgo detector network. Copied from Ref. [461] with permission.

of the potentials near the point $\phi(t) = 0$ suppresses the energy spectrum of GWs [462]. That is, cuspy potential yields stronger GW signals due to nonsmooth oscillations. In hybrid inflation, the energy scale of inflation ranges from the GUT scale to the electroweak scale. Consequently, oscillon formation generates a stochastic GW background with a typical frequency today of the order of $10^{-3} - 10^9$ Hz. Future ground-based and space-based interferometers provide the possibility to search for the GW signals with the double-peak energy spectrum.

2.4 Strongly lensed GW multimessenger

Like the strong gravitational lensing of optical signals [463–466], GW lensing attracted many interests in the last decade. The lensing of GW is very crucial for cosmology, fundamental physics, and astrophysics (see some example work in [467–476]). Though currently, we have not yet found any sufficient evidence for the GW lensing signal from the released LIGO data [477, 478], the development of the methodology of applying GW lensing to cosmology still deserves many studies. In this section, we focus on the GW strong lensing and introduce two of our work in this aspect.

The GR has been tested very precisely on solar system scales [479, 480]. However, the long-range nature of gravity on the extra-galactic scale is still loosely constrained and poorly understood. The parameterized post-Newtonian (PPN) framework [481] provides us with a systematic way to quantify the deviation from GR. The traditional strong gravitational lensing of quasars provides us with a unique opportunity to probe modifications to GR over a range of redshifts and on/above kiloparsec scales with the PPN parameterization [482–486]. Recently, the strong lensing of GW has attracted many interests, and the strongly lensed multimessenger shows significant improvements to the traditional electromagnetic (EM) experiments on cosmology, especially for the measurement of H_0 [471].

Ref. [472] proposed a new multimessenger approach using data from both GW, and the corresponding EM counterpart to constrain the modified gravity (MG) theory from the

scale-dependent phenomenological parameter γ_{PPN} . The author calculated the time-delay predictions by choosing various values of the phenomenological parameters for MG and then compare them with that from GR,

$$\Delta t_{i,j(\text{MG})} = \frac{1 + z_l}{c} \frac{D_l D_s}{D_{ls}} \Delta \phi_{i,j(\text{MG})}, \quad (2.24)$$

here the time delay $\Delta t_{i,j}$ is measured from the strongly lensed GWs and the Fermat potential difference $\Delta \phi_{i,j}$ is reconstructed from the lensed EM domain. D_X is the angular diameter distance. This strategy takes the most advantage of the information from both the GW and EM domains. For the third generation ground-based GW observatory Einstein Telescope, with only one typical event, and assuming that the dominated error from the stellar velocity dispersions is 5%, one can probe an 18% MG effect on a scale of 10 Kpc (68% confidence level). If assuming GR and a singular isothermal sphere mass model, our approach can distinguish an 8% MG effect. This work showed that the strongly lensed GW multimessenger plays an important role in revealing the nature of gravity on the galactic and extra-galactic scales.

Based on the prediction of GR, the absorption and dispersion of GWs could be neglected in a perfect-fluid Universe [487]. Such a theoretical point of view has been widely applied in some recent work, i.e., the test of Etherington distance duality relation and the opacity of the Universe at higher redshifts, with the combination of GW and EM signals [488, 489]. Up to now the hypothesis of transparent GWs in the EM domain remains experimentally untested, since the current GW detections have not yielded positive results [1, 2]. On the other hand, a large number of independent measurements of GWs indicate that DM, which constitutes a dominant component of virialized objects, could gravitationally interact with itself and with normal matter in galaxies and galaxy clusters. Many ideas have been proposed to explore the possibilities of DM self-interaction (SI) generating the cosmic accelerated expansion [490, 491] and the non-zero cosmological shear viscosity [492–494], if DM can be treated as non-ideal fluids with a viscosity term of η . In the framework of such methodology, an efficient graviton-matter conversion would be achieved with a simple relation

$$\beta \equiv 16\pi G\eta \quad (2.25)$$

between the GW damping rate (β) and DM viscosity (η). Recently a method of measuring the viscosity of DM in cosmological context has been suggested [495] and implemented on the current eleven GW events released by LIGO and Virgo Collaborations (on the assumption that DM in the Universe is treated as perfect fluids). When the GW damping rate is taken into account, the viscosity-free luminosity distance (D_L) inferred from the standard siren GW signal will be modified to

$$D_{L,eff}(z, \beta) = D_L(z) e^{\beta D(z)/2}, \quad (2.26)$$

where $D_{L,eff}$ and D represent the so-called effective luminosity distance and comoving distance, respectively. However, such strategy is hard to realize from the observational point of view, considering the failure of precise measurement of viscosity-free distances and redshift determination for inspiraling and merging binary black holes (BH). This motivates the need to probe the viscosity of DM with other plausible mechanisms.

In order to draw firm and robust conclusions about the non-gravitational behavior of DM, [475] proposed a new strategy to measure the viscosity of DM with strongly lensed GWs produced by the inspiralling NS. GWs damped by viscosity from a neutron star merger

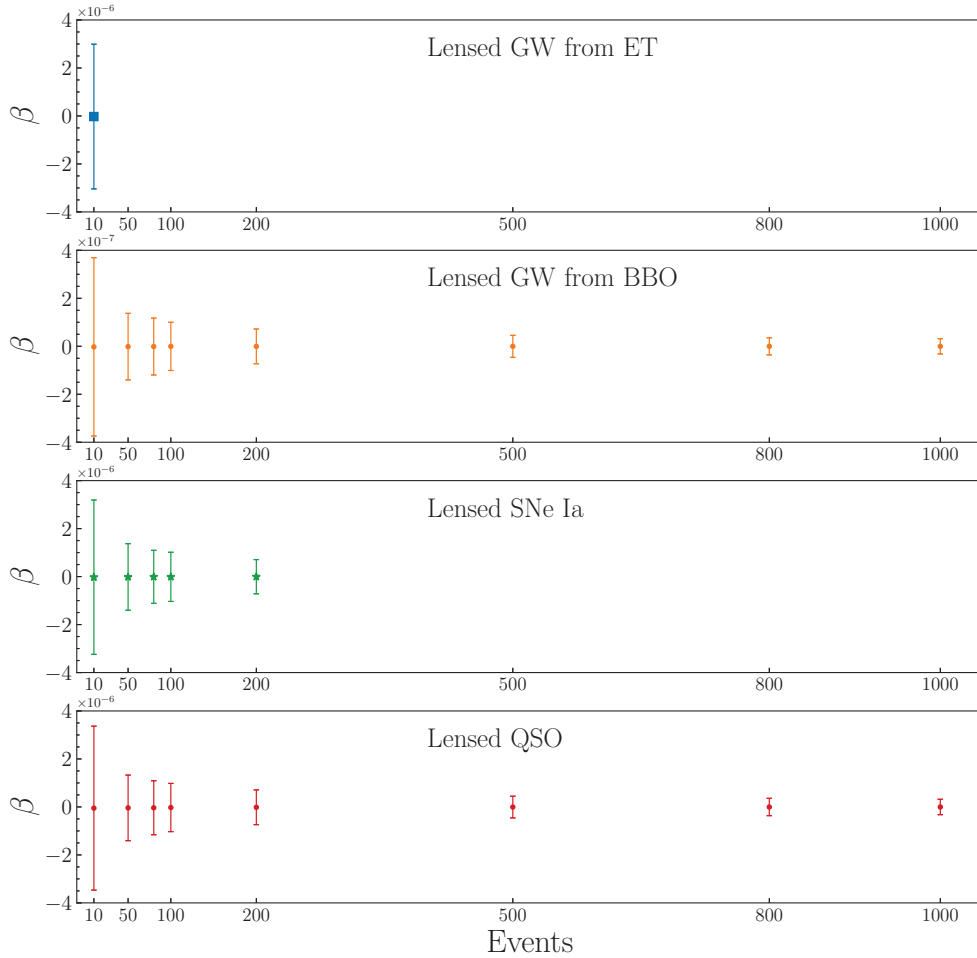


Figure 8. Constraints on the viscosity of DM with different number of strongly lensed transients: the results of the GW damping rate based on the studies of [475]. Copied from Ref. [475] with permission.

would reach the observer, with the generation of electromagnetic radiation from a short and intense burst of γ rays. One should note that besides electromagnetic counterparts, the identification of host galaxies for the majority of GW events could also contribute to unique redshift determination in the EM window. Our idea relies on the time-delay distance in a specific GW-galaxy strong lensing system (with the background GW source at redshift z_s and the lensing galaxy at redshift z_l)

$$D_{\Delta t}(z_l, z_s) \equiv \frac{D_A(z_l)D_A(z_s)}{D_A(z_l, z_s)}, \quad (2.27)$$

which could be measured precisely and accurately for time-variable GW sources, due to the

well-reconstructed Fermat potential difference ($\Delta\phi_{i,j}$) between multiple GW signals

$$\Delta t_{i,j} = \frac{D_{\Delta t}(1+z_l)}{c} \Delta\phi_{i,j}. \quad (2.28)$$

More importantly, besides the configuration of multiple signals that could be used to derive cosmological distances [496–498], the time difference ($\Delta t_{i,j}$) in the arrival times of two signals (at angular coordinates θ_i and θ_j on the sky) can also be measured with unprecedented accuracy [471], which are not affected by GW damping effect and DM viscosity. Such advantage of strongly lensed GW signals have been widely discussed concerning fundamental physics [470], cosmology [499], and dark matter [500]. In this analysis, the measured time-delay distance [Eq. (2.27)] from each strongly lensed GW (unaffected by viscous DM damping) is calibrated with the effective luminosity distances of unlensed GW signals (affected by viscous DM damping) [Eq. (2.26)].

Can the time delays be measured with sufficient precision to yield the viscosity of DM? To determine the answer, we evaluate the performance of the third-generation ground-based GW detectors, like the Einstein Telescope (ET) [501] and space-based detectors, like the Big Bang Observer (BBO) [502] and DECihertz Interferometer Gravitational wave Observatory (DECIGO) [503]. The simulations process of different GW samples follows the procedure presented in [499, 504], based on the redshift distributions of unlensed and lensed double compact objects (DCO) from the conservative SFR function [468, 505, 506]. For each specific GW event, the uncertainties of different observables (time delays, lens modeling, the line of sight contamination, etc.) will be propagated to the uncertainty of different distances ($D_{\Delta t}, D_{L,eff}$). For only 10 strongly lensed GWs from ET, the GW damping rate can be constrained to the precision of $\Delta\beta = 10^{-6} \text{ Mpc}^{-1}$. Such analysis will be significantly improved to $\Delta\beta = 10^{-8} \text{ Mpc}^{-1}$ with 1000 strongly lensed GW events detected by the BBO. More interestingly, such stringent measurements of GW damping in a viscous Universe provides another perspective to the scatter cross-section of self-interacting DM (σ_χ/m_χ):

$$\frac{\sigma_\chi}{m_\chi} = \frac{6.3\pi G \langle v \rangle}{\beta}. \quad (2.29)$$

Note that [507] recently reported a unified solution to small-scale structure from dwarfs to clusters, in which DM particles interact with each other following a hydrodynamic description and Maxwellian distribution [508]. Compared with the current operating GW detectors (LIGO and Virgo network), the third generation ground-based ET would yield more precise measurements of DM SI cross-section, especially for DM in galaxy clusters ($\Delta(\sigma_\chi/m_\chi) \sim 10^{-3} \text{ cm}^2/\text{g}$). Within the reach of the second generation space-based BBO (with more detected lensed GW events at much higher redshifts ($z \sim 5$)), both of galaxy-scale and cluster-scale DM SI are expected to be detected at high confidence levels: $\Delta(\sigma_\chi/m_\chi) \sim 10^{-6} \text{ cm}^2/\text{g}$ for dark matter in dwarf galaxies and low-surface-brightness galaxies, and $\Delta(\sigma_\chi/m_\chi) \sim 10^{-5} \text{ cm}^2/\text{g}$ in galaxy clusters. As can be clearly seen from the comparison between strongly lensed transient sources in GW and EM domain [supernovae (SNe) Ia or quasars] [Fig. 8], such recipe for measuring the viscosity of DM at different scales could helpfully alleviate the strong conflict between the collisionless CDM paradigm and N-body simulations of the small-scale structures of the Universe (known as the cusp-vs-core problem, the missing satellite problem, and the too-big-to-fail problem) [509].

2.5 Standard siren cosmology

Using GWs to measure the Hubble constant had been proposed by Schutz [510] in 1986. This feature of GWs benefits from the fact that one can infer the luminosity distance directly from the GW waveform without the external calibration, which is unavoidable in the utilization of SNe Ia as standard candles. As GW detections can be thought of as aural rather than optical, a more appropriate terminology for a GW standard candle is a “standard siren” [511]. The standard sirens rely on a very clear underlying physics, i.e., GR. The radiation emitted during the inspiral phase is well described using the post-Newtonian expansion of GR [512]. On the contrary, SNe Ia standard candles are poorly understood in physics and systematics [513, 514].

However, one disadvantage of the standard sirens is the missing redshift information which is completely entangled with the mass and frequency parameter in the waveform. For using standard sirens to investigate cosmology, one needs the redshift information from an independent strategy. The most promising way is from the EM counterparts associated with the GWs. We call this type of standard sirens “bright sirens”. For instance, it has long been argued that BNSs and NS-BH mergers are likely to be accompanied by a gamma-ray burst (GRB) [515–518]. The applications of using short GRBs as the EM counterparts of GW standard sirens on cosmology were investigated in details in [519–523]. The GRB counterpart to the GW source can not only provide a precise sky localization, which is useful for determining the redshift to the source galaxy, but also significantly improve the GW determination of luminosity distance by breaking the degeneracies between distance, position, and orientation angles. Thus it can measure the expansion history of our Universe back to redshift up to around 2 [521, 522].

The first joint observations of GW from a BNS GW170817 with its EM counterpart GRB 170817A [2, 524, 525] mark a significant breakthrough for multimessenger astronomy. By identifying the host galaxy NGC 4993, the first measurement of the Hubble constant from standard sirens has been reported [526]. Recently, [527] reported the first plausible optical EM counterpart to a (candidate) BBH merger GW190521, detected by the Zwicky Transient Facility (ZTF). The corresponding measurements of the Hubble constant and other cosmological parameters have also been investigated [528, 529]. Though at the present stage they cannot resolve the Hubble tension due to the large uncertainty, the future second-generation GW detector network LIGO-Hanford+advanced LIGO-Livingston+advanced Virgo+KAGRA+LIGO-India (HLVKI) could provide a much tighter constraint [530].

In addition to BNS, the massive black hole binaries (MBHBs) are assumed to produce observable EM emissions at the merger from the production of an optical accretion-powered luminosity flare, and also the radio flares and jets. The EM emissions is based on results from general-relativistic simulations of merging MBHBs in an external magnetic field [531]. Several studies found that MBHBs could emit radiation in different bands of the EM spectrum both at merger and during long-lasting (ranging from weeks to months) afterglows [532, 533]. Moreover, pre-merger EM observational signatures could even be spotted during their inspiral phase [534–537]. The standard sirens of MBHB detected with future space-based detector LISA on cosmology have been investigated [538–543]. Compared to the BNS standard sirens with the ground-based detector, the MBHB standard sirens with a space-based detector can approach redshift up to 6–7, thus measuring the expansion history of Universe back to a much earlier time [540].

The bright sirens not only could measure the expansion history of our Universe, thus constraining such as the Hubble constant and the dark-energy equation of state, but also test

gravity theories. For instance, the GW170817 with its EM counterparts has put a very tight constraint of the speed on GW, $(c_T - c)/c < \mathcal{O}(10^{-15})$ [525]. It has a very strong implication on dark energy model and modified gravity theory [544–550] or even some dark matter model [551]. In addition to the speed of GW, the bright sirens can constrain the modified gravity theory from the propagation of GW in the cosmic distance. Several studies have shown the potential of the BNS and MBHB standard sirens on testing GR through GW propagation from the ground/space-based GW detectors [552–562].

With advanced LIGO and advanced Virgo reaching their target sensitivity, and other detectors such as Kamioka Gravitational wave detector (KAGRA) and LIGO-India joining the search in the near future, the second-generation ground-based detector network HLVKI would be in operation. On a longer timescale, around the 2030s the third-generation ground-based detectors, such as ET [7] and CE [8], and the space interferometer LISA will be ready for operation. During the same period, Chinese space-based GW detectors Taiji [11–13] [proposed by the Chinese Academy of Sciences (CAS)] and TianQin [17–19] [proposed by the Sun Yat-Sen University (SYSU)] will be launched. The synergic operation of these GW networks would contribute greatly on cosmology and the test of GR [530, 561, 563–568].

Bright sirens

In this subsection, we wish to highlight some work of using GWs with EM counterparts as bright sirens to probe the evolution of the universe and test GR.

- For forecasting the ability of third-generation ET on constraining the cosmological parameters such as Hubble constant, matter density and the dynamics of dark energy, [523] simulated a series of GW standard sirens of BNS and NS-BH with short GRB as the EM counterparts. Using the inspiral phase of waveform which is computed in the post-Newtonian formalism up to 3.5 PN, the Signal-to-Noise-Ratio (SNR) can be calculate from the matched filtering with an optimum filter in the ideal case of Gaussian noise,

$$\rho^2 = \frac{5}{6} \frac{(G\mathcal{M}_c)^{5/3} \mathcal{F}^2}{c^3 \pi^{4/3} d_L^2(z)} \int_{f_{\min}}^{f_{\max}} df \frac{f^{-7/3}}{S_n(f)}, \quad (2.30)$$

here \mathcal{M}_c is the redshifted chirp mass $\mathcal{M}_c = (m_1 m_2)^{3/5} / (m_1 + m_2)^{1/5} (1 + z)$. d_L is the luminosity distance. $S_n(f)$ is the one-sided noise power spectral density (PSD) of the detector. The factor \mathcal{F} is to characterize the detector response, $\mathcal{F}^2 = \frac{(1 + \cos^2 \iota)^2}{4} F_+^2 + \cos^2 \iota F_\times^2$. F_+ and F_\times are the antenna response functions to the GW + and \times polarizations. One can easily estimate the uncertainty of the inferred luminosity distance from the Fisher information matrix. In that work, the authors considered the beam feature of short GRB which can help to break the degeneracy between inclination angle ι and luminosity distance d_L . But they still give a conservative estimation of $\sigma_{d_L}^{\text{inst}} = 2d_L/\rho$ from the instrument together with the weak lensing uncertainty $0.05zd_L$. From these distance uncertainties and the merger rate distributions of BNS and NS-BH, the authors simulated 100-1000 standard sirens from ET. Then they adopted the Markov chain Monte Carlo (MCMC) approach to constrain the cosmological parameters H_0 and Ω_m under the baseline Λ CDM model. From the nonparametric Gaussian (GP) process regression method, they reconstructed the equation of state of dark energy $w(z)$ in the redshift range 0–1. The results showed that with about 500-600 GW events from ET one can constrain the Hubble constant with precision comparable to Planck 2015 results. Using GP and with 1000 GW events, one can constrain $w(z)$ with an error of 0.03 in the low redshift region. This work gave an impression of what we can do with

the mock future standard sirens to constrain the cosmological parameters by different data interpretation techniques.

- The interaction between dark energy and DM is a very crucial problem to understand the nature of the dark sector of our Universe. [543] performed a forecast analysis of the ability of the LISA space-based interferometer to reconstruct the dark sector interaction using MBHB standard sirens at high redshift. Using the MBHB catalogs constructed from three different astrophysical scenarios (i.e., light-seeds popIII, heavy-seeds with time delay Q3d and without time delay Q3nod) for the evolution of massive black hole mergers based on the semi-analytic model [569], this work constructed the catalogs of MBHB standard sirens by LISA, with an electromagnetic counterpart detectable by future telescopes. Then the authors employed Gaussian process methods to reconstruct the dark sector interactions in a nonparametric way,

$$q = 2 \left(\frac{3D''^2}{D'^5} - \frac{D'''}{D'^4} \right) (1+z)^2 + 4 \frac{D''}{D'^4} (1+z), \quad (2.31)$$

where D is the normalized comoving distance $D = H_0 d_L / (c(1+z))$. $q \equiv Q/H_0^3$ is the dimensionless interacting term between the matter and vacuum energy. The continuity equations for DM and the vacuum energy are $\dot{\rho}_m + 3H\rho_m = -Q$ and $\dot{\rho}_v = Q$. Using MBHB standard siren alone, LISA can reconstruct the interaction well from $z \sim 1$ to $z \sim 3$ (for a 5 years mission) and to $z \sim 4$ or even $z \sim 5$ (for a 10 years mission). When combined with the simulated Dark Energy Survey (DES) SNe Ia datasets, the low redshift below 1 can be also covered and reconstructed well. These results suggested that MBHB standard sirens from LISA are a very promising tool to test and constrain possible deviations from the standard Λ CDM dynamics, especially at high redshift.

- The cosmic anisotropy with a dipole amplitude have been constrained with CMB, SNe Ia and large scale structure data sets [570–574]. GW standard sirens as excellent indicators of the cosmic distance are very suitable for the test of anisotropy of our Universe. [575] simulated a series of standard sirens of BNS and NS-BH from ET and DECIGO, and of MBHBs from LISA. These standard sirens can be used as a probe of the cosmic anisotropy with a dipole form

$$d_L(\hat{z}) = d_L^0(z)[1 + g(\hat{n} \cdot \hat{z})], \quad (2.32)$$

where they parameterized the dipole modulation simply by its amplitude g and direction \hat{n} given by $\hat{n} = (\cos \phi \sin \theta, \sin \phi \sin \theta, \cos \theta)$. d_L^0 is the isotropic luminosity distance calculated from the fiducial cosmology. Thus it is very straightforward to adopt MCMC to constrain the amplitude and direction of the dipole anisotropy from the mock GW data generated with different sky locations. The results of this work can be summarized as follows. For LISA, the cosmic anisotropy can be detected at 3σ C.L. if the dipole amplitude is larger than 0.03, 0.06, and 0.025 (for MBHB seed models Q3d, pop III, and Q3nod, respectively). In the meanwhile, the dipole direction can be constrained roughly around 20% at 2σ C.L.. For ET with no less than 200 GW events, one can detect the cosmic anisotropy at 3σ C.L. if the dipole amplitude is larger than 0.06, and the dipole direction can be constrained within 20% at 3σ C.L. if the dipole amplitude is about 0.1. For DECIGO with no less than 100 GW events, the cosmic anisotropy can be detected at 3σ C.L. for dipole amplitude larger than 0.03, and the dipole direction can even be constrained within 10% at 3σ C.L. if dipole amplitude is larger than 0.07. This work manifested the potentials of using the standard sirens approach in the the detection of the cosmic anisotropy.

- Recent work has shown that the modified GW propagation can be used as a powerful probe of dark energy and modified gravity. In theories where GR is modified on cosmological scales, from standard sirens we do not measure the same luminosity distance as electromagnetic probes. The general models of modified gravity that pass the speed-of-gravity test still can modify the friction term of the equation of motion of GW,

$$h_A'' + 2[1 - \delta(\eta)]\mathcal{H}h_A' + k^2 h_A = 0. \quad (2.33)$$

Here $\delta(\eta)$ is used to denote the deviation from GR. Then one can show, from the canonical inference of the GW amplitude, the luminosity distance is actually

$$d_L^{\text{gw}}(z) = d_L^{\text{em}}(z) \exp \left\{ - \int_0^z \frac{dz'}{1+z'} \delta(z') \right\}. \quad (2.34)$$

In [562], the authors investigated using the technique of Gaussian processes to reconstruct the δ function by combining the GW luminosity distance from simulated joint GW-GRB detections with the electromagnetic luminosity distance from simulated DES data, without assuming any parameterizations. This work showed that from future HLVK and ET detectors, the δ function which denotes the deviation from GR in terms of the tensor propagation can be reconstructed very precisely with the Gaussian process.

- In addition to the second-generation ground-based network HLVKI, the third-generation ground-based ET+2CE and space-based LISA-Taiji networks have also been proposed and investigated. The synergy of the networks would not only improve the SNR thus detecting more GW events, but also help to measure the GW parameters more precisely. [568] constructed the catalogs of standard sirens with the joint GW+EM detections for 10 years detections of HLVKI, 5 years detections of ET+2CE, and 5 years of detections of LISA-Taiji, which are estimated to be available and released in the 2030s. With a combined Hubble diagram from these ground and space-based detector networks which can explore the expansion history of our Universe from redshift 0 to 7, as shown in figure 9. The author adopted several methodologies such as MCMC, Gaussian process, and Artificial Neural Networks to investigate the potential of future bright sirens on cosmology and modified gravity theory. The results show that the combined standard siren alone can constrain the Hubble constant at the precision level of 0.34%, 1.76 times more tightly than the current most precise measurement from *Planck*+baryon acoustic oscillation (BAO)+Pantheon. The joint standard siren with current EM experiments will improve the constraints of cosmological parameters significantly. The modified gravity theory can be constrained with 0.46% error from the GW propagation. This work showed the bright sirens in the 2030s are powerful probes of cosmology and gravity theory in addition to the traditional EM experiments.

Standard sirens combined with other cosmological probes

In the above part, several examples of using GW standard sirens to explore the cosmic evolution and test gravity theories are provided; but the focus is on the cases of solely using the standard sirens as a cosmological probe. Actually, the more important role that the GW standard sirens will play in the exploration of the universe in the future relies on the fact that once they are combined with other EM cosmological probes, the degeneracies between cosmological parameters can then be well broken. Thus, from a perspective of comprehensive analysis on cosmology, GW standard sirens would provide an extremely important cosmological probe to precisely measure cosmological parameters in the next decades. In the

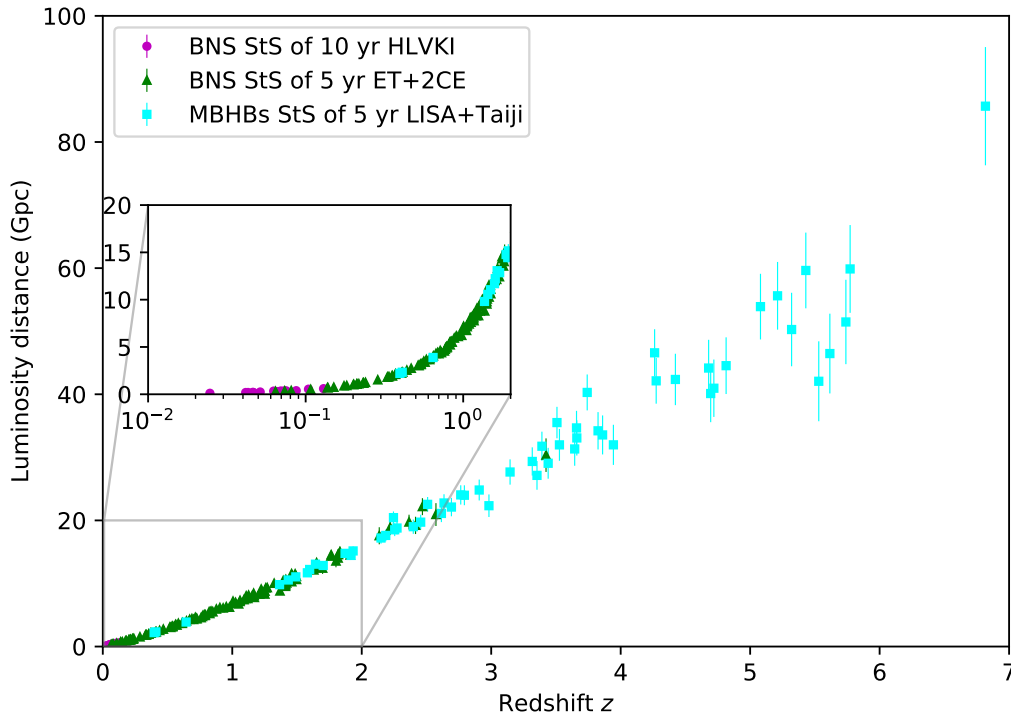


Figure 9. The Hubble diagram of one realization of mock standard sirens from future GW detector networks. Copied from [568] with permission.

following, we shall focus on the discussions on the role that standard sirens would play in precisely measuring cosmological parameters in synergy with other cosmological probes.

Precisely measuring cosmological parameters has always been one of the most important tasks in cosmology because almost all the important scientific questions in cosmology are relevant to precision measurements of cosmological parameters. Currently, there are two main problems concerning the measurements of cosmological parameters: (i) tensions appear between the early and late universe observations [241, 576–579]. For example, for the Hubble constant H_0 , the Planck- Λ CDM results [241] are in significant tension with the local measurements (which prefer a higher value) [580]; (ii) in the extended cosmological models (beyond Λ CDM), extra cosmological parameters (from “new physics”) cannot be tightly constrained by current cosmological observations, since parameter degeneracies are usually serious. For example, dark-energy equation of state (EoS) w , total neutrino mass $\sum m_\nu$, and other extra parameters still cannot be well constrained by the current observations [581–591], due to the strong parameter degeneracies. Since GW standard sirens can measure absolute cosmological distances, they can be used to effectively break the parameter degeneracies existing in the constraints from the traditional EM cosmological observations [592]. Hence, it can be expected that GW standard siren observations could play an important role in precisely measuring cosmological parameters. Next, we highlight some work concerning using GW standard sirens to break cosmological parameter degeneracies.

- In Refs. [593–602], a series of analyses have been made for the cosmological parameter

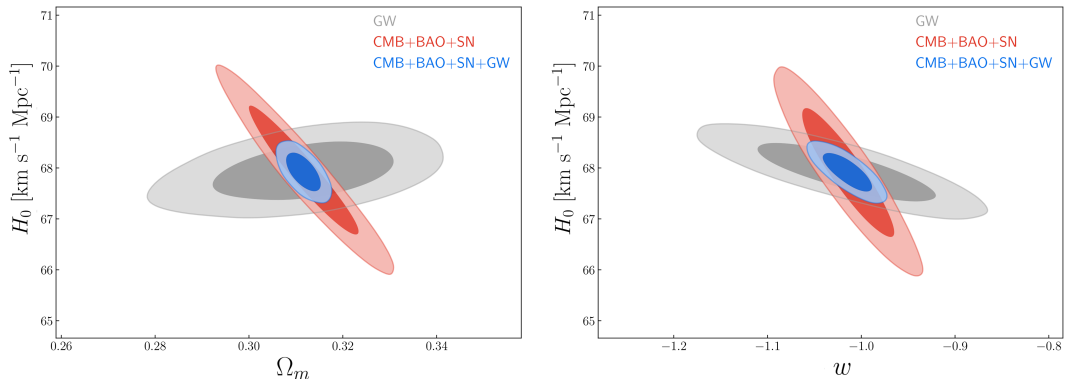


Figure 10. Two-dimensional marginalized contours (68.3% and 95.4% confidence level) in the Ω_m - H_0 and w - H_0 planes for the w CDM model, by using the data of GW, CMB+BAO+SN, and CMB+BAO+SN+GW. Here, GW represents 1000 standard sirens of BNS mergers simulated for CE's 10-year observation. Copied from Ref. [602] with permission.

estimation in various dark energy models using the combination of GW and EM observations (e.g., CMB, BAO, and SN). These analyses show that standard sirens alone cannot provide very tight constraints on the cosmological parameters except H_0 , but the combination of GW and EM observations can effectively break the parameter degeneracies and thus greatly improve the constraint accuracies. For example, Jin *et al.* [602] find that the future GW standard siren data from CE can well break the cosmological parameter degeneracies generated by the EM observations, as shown in Figure 10 (1000 simulated standard siren data are used). When adding the GW data to the data combination of CMB+BAO+SN, the constraint precisions of Ω_m and H_0 could be improved from 1.59% and 0.49% to 0.71% and 0.21%, respectively, in the Λ CDM model; the constraint precision of w can be improved from 3.15% to 1.68% in the w CDM model. The standard siren observation can also be combined with the fast radio burst observation to provide an independent low-redshift probe [603].

- The work discussed above focus on the standard sirens of using the GWs emitted by BNSs, now we turn to the scenario with the GWs emitted by MBHBs. We have mentioned that MBHB mergers are expected to produce powerful EM radiation [531, 535, 569, 604, 605] and thus one can determine the redshifts of the sources through identifying the EM counterparts. If GW detectors can locate the positions of sources within 10 deg², it can reach the same orders of magnitude as the fields of view of the Vera C. Rubin Observatory (formerly LSST) [606], the European Extremely Large Telescope (E-ELT) [607], and the SKA [608], making it possible to identify EM counterparts. In Ref. [540], the authors show that the number of events that EM counterparts can be observed is only a few dozen within the 5-year observation. Even so, the high-redshift MBHB standard siren data would provide an important supplement to low-redshift observations. In Ref. [609], Zhao *et al.* take the Taiji mission as a representative to study the capability of space-based GW detection of breaking the degeneracies of cosmological parameters. As shown in Figure 11, although the Taiji data alone cannot constrain cosmological parameters well enough, it can effectively

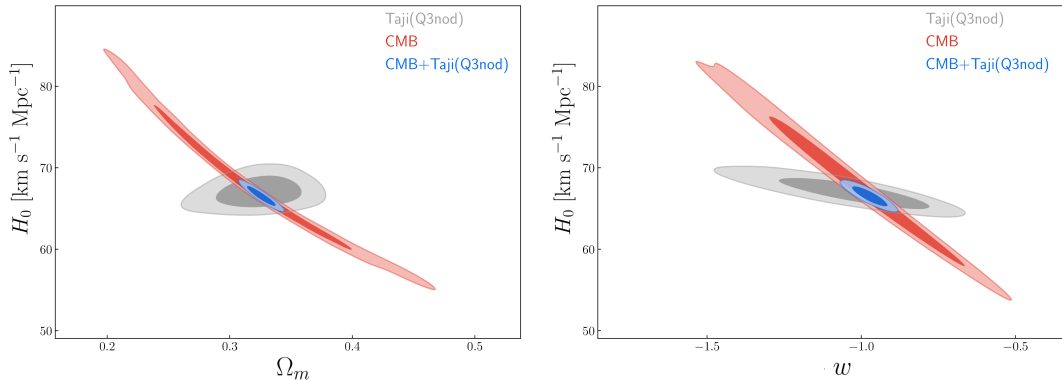


Figure 11. Two-dimensional marginalized contours (68.3% and 95.4% confidence level) in the Ω_m – H_0 and w – H_0 planes for the w CDM model, by using the data of Taiji, CMB, and CMB+Taiji. Here, Taiji represents the simulated standard sirens of MBHB mergers detected by the Taiji mission (5-year observation) based on the Q3nod model. Copied from Ref. [609] with permission.

break the parameter degeneracies inherent in the CMB data, thus greatly improving the constraint accuracies of parameters. For example, for the constant dark-energy EoS w , the data combination of Taiji+CMB can constrain it to an accuracy of 4%, which is comparable to the result of about 3%–4% from the CMB+BAO+SN data combination. In addition, Wang *et al.* [610] also conduct a similar analysis on TianQin and reach the same conclusion.

- Moreover, the space-based GW observatories, such as LISA, Taiji, and TianQin, could form a space-based GW detection network in the future [564]. In Ref. [564], Ruan *et al.* find that the LISA-Taiji network may achieve four orders of magnitude improvement on the source localization (solid angle increased by three orders and luminosity distance increased by one order) compared to the single detector. The improvement by the LISA-Taiji network compared to the single Taiji mission in constraining cosmological parameters is discussed in Ref. [567]. It is shown that, even in the conservative scenario where only the inspiral phase is used to locate GW sources, the constraint precision of H_0 could reach 1.3% by solely using the standard sirens from the LISA-Taiji network. Moreover, the CMB+network data could improve the constraint on w by 56.7% compared with the CMB+Taiji data, and the constraint precision of w reaches about 4%, which is comparable with the result of CMB+BAO+SN. We can conclude that the GW detection network composed of multiple space-based GW observatories will play an important role in understanding the nature of dark energy in the future.

- Actually, for the dark-energy EoS parameter, using the $d_L - z$ relation to constrain $w(z)$ will lead to information loss due to the two integrals in the expression of distance relating to $w(z)$. In Ref. [611], the authors use the multi-messenger (GW standard sirens) and multi-wavelength (optical band, ELT; radio band, SKA) observations to probe the nature of dark energy through direct measurements of the Hubble parameter $H(z)$. As shown in Figure 12, each of these three observations cannot constrain H_0 and Ω_m well, but the combination of them can effectively break the parameter degeneracies. For the dark-energy EoS parameters

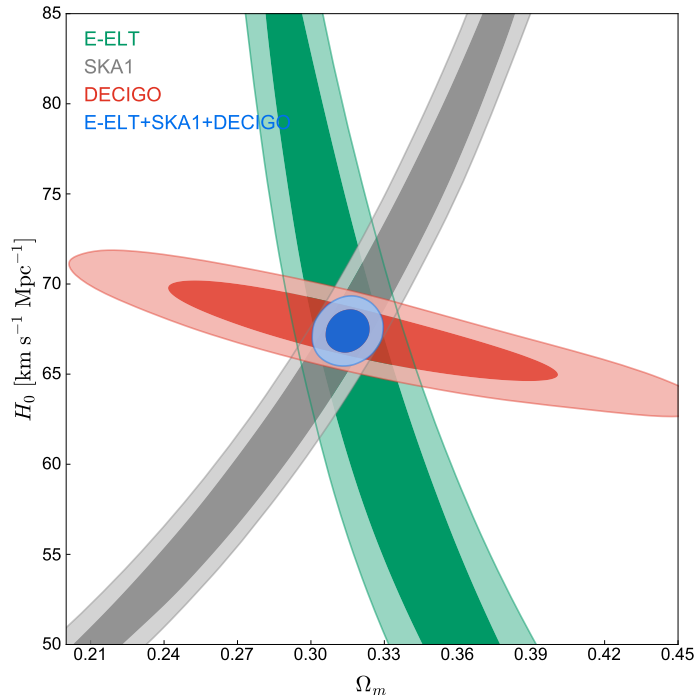


Figure 12. Two-dimensional marginalized contours (68.3% and 95.4% confidence level) in the Ω_m – H_0 plane for the Λ CDM model from E-ELT, SKA1, DECIGO, and E-ELT+SKA1+DECIGO. Here, DECIGO represents the simulated standard sirens of BNS mergers detected by the DECihertz Interferometer Gravitational wave Observatory (1-year observation). Copied from Ref. [611] with permission.

in the w CDM and CPL models, the authors find that the joint data analysis gives better constraints than the results of CMB+BAO+SN. It is concluded that future GW observations combined with other EM observations will provide great help in revealing the nature of dark energy.

Dark sirens

The results above are derived based on the analyses in which EM counterparts of GW sources are assumed to be directly detected. Actually, even without EM counterparts, the corresponding redshift information of GW sources can still be acquired with a galaxy catalog using Bayesian inference [530, 612–615]. By using the BBH detections from the first and second observing runs of the Advanced LIGO–Advanced Virgo detector network, the joint standard siren–dark siren measurement on H_0 is improved by about 4% over the result from GW170817 [616]. Some other GW-only standard siren analyses are also made assuming that the properties of the source population are known, such as the mass distribution of compact binaries [617–621] or the EoS of neutron star [622–624]. The dark siren method can be used to examine the results from standard sirens alone and to extend the application potential of GWs in cosmology.

In [565], the authors investigated the potential of using dark sirens from the LISA–Taiji network to measure the Hubble constant. Inspired by the fact that the LISA–Taiji network can improve the localization of the GW sources significantly, which is very helpful for the identification of host galaxy and thus obtaining the redshift information of dark sirens.

Considering 3 different massive black hole formation models with different black hole seedings and time delays, it is showed that within a 5-year operation time, the LISA-Taiji network is able to constrain H_0 to within 1% accuracy and possibly beats the scatters down to 0.5% or even better.

In conclusion, the GW standard siren observation can directly measure the absolute distance, which is very important for the study of cosmology. If the EM counterparts of GW events can be identified, the $d_L - z$ relation can be established to constrain the cosmological parameters. The multi-messenger standard sirens alone can accurately measure the Hubble constant, but they cannot provide precise measurements for other parameters, such as the EoS of dark energy. Nevertheless, according to a series of studies, we find that the combination of GW standard sirens and EM observations can effectively break the parameter degeneracies and thus greatly improve the constraint accuracies. In the next two decades, multi-band GW observations combined with the optical, near-infrared, and radio observations will usher in a new era of cosmology.

3 GW astrophysics

The detection of GWs by ground-based GW observatories has opened a new window to probe various astrophysical GW sources. The main astrophysical GW sources include the stellar compact binaries [SCBs; double-white-dwarfs (DWDs), NS-WD binaries, BNSs, NS-BH binaries, BBHs, etc.], SMBBHs, EMRIs, and so on. GW observations can provide rich information for investigating the formation and evolution of these sources, which may not be able to obtain only by EM observations. We mainly focused on investigating the formation and evolution of these SCBs and SMBBHs across the cosmic time, the physical processes involved in their formation and evolution, the observation/detection (methods) of the EM signatures and GWs radiated from these sources, and the implications of their GW and EM observations.

We have made significant progress in various aspects of GW astrophysics in the past several years. For example, we have carefully studied the evolution of NS-WD binaries, especially on the orbital evolution of ultra-compact X-ray binaries and its GW radiation [625, 626]. We have investigated in details about the EM properties of BNS and NS-BH mergers and the constraints on the merger products and equation of state (EOS) of NSs that can be obtained from both GW and EM observations of GW170817, the first GW source with multi-wavelength EM counterparts detected [627–631]. We have studied the formation and evolution of stellar BBHs (sBBHs) and BNSs and its relation to the properties of the host galaxies of BBH mergers [632], and we predicted the SGWBs resulting from sBBHs and BNSs [633]. We have helped to organize the Chinese PTA (CPTA) collaboration to search for nano-Hertz GW radiation and have been collecting data through FAST and other radio telescopes in China. We have performed serial work on the solar system ephemeris (SSE) by using PTA data [634, 635], which is necessary for further extract GW signals from the CPTA observations. We have investigated the detection of individual SMBBHs by current and future PTAs and its possible cosmological application to constrain cosmological parameters [636–638]. We have found a number of SMBBH candidates [639, 640], investigated the detailed observational properties of some SMBBH candidates [641, 642], and introduced several new methods to identify BBH candidates and distinguish it from alternative interpretations [643–646], investigated the cosmic evolution of SMBBHs and predicted the SGWBs resulting from inspiralling SMBBHs and SMBBH merger rate [647].

Below we highlight some of our recent work, ranging from the evolution of NS-WD/ultra-compact binaries in the Milky Way, the detected BNS GW170817, solar system ephemeris (SSE) for PTA GW observations, GW background and SMBBH observations by future PTAs, SMBBHs searching and its PTA detection, to the estimation of SGWBs.

3.1 Orbital evolution of NS – Roche-Lobe filling WD binaries and their GWs

Neutron star (NS)-white dwarf (WD) binaries may have extremely short orbital periods and radiate GWs in the frequency range of $10^{-4} - 1$ Hz. These compact binaries are therefore of interest for the GW detections of LISA [648, 649], Taiji [650], and TianQin [651]. The model of a NS accreting a Roche-lobe filling (RLF) WD companion with orbital period in the range of $\sim (10 - 80)$ minutes can well explain the observed properties of ultracompact X-ray binary stars (UCXBs), whilst the model of a NS plus a low-mass RLF He star may also be one of the formation channels of UCXBs (e.g., [652]). Recently, UCXBs are also proposed to be dual-line GW sources for both LISA-like and LIGO-like detectors (e.g., [653, 654]). Measurement of the GW signals generated by the UCXBs and NS-WD binaries will allow us to infer their orbital parameters (masses, orbital separations and eccentricities), which can provide important information and clues to understand their chemical composition, magnetic activities, tidal interaction, as well as the mass transfer process, common envelope evolution, spatial distribution and so on (e.g., [626, 653, 655–657]).

We studied the effects of mass transfer and GW radiation on the orbital evolution of NS-RLF WD binaries, and the detectability of these binaries by space GW detectors (e.g., LISA; Taiji; TianQin) in a recent work [626]. The GW frequency generated by a circular orbit binary, with WD mass $\sim 0.05 - 1.4M_{\odot}$, is in the range of $\sim 0.0023 - 0.72$ Hz when the Roche lobe overflow is just onset, weakly depending on the NS mass. We find that high-mass NS-WD binaries may undergo direct coalescence after unstable mass transfer if the mass of the WD component $m_{\text{wd}} \gtrsim 1.25 M_{\odot}$. If the WD mass $m_{\text{wd}} < 1.25 M_{\odot}$, NS-WD binaries may avoid direct coalescence because mass transfer after contact can lead to a reversal of the orbital evolution. The orbital evolution of the well-known UCXB source 4U 1820–30 can be well explained in details by using the NS-RLF-WD binary model with component masses of $(1.0 + 0.065)M_{\odot}$. Assuming this model, the expected signal-to-noise-ratio (SNR) of 4U 1820–30 is $\sim 11.0/10.4/2.2$ by a 4-year observations of LISA/Taiji/TianQin with the designed sensitivities. For a $(1.4+0.5)M_{\odot}$ NS-WD binary close to contact, the expected SNR is $\sim 27/40/28$ for a 7-days observation by LISA/Taiji/TianQin. For NS-WD binaries with masses of $(1.4+ \gtrsim 1.1)M_{\odot}$, the significant change of GW frequencies and amplitudes may be measurable, and thus it is possible to determine the binary evolution stage. At distances up to the edge of the Galaxy (~ 100 kpc), high-mass NS-WD (e.g., $\sim (1.4 + 0.5)M_{\odot}$) binaries will be still have $\text{SNR} \gtrsim 1$. This suggests that the direct coalescence events of NS-WD binaries in the Galaxy, if any, may be detected by LISA/Taiji/TianQin in the future.

In order to compare the GW signals from different type of sources in the Galaxy, we have also calculated the GW characteristic strain of some other UCXB sources with known distances and orbital parameters, detached double white dwarfs, AM CVn stars, and hot-subdwarf binaries, and show them Fig. 13 [626] with the sensitivity curves of the proposed space GW detectors LISA, Taiji, and TianQin, as well. We have also investigated the influences of eccentricities of NS-WD binaries on their GW signals. Our results indicate that the NS-WD binaries with high eccentricities evolve faster than those with low ones, and with increase of the eccentricity, the GW harmonics gradually emerge. As an example, Fig. 14 shows the evolution of the power spectrum distributions (PSD) of $(1.4 + 1.25)M_{\odot}$ NS-WD

binaries, with eccentricities of $e = 0.0$ (panel a), 0.1 (panel b), 0.3 (panel c), and 0.5 (panel d), respectively, as a function of GW frequency and time, which would be compared with space-based GW observations to constrain the parameters in our models. We here take the initial orbital period approximately 30s.

3.2 Constraints on the neutron star maximum mass from GW170817

Depending on the size relationship between the merger remnant (gravitational) mass and the maximum mass of a single NS, a BNS merger can give a variety of post-merger products [658–662]: (1) a black hole (BH) by immediate collapse after the merger; (2) a differential rotation supported hypermassive NS (HMNS), which would survive $10 \sim 100$ ms before collapsing; (3) a rigid rotation supported supermassive NS (SMNS), which would collapse after the NS spins down; and (4) a stable NS (SNS). Before the detection of GW170817, it has been well discussed that binary neutron star (BNS) merger events could be used to constrain the maximum mass of a non-spinning neutron star, M_{TOV} (see Ref. [662] and references therein). With the observations of GW170817, we applied some EOS-independent universal relations for rapidly spinning NS to discuss the constraints one may pose on M_{TOV} . Here we briefly introduce our research methods and results (see Ref. [630] for details).

Given an EOS, one can derive its corresponding M_{TOV} by solving the Tolman-Oppenheimer-Volkoff (TOV) equations [663]. Rotation, either rigid or differential, could enhance the gravitational mass by a certain factor $\chi = (M - M_{\text{TOV}})/M_{\text{TOV}}$. One can define the maximum mass of a rotating NS as

$$M_{\text{max}} \equiv (1 + \chi_{\text{max}})M_{\text{TOV}}, \quad (3.1)$$

$$M_{\text{max,d}} \equiv (1 + \chi_{\text{d,max}})M_{\text{TOV}}, \quad (3.2)$$

where χ_{max} and $\chi_{\text{max,d}}$ are used to denote the maximum enhancement factors for uniform and differential rotations, respectively. Due to the change of rotation properties, the gravitational mass of the merger remnant will change with time. Here we define M_{rem}^0 as the remnant mass right after the merger, M_{rem}^k as the remnant mass when the NS starts to spin with a Keplerian rotation ($P = P_k$) and M_{rem}^∞ as the remnant mass with no rotation ($P = \infty$). When $M_{\text{rem}}^0 > M_{\text{max,d}}$, the post-merger product would be a BH by immediate collapse. Otherwise if $M_{\text{max}} < M_{\text{rem}}^k < M_{\text{rem}}^0 \leq M_{\text{max,d}}$, the post-merger product would be a HMNS and collapse into a BH after losing angular momentum as well as mass. If, however, $M_{\text{rem}}^k \leq M_{\text{max}}$, the merger remnant would first go through a HMNS phase and then form a uniformly rotating NS. In this case, when $M_{\text{rem}}^\infty > M_{\text{TOV}}$, the merger remnant would eventually collapse into a BH after the NS spins down; when $M_{\text{rem}}^\infty \leq M_{\text{TOV}}$, the remnant would never collapse. The total baryonic mass of the system should be conserved during the merger. We denote the baryonic mass of the remnant as M_b and the maximum baryonic mass for non-rotational NSs predicted by an EOS as $M_{b,\text{TOV}}$. In the uniformly rotating phase, we define χ_{col} and χ_{TOV} as the enhancement factors when SMNS collapses to BH and when $M_b = M_{b,\text{TOV}}$. Using *RNS* code, we find that, for selected EoSs with $2.08M_\odot < M_{\text{TOV}} < 2.78M_\odot$ (*SLy* [664], *WFF1* [665], *WFF2* [665], *AP4* [666], *Bsk21* [667], *AP3* [666], *DD2* [668], *MPA1* [669], *Ms1* [670], *Ms1b* [670]), χ_{col} and χ_{TOV} as functions of P , are almost independent on the EOS adopted, which could be expressed as,

$$\log \chi_{\text{col}} = (-2.740 \pm 0.045) \log \mathcal{P} + \log(0.201 \pm 0.005), \quad (3.3)$$

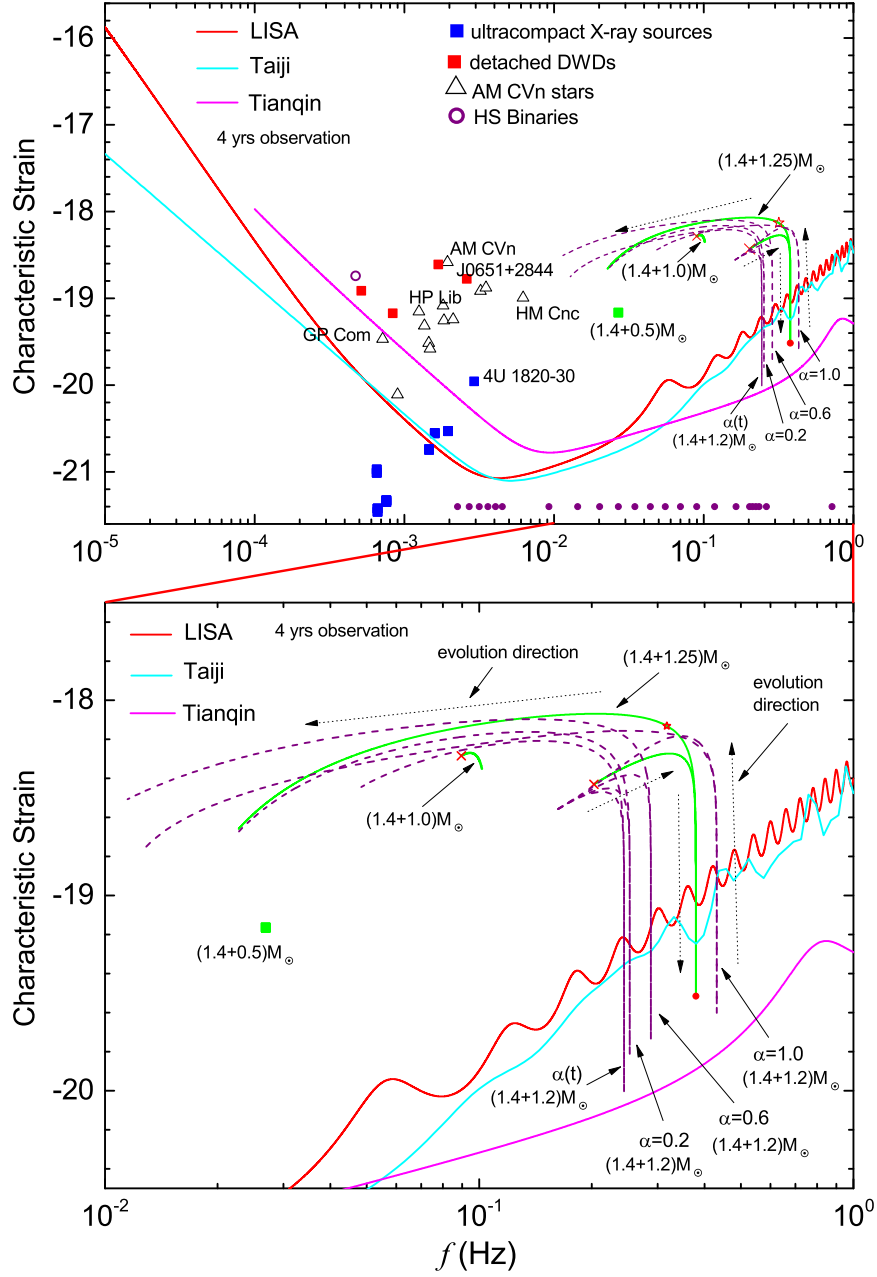


Figure 13. Top panel: GW characteristic strains of example NS-WD binaries (assuming a 4-year observation period). For comparison, the GW strains of the observed detached double WDs (red squares), AM CVn stars (open triangles), and hot subdwarf (HS) binaries (purple circles), are also plotted. Green squares and lines show the evolution track of NS-RLF-WD binaries with masses of $(1.4 + 0.5/1.0/1.25)M_{\odot}$, respectively. The red crosses on the two green lines denote the onset of the mass transfer. Purple dashed lines show the evolution of $(1.4 + 1.2)M_{\odot}$ binary with α being the accretion parameter (time-dependent in our model). Red solid circle and open star mark the points where the GW frequency reaches its maximum value and the mass loss rate reaches the peak value, respectively. The sensitivity curves of LISA, Taiji, and TianQin are shown by the red, cyan, and magenta lines, respectively. The row of purple points at the bottom denote the contact frequencies of NS-RLF-WD binaries with different WD masses. Enlarged bottom panel: the region $f = 0.01 - 1$ (Hz) and GW strain $= -20.5 - -17.5$ in the top panel is enlarged to show the evolution of massive NS-RLF-WD binaries more clearly. Copied from Ref. [626] with permission.

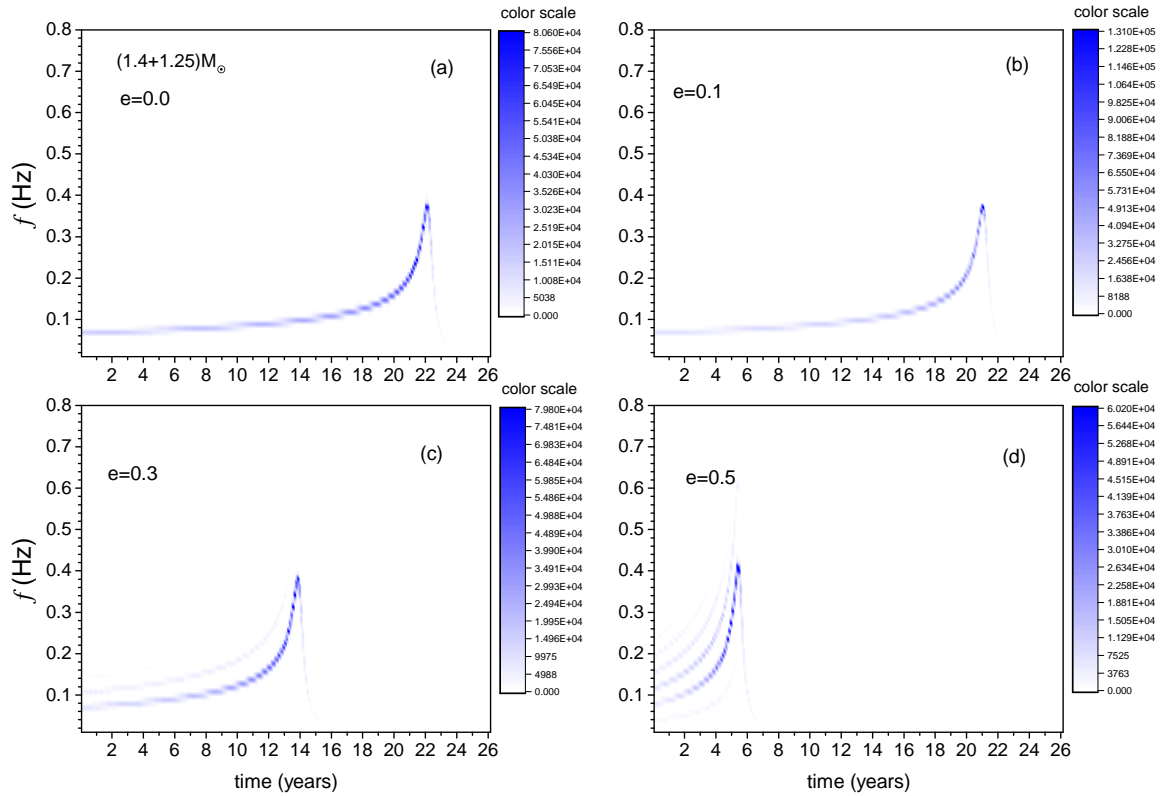


Figure 14. The arbitrary power spectrum distribution of $(1.4 + 1.25)M_{\odot}$ NS-WD with eccentricity $e = 0.0, 0.1, 0.3$ and 0.5 (panel (a)-(d)) as a function of GW frequency and evolution time. We here take the initial orbital period approximately 30s.

$$\begin{aligned} \log \chi_{\text{TOV}} = & (1.804 \pm 0.268)(\log \mathcal{P})^2 + (-3.661 \pm 0.190)\log \mathcal{P} \\ & + \log(0.101 \pm 0.007), \quad P > P_{k,\text{TOV}}, \end{aligned} \quad (3.4)$$

where $\mathcal{P} = P/P_{k,\text{min}}$ and $P_{k,\text{min}}$ is the minimum Kepler period for a uniformly rotating NS. When $P = P_k$, we have $\chi_{\text{col}}^k = \chi_{\text{max}} = 0.201 \pm 0.017(0.008)$ and $\chi_{\text{TOV}}^k = 0.046 \pm 0.008(\pm 0.004)$ with the errors indicating 2σ (1σ) confidence level, respectively. The enhancement factor of a SMNS at the time when differential rotation damps (χ^k) must satisfy $\chi_{\text{TOV}}^k < \chi^k < \chi_{\text{max}}$, as shown in Figure 15 (see also figures 1-2 in Ref. [630]).

For GW170817, the total gravitational mass of the system at infinite binary separation is estimated as $2.74_{-0.01}^{+0.04} M_{\odot}$, and the mass ratio is constrained to the range of $(0.7 - 1)$ [2]. Assuming non-spinning progenitors with equal mass, convert the gravitational mass for each NS ($1.37M_{\odot}$) to baryonic mass and add them together, then subtract the mass being ejected ($M_{\text{ejc}} = 0.06 \pm 0.01$) during merger. Finally, convert the baryonic mass of the remnant back to the gravitational mass. The relationship between M_{rem}^k and M_{TOV} are shown in Figure 15, which reads (see also Ref. [631])

$$M_{\text{rem}}^k = (2.354 \pm 0.074) + (0.076 \pm 0.032)M_{\text{TOV}}, \quad (3.5)$$

with the errors indicating 2σ confidence level. Comparing M_{rem}^k , as well M_b , with the critical masses, one can determine what kind of remnant was produced. In reverse, one can

put constrains on EOSs. With the universal relations shown above, we reach to the results: If GW170817 produces a short-lived HMNS, one has $M_{\text{TOV}} < 2.09_{-0.09}^{+0.11}({}_{-0.04}^{+0.06})M_{\odot}$; If GW170817 produces a long-lived SMNS, the constraint should be $2.09_{-0.09}^{+0.11}({}_{-0.04}^{+0.06})M_{\odot} \leq M_{\text{TOV}} < 2.43_{-0.08}^{+0.10}({}_{-0.04}^{+0.06})M_{\odot}$; If GW170817 produces a stable NS, the constraints should be $M_{\text{TOV}} \geq 2.43_{-0.08}^{+0.10}({}_{-0.04}^{+0.06})M_{\odot}$. The quoted uncertainties are at the 2σ (1σ) confidence level.

3.3 Identifying supermassive binary black holes

Identifying SMBBHs with separations less than a few pc is crucial for a broad range of topics in contemporary astrophysics, including the growth and evolution of SMBBHs, galaxy mergers, nano-Hertz GWs, etc. A large number of possible SMBBH candidates have been discovered through periodic variability from time-domain surveys (e.g., [671–673]) and serendipitous exploration over historical data compilations (e.g., [639, 640, 674, 675]), or through other approaches with predicted signatures of SMBBHs (e.g., [676, 677]; see also [678] for a review). However, there is currently no exclusively confirmed SMBBH because of the challenges in establishing effective criteria before the detection of nano-Hertz GW from SMBBHs via PTAs. In this sense, there is no doubt that developing new approaches for identifying SMBBH candidates are of great importance.

In a recent work [679], we illustrated that a SMBBH provides necessary tidal torques to prevent the counter-rotating disk between 0.2 and 7 pc detected in the nucleus of the nearby galaxy NGC 1068 (see Figure 16) from the Helvin-Helmholtz instability, which can result in a catastrophe at the interface between the reversely rotating parts. In other words, counter-rotating disks can avoid the Helvin-Helmholtz instability in the presence of SMBBHs that supply angular momentum to the disks. Meanwhile, such angular momentum transfer can also efficiently remove the SMBBH’s orbital angular momentum and expedite the orbit hardening, providing an alternative paradigm for solving the “final pc problem”. For NGC 1068, we estimated the total mass of the SMBBH to be $1.3 \times 10^7 M_{\odot}$, mass ratio to be $\gtrsim 0.3$ and orbit separation to be ~ 0.1 pc (see [679] for the detail). With these fiducial estimates, the SMBBH is radiating GWs at frequency $f \approx 0.1$ nHz with an intrinsic strain of $h_s = 5 \times 10^{-19}$. The GW backgrounds emitted from NGC 1068-like SMBBHs are likely to be detected through the forthcoming PTA observations of the Square Kilometer Array ([680]). The putative SMBBH in NGC 1068 has an angular size of 2 mas, which could be resolved by the Event Horizon Telescopes if both the black holes radiate radio emissions. Such an identification basis as in NGC 1068, that is, counter-rotating disks, can serve as a new strategy to search for SMBBH candidates in nearby galaxies. A thorough high-resolution survey with Atacama Large Millimeter/Submillimeter Array (ALMA) over the nuclei of nearby galaxies is therefore highly worthwhile to find out those NGC 1068-like counter-rotating disks and identify the SMBBH candidates residing therein.

3.4 GW background from stellar compact binaries

There are numerous sBBHs and BNSs inspiralling and merging across the cosmic time as predicted by theoretical models [681] and supported by ground-based GW observations [1, 2, 346]. LIGO and Virgo have put strong observational constraints on the local merger rate densities of sBBHs and BNSs after the observing run O3a, i.e., $19.1_{-9.1}^{+15.9} \text{ Gpc}^{-1}\text{yr}^{-1}$ for sBBHs and $320_{-240}^{+490} \text{ Gpc}^{-1}\text{yr}^{-1}$ for BNSs [346]. Currently, there are several different models for the origin of the sBBHs, the leading ones are: 1) sBBHs are the final products of the evolution of massive binary stars (hereafter denoted as the EMBS channel) [682], 2) sBBHs

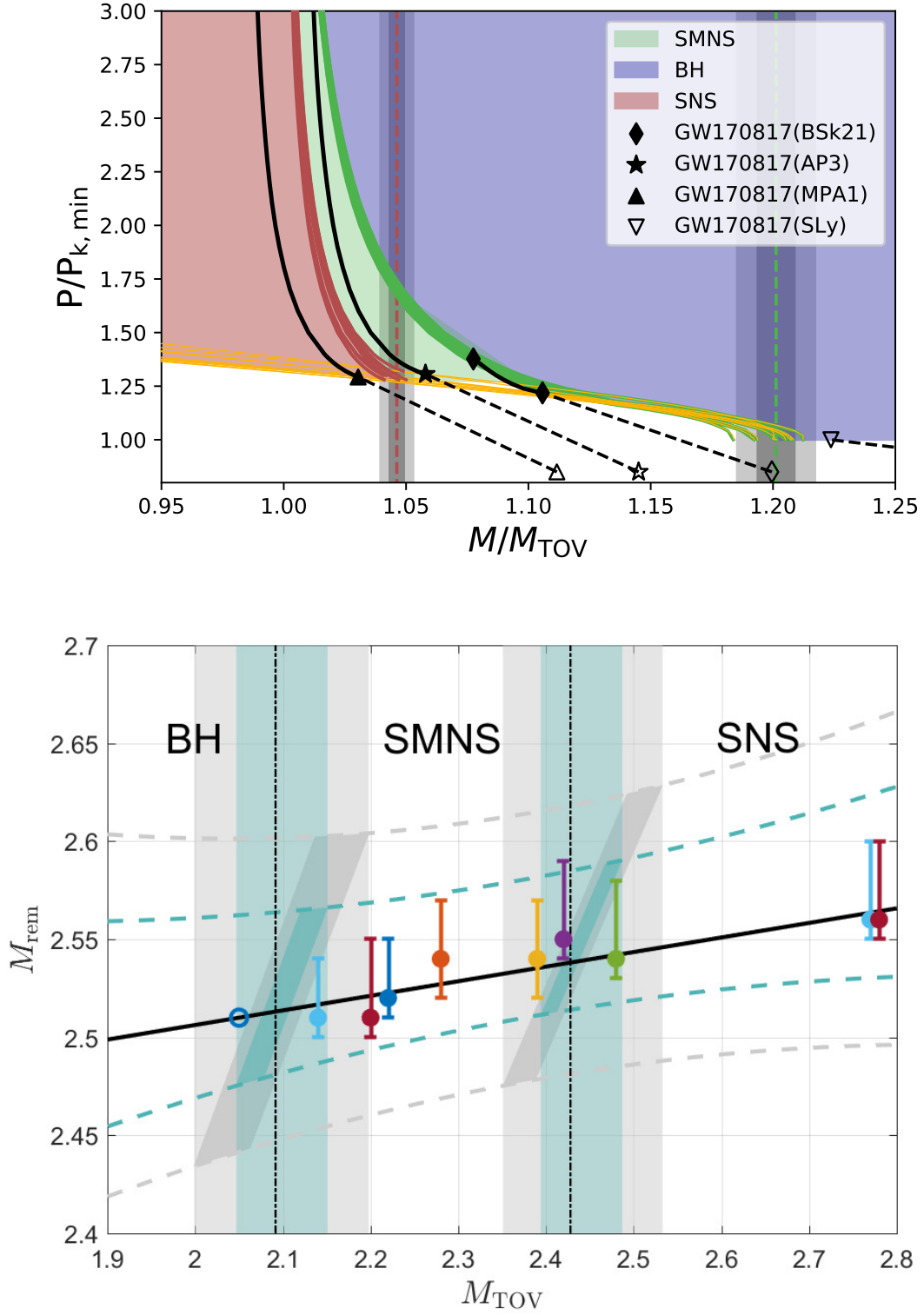


Figure 15. Constraints on M_{TOV} with GW170817 observations in case of different merger products. The top panel shows the mass-dependent normalized Keplerian period \mathcal{P}_k lines (orange), the constant $M_{\text{TOV},b}$ lines (red) and the boundary lines for SMNS collapsing into BH (green). The bottom panel shows the separation M_{TOV} values for different merger products (dot-dashed vertical lines) and the best fitting relation between M_{TOV} and M_{rem} (black solid line). Copied from Ref. [630] with permission.

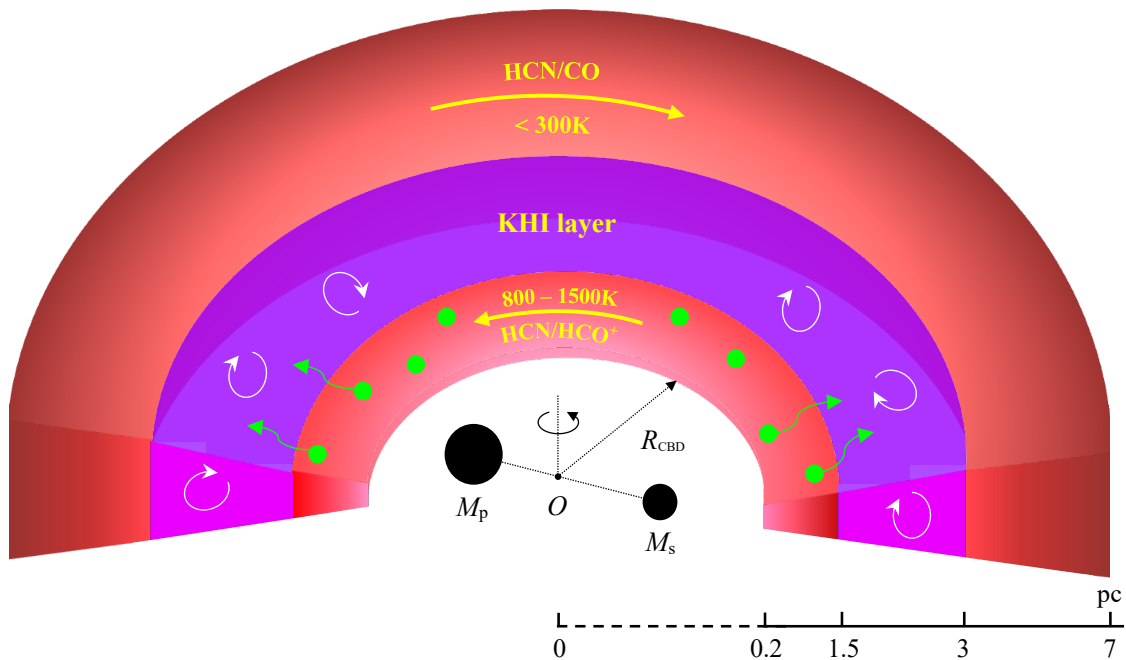


Figure 16. Cartoon of a CB-SMBH maintaining one circumbinary disc (CBD) composed of the prograde ($R \lesssim 1.5$ pc) and the retrograde ($3\text{pc} \lesssim R \lesssim 7\text{pc}$) parts in NGC 1068. Copied from Ref. [679] with permission.

are originated from the dynamical interactions in dense stellar systems, including globular cluster and galactic nuclei (hereafter denoted as the dynamical channel) [683]. The dynamical channel becomes even more important with the recent discovery of the most massive sBBHs GW190521 [684, 685], and it is anticipated that the contribution from the dynamical channel to the formation of sBBHs is significant or even dominant. The dynamical channel may produce sBBHs with extremely high eccentricities (close to 1), while the EMBS channel produces sBBHs with small eccentricities. At the low frequency range ($10^{-4} - 10^{-2}$ Hz), many inspiralling sBBHs may have significant eccentricities, if originated from the dynamical channel, because their orbits cannot be immediately circularized at this frequency range [633]. BNSs are mostly, if not all, formed via the evolution of binary massive stars and it may have small eccentricities in the frequency range $> 10^{-4}$ Hz.

GWs radiated from cosmic sBBHs and BNSs form a SGWB at frequencies spanning $10^{-4} - 1000$ Hz). This SGWB is the main target for both the ground-based GW detectors (LIGO/VIGO/KAGRA/ET/CE) with working frequency at $10 - 1000$ Hz and the space GW detectors (LISA, Taiji, and TianQin) with working frequency at $10^{-4} - 1$ Hz. GWs from eccentric binaries may result in detectable signatures in the SGWB. We have considered various models for the sBBH formation and the BNS formation to predict the SGWB and estimate the SNR of this SGWB that may be detected by space GW detectors (LISA/Taiji/TianQin) and ground-based GW detector LIGO. Here for simplicity, we show the results from two models for sBBHs: 1) the EMBS-origin-dominant model: we assume 75% of cosmic sBBHs are formed from the EMBS channel and the rest 25% are originated from the dynamical channel; 2) the dynamical-origin-only model: all cosmic sBBHs are from the dynamical

channel. Figure 17 shows the resulting SGWB energy density spectrum due to sBBHs and BNSs from EMBS-origin-dominant model and dynamical-origin-only model, respectively [c.f. 633]. The total SGWB energy density at 25 Hz is predicted to be $\Omega_{\text{GW}} = 6.57_{-3.95}^{+7.65} \times 10^{-10}$ and $8.17_{-4.71}^{+8.98} \times 10^{-10}$ for the EMBS-origin-dominant and dynamical-origin-only model, respectively. Note that the values of Ω_{GW} obtained here are substantially smaller than those estimated in [633, 686, 687] because the local sBBH and BNS merger rate densities are re-scaled to the LIGO/VIRGO O3a constraints [346] but not the LIGO/VIRGO previous constraints. As seen from figure 17, the SGWB spectrum deviates from a single power law with the canonical slope of 2/3 at frequency $\lesssim 10^{-3}$ Hz because of the contribution from highly eccentric sBBHs originated from the dynamical channel. The deviation is quite significant in the dynamical-origin-only model and the SGWB may be better described by a broken power law. We suggest that the future detection of SGWB and its shape at low frequency may put a strong constraint on the origin of sBBHs and distinguish different models for sBBHs.

The SGWB signal from inspiralling sBBHs and BNSs can be detected by LISA, Taiji, and TianQin, but may be difficult for LIGO to detect it with the designed sensitivity. Assuming an observation time period of 4 years, we predicted that the SGWB is expected to be detected by LISA, Taiji, and TianQin with a SNR of 92_{-56}^{+109} , 86_{-52}^{+102} , and $7.29_{-4.42}^{+8.61}$, respectively, for the EMBS dominated model. For the SGWB from sBBHs alone, the expected SNR for LISA, Taiji, and TianQin are 46_{-22}^{+39} , 44_{-21}^{+36} , and $3.83_{-1.83}^{+3.19}$, respectively. For the model with all sBBHs originated from the dynamical channel, the estimates of SNR of total SGWB detected by LISA, Taiji, and TianQin are 104_{-62}^{+119} , 99_{-58}^{+114} , and $8.81_{-5.14}^{+9.86}$, respectively. The SGWB from sBBHs detected by LISA, Taiji, and TianQin are 59_{-28}^{+49} , 58_{-28}^{+48} , and $8.81_{-5.14}^{+9.86}$, respectively. We also estimated that the SNR of the SGWB monitored by LIGO with the designed sensitivity over an observation period of 4 years would be $1.59_{-0.95}^{+1.84}$ and $2.00_{-1.14}^{+2.17}$ for the EMBS-origin-dominant model and the dynamical-origin-only model, respectively. This apparently suggests that the detection of the SGWB for LIGO needs to wait for many more years, different from previous expectation [686, 687].

3.5 PTA probing solar system dynamics and constructing planet ephemeris

Pulsars, particularly the millisecond pulsars (MSPs), are of high rotational stability, which is comparable to that of time-keeping atomic clock. The stability had been revealed and confirmed using the pulsar timing method, where the difference (called timing residuals) between the measured time of arrival of pulsed signals and a low-order polynomial predication can reach sub-100 ns level. By monitoring multiple MSPs, one can study the correlation between timing residuals of pulsar pairs. The correlated common signal provides opportunities to probe fundamental physics, which includes detecting nano-Hertz GWs [688], investigate the stability of reference terrestrial time standards [689], and study the Solar System dynamics [690]. These applications make use of so-called PTAs, which are an ensemble of pulsars, typically millisecond pulsars, in different sky positions [691].

One of the noise sources preventing from successful GW detection using PTA is the uncertainties in modeling the Solar system dynamics. It introduces correlated signals in PTA data, and can mimic, to a certain level, the properties of GW. The error in the Solar System ephemeris (SSE) will lead to dipolar correlations in the residuals of pulsar timing data for widely separated pulsars. We have performed serial work in order to solve the SSE problem. As a first step, we tackled the problem with a perturbative approach [692]. The SSE error induces a dipole correlation. We utilized the signals and constructed a Bayesian

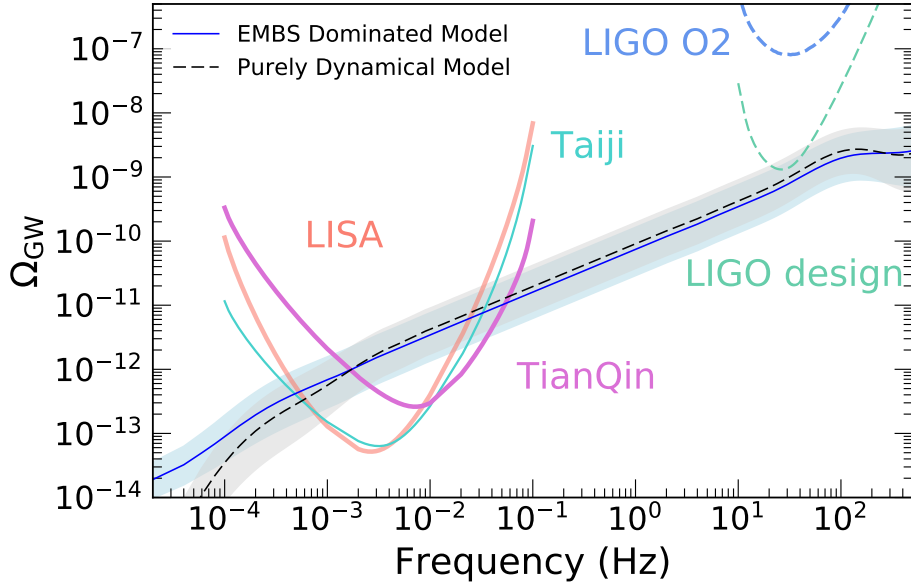


Figure 17. The energy density spectrum of stochastic SGWB from sBBHs and BNSs. Blue solid and black dashed lines represent the total Ω_{GW} resulting from the models with sBBHs formed mainly from the EMBS channel and the purely dynamical channel, respectively. Cyan solid, red solid, magenta solid, blue dashed, and green dashed curves show the sensitivity curves of Taiji, LISA, TianQin, LIGO O2, and LIGO design, respectively. Copied from Ref. [633] with permission.

data-analysis framework to detect the unknown mass in the Solar System and to measure the orbital parameters. In this way, we can probe if there is any unknown point mass in our Solar system [634]. We expect that the future PTA data can limit the unknown massive objects in the Solar System to be lighter than 10^{-11} to $10^{-12}M_{\odot}$, or measure the mass of Jovian system to fractional precision of $10^{-8} - 10^{-9}$. Using the data from international PTA, we also measured the mass of planets and heavy asteroids using the perturbative method. Then we started to look into the nonlinear aspect of Solar system dynamics. To better understand the effects on pulsar timing caused by the uncertainties of SSE, we implemented the fully dynamical model of the Solar system [635], based on the SSE of Guangyu Li. Under the same initial condition, we demonstrated that the planetary positions and velocities are compatible with DE435 at centimeter and 10^{-4} cm/s level over a 20-year timespan. We noted that the dominant effects on the inner and outer planets are different between the perturbative and full-dynamic models. For the outer planets, the timing residuals are dominated by the SSE shift, the two models produce similar results. However, for inner planets, the variations in the orbit of the Earth are more prominent, which makes the leading-order approaches insufficient and leads to larger effects on pulsar timing. Furthermore, the power spectrum of planet ephemeris induced signal is much more complex than simple harmonics assumed before. Armed with the full dynamic model of Solar system dynamics, we studied [635] 1) how to mitigate the Solar system noise in pulsar timing data processing, and 2) how to constrain the Solar system model itself by using PTA data. We are now able to systematically account for the effects of errors in the orbital elements, which making our search for GWs, errors in SSE parameters and planetary mass constraints, more robust. Because most of planet ephemeris are closed-source, our work in Solar system model becomes one of the

major support for our independent PTA data analysis in the future.

3.6 Detecting GWs using PTAs in the SKA era

PTA is the most promising experiment to open the very low frequency window ($\sim 1 - 100$ nHz) of GW astronomy. There are three major regional PTA consortia that have been in operation for more than a decade: NANOGrav, the European Pulsar Timing Array (EPTA), and the Parkes Pulsar Timing Array (PPTA), which are currently monitoring 47 [693], 42 [694] and 26 [695] millisecond pulsars, respectively. The International Pulsar Timing Array (IPTA), as the umbrella of the three PTAs, contains 65 pulsars in its most recent data release (DR2) [696]. Meanwhile, the Chinese PTA (CPTA) [697] and Indian PTA (InPTA) [698] are both in rapid development and will join in the IPTA's effort in detecting GWs.

In the past several years, PTAs have already put astrophysical meaningful constraints on the stochastic GW background [419–421], continuous wave signals from resolvable SMBBHs [699–701], and bursts with memory [702, 703]. Recently, based on the 12.5-yr data collected between 2004 and 2017, the NANOGrav has found strong evidence of a common-spectrum stochastic process with a median characteristic GW strain amplitude of 1.92×10^{-15} at $f = 1/\text{yr}$ for the fiducial $f^{-2/3}$ spectrum. However, no statistically significant evidence has been found for the inter-pulsar quadruple spatial correlation (Hellings-Downs curve [704]) of the timing residuals induced by the GW from an unresolved SMBBH population [25]. This result has been confirmed by the other PTAs.

While the current PTAs are on the verge of making a first detection of the stochastic GW background in the coming years, this nascent GW astronomy in the very low frequency will experience a leap with the next generation large-scale radio telescopes, namely FAST [705] and SKA [706], which will increase the number of the pulsar timed with a precision of $\lesssim 100$ ns to $O(10^3)$ [707] and allow us to observe GWs generated by individual SMBBHs, early cosmic phase transition, cosmic string decay and primary black holes [708]. These anticipated discoveries will have a profound impact on our understanding of the evolution of the early universe, large-scale structure and galaxy formation, and fundamental theory of gravitation.

With the growing timing precision and the number of pulsars, the data analysis challenges in PTA also become more difficult. For example, the N_p unknown pulsar phase parameters, where N_p is the number of pulsars, brought by the so-called pulsar terms in the GW induced timing residual signal exponentially enlarges the volume of the search space. Using fully coherent methods that can handle these phase parameters semi-analytically [709, 710], we have assessed the performance of the SKA-era PTA with 10^3 pulsars timed to 100 ns level [711]. Our work shows that, for the SKA-era PTA, the sky-averaged upper limit on GW strain amplitude will be

$$h = 5.2 \times 10^{-16} \times \left(\frac{f_{\text{gw}}}{2 \times 10^{-8} \text{ Hz}} \right), \quad (3.6)$$

if the network SNR $\rho = 30$ is adopted as a detection threshold. At the frequency $f_{\text{gw}} = 2 \times 10^{-8}$ Hz, $h = 5.2 \times 10^{-16}$ which is about 2 orders of magnitude improvement over the existing limits. Given a redshifted chirp mass of $4 \times 10^9 M_\odot$ ($4 \times 10^{10} M_\odot$), the SMBBH will be visible out to the cosmological redshift $z \approx 1$ (28). With this distance reach, some of the SMBBH candidates that are found by the electromagnetic observations, such as PG 1302-102 and PSO J334+01, can be either confirmed or ruled out. In addition, our work unveiled the relationship between the parameter estimation uncertainty and the condition number of the

response matrix in the signal model. The latter indicates the ill-posedness that is inherent in coherent GW data analysis as is already known for ground-based detector networks [712–714]. For example, the estimated right ascension and declination of the sources at locations with increasing condition numbers tend to have larger variance and bias for a given ρ ($\neq 0$). For the noise-only case ($\rho = 0$), the estimated locations of sources are attracted towards the Galactic North and South poles where the condition numbers approach unity.

For the resolvable sources, we have demonstrated that the high frequency reach of PTAs is not limited by the Nyquist frequency of single pulsar observations [715]. Actually, one can take advantage of asynchronicity, a feature inherent in PTA, to reconstruct the high frequency component of the GW signals that is preserved in the data due to aliasing in the observation sequences of an array of pulsars. Using asynchronous observations which we call *staggered sampling*, one can effectively extend the GW search frequency range by a factor of up to N_p without increasing the total allocated time for pulsar timing observations and the average observation cadence per pulsar. Given the typical average observation cadence of 1/(2 weeks), the staggered sampling can increase the Nyquist frequency from 4×10^{-7} Hz to 2×10^{-5} Hz for the existing PTAs with about 50 pulsars and 4×10^{-4} Hz for the SKA-era PTA with 10^3 pulsars [715]. This will bridge the μ Hz band between the conventional PTAs and the space-borne interferometric detectors, such as LISA [10], TianQin [17] and Taiji [15]. Taking the SKA-era PTA as an example, we have shown the significant astrophysical implications in the light of this frequency increase: (1) the GW strain upper limit in [10, 400] μ Hz will be improved by around 3 orders of magnitude over the current high-cadence experiments [716]; (2) PTA will not only sensitive to the GWs from SMBBHs in the early inspiral phase, but also the more dynamic merger and ringdown phases, which can be used to test GR with high precision. For example, the no-hair theorem can be tested to $\approx 2\%$ level, compared to the $\approx 10\%$ level archived by LIGO [717]; and (3) measuring the Hubble constant by using only GW observations (no need for an electromagnetic counterpart). This is realized by measuring the additional timing residuals rooted in the curvature of the GW wavefront and inferring the co-moving distance of the source D_c . $D_c = D_L/(1+z)$, where D_L is the luminosity distance obtained from GW signal simultaneously. From the Fresnel criterion, it follows that this effect will manifest itself more clearly at higher frequencies [718].

3.7 Forecasting SKA-PTA detection of individual SMBBHs

As mentioned before, PTA is not only aiming at detecting the stochastic GW background from numerous cosmic SMBBHs but also individual SMBBHs in nearby and faraway Universe. We have quantified the potential of detecting GWs radiated from individual SMBBHs by the SKA-PTA [636]. Our calculations demonstrate, for the first time, that even a small number (about 20) of high-quality MSPs monitored by SKA will deliver valuable information about the redshift evolution of SMBBHs. Based on infrared galaxy samples and statistical assumptions of the SMBBH population, we carried out a semi-analytical numerical simulation to estimate the number of detectable SMBBHs with SKA-PTA. Different from the hundreds of pulsars commonly assumed to be necessary in previous work, the new calculations demonstrate that a SKA-PTA consisting of merely ~ 20 pulsars is capable of detecting single GW sources within 5 years and approaching a ~ 100 SMBBHs/yr detection rate within 10 years. 30 years of SKA-PTA operation will detect about 60 individual SMBBHs with $z < 0.05$ and more than 10^4 within $z < 1$ (Fig. 18). With such a substantial number of expected detections, SKA-PTA will open a new window into the SMBBHs, their host galaxies, and the evolution of the SMBBH population through redshifts.

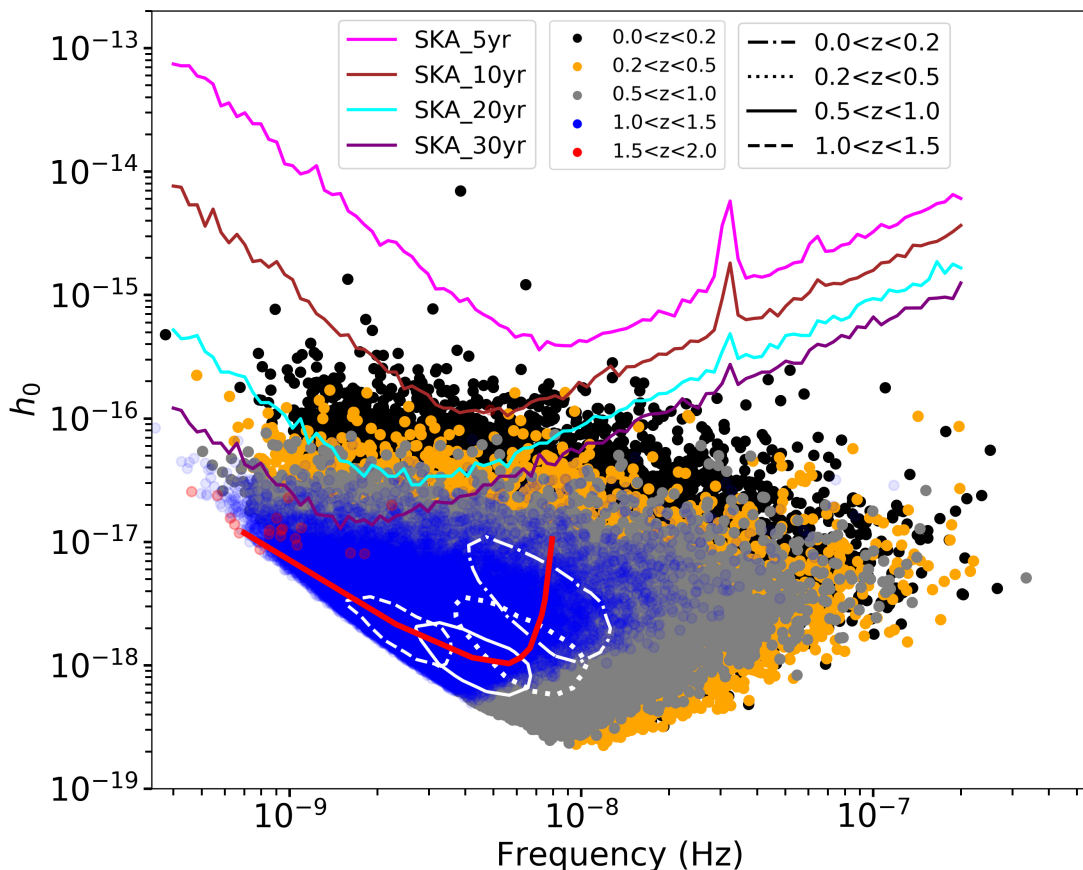


Figure 18. Colored curves show the detection threshold for SKA-PTA at different year mark from the initiation of its operation . Black, orange, gray, blue, red dots represent SMBBH population hosted by 10^6 galaxies from $0.0 < z < 0.2$, $0.2 < z < 0.5$, $0.5 < z < 1.0$, $1.0 < z < 1.5$, $1.5 < z < 2.0$ respectively. Dash-dotted, dotted, solid, dashed number density contours represent 50% of the peak value for $0.0 < z < 0.2$, $0.2 < z < 0.5$, $0.5 < z < 1.0$, $1.0 < z < 1.5$ respectively. The red curve crossing the contour centers shows the evolution trend of SMBBH population from low to high redshifts: the GW frequencies increase; the GW strains decrease first and then increase. Copied from Ref. [636] with permission.

More than 10^4 SMBBHs detected in the Square Kilometre Array era (in an optimistic case) is a treasure trove for nano-Hertz multi-messenger astronomy. We are preparing for such an amazing party:

- Use available IPTA data to get a good understanding of PTA data and carry out PTA sciences. We investigated the long-term timing observations of the pulsar PSR J1909–3744 from the Parkes radio telescope and managed to derive the most stringent constraints to date on the chirp masses of a set of SMBBH candidates [637]. Our results are between 2 to 7 times smaller than previous limits. The estimated detection thresholds are still much larger than expected chirp masses, with that of 3C 66B being the closest at about 3 times more massive. Our analysis also demonstrated that, unlike the stochastic GW background, the detection of single GW sources can be impervious to uncertainties in

the solar system ephemeris and can benefit significantly from a priori knowledge of the SMBBH orbits.

- As part of the CPTA efforts, we investigated methods to improve timing precision. With FAST, We found multiple jitter modes in PSR J1022+1001[719]. This marks the initial step of understanding single pulse behaviours of PTA MSPs with FAST and the FAST’s potential to better reveal GW [705, 720].
- We developed machine learning procedures for classification and detection of GW signals from specific SMBBHs in simulated PTA data sets. Our convolutional neural network achieves high accuracy when the combined SNR is > 1.33 [721]. Due to the lack of confirmed SMBBH sources and their weak estimated strain, the mainstream PTAs have been focusing on the stochastic background GW, which is in essence a noise term, and even when detected, will provide only limited, congregated astrophysical information. Preparation for LIGO type individual source-detection pipeline is thus necessary for GW astrophysics using PTAs.

4 Numerical relativity and gravitational waveform template

Compact binary coalescences are the most important and promising GW sources for both the ground-based and space-based GW detectors. In the past years, LIGO and Virgo have completed three observation runs. And more than 50 GW events have been announced. All of these events and other GW event candidates are compact binary coalescences.

Due to the weakness of the GW strain, the detected data by the GW detectors are typically weak signals hidden in strong noises. Consequently, a special data analysis technique, matched filtering, is required to dig out the weak GW signal. In order to let the matched filtering scheme work, accurate and complete waveform templates are indispensable.

On the other hand, the GW sources are extremely general relativistic on the GW generation side. The typical characters include extremely strong gravitational force and highly dynamical evolution. Because of these issues, numerical relativity is almost the unique method to treat GW source modeling problems. Since numerical relativity admits no approximation to Einstein equation, numerical relativity is very reliable to model GW sources.

The task of numerical relativity is solving Einstein equation with a numerical method. At first glance, one need only code the Einstein equation and put it in a supercomputer. Afterwards, the numerical relativists just sit and wait for the results. The real life for numerical relativists is much harder [722]. The first issue numerical relativists need to face is how to make the numerical solution process stable. Otherwise, the code will break down soon and nothing can be obtained except a mount of ‘NaN’ (not a number). From the 1960s to 2005, numerical relativists worked hard to solve this stability problem. After 2005, stability problem of numerical relativity is solved [723–725] in the sense that properly implemented numerical techniques can make specific binary merger calculation stable [726–728]. On the other hand, there is no concrete mathematical theorem to guarantee a sufficient condition for the stability of numerical relativity. Numerical relativists need to extend existing experiences to new problems and make the calculation stable.

Along with the ground-based detection development for GW, several GW templates have been constructed including post-Newtonian approximation ones, numerical relativity surrogate ones, effective one body (EOB) numerical relativity series, and IMRPhenomenon series [729]. The state of art for the gravitational waveform template of compact binary

coalescence is as following. The binary’s total mass can be regarded as a unit to make all of the involved quantities in the system dimensionless. Consequently, the waveform models are available for any total mass. The mass ratio is an essential parameter. If the mass difference between the two objects is too large, the computational requirement is huge. Reliable numerical relativity results are available till mass ratio 1 to 20. Recently many efforts have been paid to binary black hole simulations with a mass ratio around 1 to 100 [730–732]. The mass ratio problem provides a computational efficiency challenge to numerical relativity. Before our project, complete inspiral-merger-ringdown waveform models only work for circular binaries. We developed complete waveform models for eccentric binaries. Based on the prediction of GR, GW admits memory. Before our project, there are some intuitive waveform models inspired by post-Newtonian approximation for GW memory. We proposed a new method to calculate GW memory accurately for the full inspiral-merger-ringdown process. In the following, we will give an introduction about our progress on the efficiency problem of numerical relativity, waveform model for eccentric binaries, and the GW memory model.

4.1 Finite element Numerical relativity

Numerical methods solving partial differential equations include finite difference method, spectral method, and finite element method. Numerical relativity codes based on finite difference method or spectral method have been widely used to simulate binary black holes for waveform model construction. There is no finite element code for numerical relativity having been used for binary black hole merger yet.

The existing numerical relativity codes based on finite difference method and the ones based on spectral method have their advantages and limitations respectively. The adaptive mesh refinement (AMR) is necessary to treat the multi-scale problem met in the binary black hole problem for finite difference code. AMR technique is powerful, but the strong parallel scaling ability is highly limited by the grid numbers on each mesh level. Current numerical relativity commonly uses about $100 \times 100 \times 100$ grid boxes. Consequently finite difference code can not use too many cores to simulate binary black hole systems [733]. The parallel scaling ability of pseudo-spectral code is much worse due to the global data change among the spectral domain. The advantage of pseudo-spectral code is the high convergence property. The pseudo-spectral code needs much less cores than finite difference code for binary black hole system simulations [734]. Unfortunately when the mass ratio increases, it is quite hard to tune the pseudo-spectral code to make it work.

The finite element has a local data property as finite difference when discriminating the space. So finite element method has comparably high parallel scaling advantage as finite difference method. The high order polynomial function basis and/or spectral function basis in each element are similar to the spectral method (spectral element method). Consequently, the finite element method could combine the high parallel scaling property as the finite difference method and the high convergence property of the pseudo-spectral method. So it is possible to use the finite element method to treat the unsmooth region with small element and to treat the smooth region with large element but high order basis or spectral basis. The finite difference method have to transfer data between different mesh levels. So the size of single mesh limits the strong parallelization scalability for the finite difference method. All elements in the finite element method are treated as the same level. Consequently the finite element method may admit higher strong parallelization scalability than both the spectral method and the finite difference method.

Although the finite element method admits above attractive properties, it is still unclear how to construct a finite element code for binary black hole merger. Especially it is not clear yet how to make the numerical calculation based on finite element stable. The key details include that the weak form of Einstein equation is difficult to design, the gauge condition and the boundary condition are highly nontrivial to construct.

When we use the finite element method to solve Einstein equations numerically, we decompose the Einstein equations into the evolution part and constraint part and taking the whole task as a Cauchy problem. As the first step, we apply the finite element method to solve the constraint part for the initial data of the Cauchy problem [735].

Based on 3-metric γ_{ij} and external curvature K_{ij} , the constraint equations can be written as following

$$\mathcal{H} \equiv R - K_{ij}K^{ij} + K^2 - 16\pi\rho = 0, \quad (4.1)$$

$$\mathcal{M}_i \equiv D_j K^j_i - D_i K - 8\pi s_i = 0, \quad (4.2)$$

where the R is the scalar curvature with respect to the spatial metric γ_{ij} . D is the covariant derivative operator consistent with the spatial metric. ρ and s_i are the mass density and momentum density of matter. We refer our reader to [726] for a detailed description of the quantities involved in the above constraint equations. Borrowing the experience in the previous numerical relativity schemes, we consider the puncture scheme proposed in [736] with conformally flat assumption. In this scheme, the momentum constraints are solved analytically. After that, the 3-metric and the extrinsic curvature can be determined by the spins and velocities of the two black holes. In addition, a conformal factor ψ is involved. And the conformal factor ψ is determined by the Hamiltonian constraint equation

$$-(\partial_x^2 + \partial_y^2 + \partial_z^2)\psi = \frac{1}{8}\hat{K}^{ij}\hat{K}_{ij}\psi^{-7} + 2\pi\rho\psi^{-3}. \quad (4.3)$$

The positions of the black holes are singular and they are called puncture points. We can transform to a regular variable u . The authors in [736] have proved that the solution u is only C^4 around the puncture points. This unsmoothed behavior can be well treated by the weak form of our finite element method. Binary black hole systems are theoretically described by a vacuum, so $\rho = s_i = 0$.

Using regular variable u the Hamiltonian equation can be written as an non-linear Poisson equation

$$-\nabla^2 u = f(u) \text{ in } \Omega. \quad (4.4)$$

Based on the finite element scheme we approximate the domain \mathbb{R}^3 with some finite domain Ω . At the boundary of Ω we consider both Dirichlet boundary condition and Robin boundary condition.

For the non-linear Poisson equation (4.4) and the Robin boundary condition, we use integration by part to construct the weak form. With the basis function of the finite element ϕ_i , we expand the unknown function as $u = u^i \phi_i$. Accordingly, we discretize the above weak form equation and use the Newton iteration method to solve the set of non-linear equations for u^i . Noting that all the involved matrices are symmetric, we use the preconditioned conjugate gradient to solve the linear equations. The diagonal elements of the matrix in question are used as the preconditioner. Aided with the mentioned preconditioner we can get the converged solution soon. The numerical scheme for the Dirichlet boundary condition is similar. We refer our reader to the reference [735] for details.

After the initial data is ready, we come to the evolution equations [737]. There are well developed finite element methods for Hamilton-Jacobi-like equations [738]

$$u_t + H(u_x) = S(u) \quad (4.5)$$

where u denotes general unknown functions. H and S are some specific functions depending on u_x and u respectively.

Denote the discretized domain as $I_j = (x_{j-\frac{1}{2}}, x_{j+\frac{1}{2}})$, $j = 1, \dots, N$. $x_j = \frac{1}{2}(x_{j-\frac{1}{2}} + x_{j+\frac{1}{2}})$ corresponds to the center of the cell I_j and $\Delta x_j = x_{j+\frac{1}{2}} - x_{j-\frac{1}{2}}$ as the size of the cell. The function space corresponding to the numerical solution is defined as a piecewise polynomial space, There is no continuity requirement at the interfaces $x_{j\pm\frac{1}{2}}$. This non-continuity property means a discontinuous Galerkin method.

The Legendre polynomials are used to decompose functions in the approximation space. Our local discontinuous Galerkin finite element method includes two steps. As the first step, we calculate the derivative u_x by solving the equation $\psi = u_x$. We have two numerical solutions p_1 and p_2 to the equation of ψ . Then the Lax-Friedrichs numerical Hamiltonian can be constructed

$$\hat{H}(p_1, p_2) = H\left(\frac{p_1 + p_2}{2}\right) - \frac{1}{2}(p_1 - p_2). \quad (4.6)$$

As the second step, we calculate u_t through

$$\int_{I_j} u_t v dx + \int_{I_j} \hat{H}(p_1, p_2) v dx = \int_{I_j} S(u) v dx. \quad (4.7)$$

We use this u_t to update u with respect to time based on the fourth-order Runge-Kutta method.

A limiter is used during the evolution to alleviate the high frequency numerical error.

Following the idea we proposed in [739], a buffer cell is added for boundary condition treatment.

For a spherically symmetric spacetime, we can write the Einstein equation as [737, 740]

$$\partial_t u^\mu + A^\mu{}_\nu \partial_r u^\nu = S^\mu, \quad (4.8)$$

where the unknown variables u^μ and the related $A^\mu{}_\nu(u^\sigma)$ and $S^\mu(u^\sigma)$ are given in [737]. The Eq. (4.8) is Hamilton-Jacobi-like. We apply directly the above finite element numerical scheme to the Eq. (4.8). We realized stable evolution of a Schwarzschild black hole based on Kerr-Schild coordinate, isotropic coordinate and Painleve-Gullstrand-like (PG) coordinate.

For a general spacetime without symmetry, we note that the generalized harmonic formalism of Einstein equations is Hamilton-Jacobi-like [741]. Accordingly, we apply the finite element method to the generalized harmonic formalism of Einstein equations based on the Parallel Hierarchical Grid (PHG) library [735, 742, 743]. Since the continuous Galerkin module is more well developed than the discontinuous Galerkin module in PHG library, we used continuous Galerkin instead of discontinuous Galerkin in [744]. Similar to the above filter, we adopt the filter [745, 746]

$$F_\alpha = \alpha F_{N-1} + (1 - \alpha)I, \quad (4.9)$$

where F_{N-1} is the interpolation operator from the space of the polynomials of maximum degree N to the space of the polynomials of maximum degree $N - 1$, I is the identity operator, and $\alpha \in (0, 1]$ is the relaxation parameter which allows us to filter only a fraction of the highest mode. Since this filter is based on interpolations in physical space, the filtered solution will still be continuous at the boundaries between each two elements. In another word, this filter is consistent with the continuous Galerkin implemented here. With these numerical skills, we can evolve single Schwarzschild black hole stably.

4.2 Gravitational waveform models for eccentric compact binaries

More than 50 compact binary coalescence (CBC) events have been detected by LIGO and VIRGO. One possible channel for the formation of merging binaries is isolated evolution in the field. Another possible channel is through dynamical interaction in dense stellar environments such as globular clusters or galactic nuclei. Currently, it is not clear the detected binaries are formed through which channel. The binaries formed in the field can radiate away their eccentricity. The dynamically formed binaries may still have significant residual eccentricity when their GWs enter the LIGO-Virgo band. People may infer the formation channel of the binary through the eccentricity detection. For space-based detectors including LISA [9, 10, 387], Taiji [11–13] and TianQin [17–19], the orbit of the concerned binary black hole systems may be highly eccentric [747, 748]. Consequently more and more attention is paid to the eccentricity detection recently [749–772].

In order to estimate the eccentricity, an accurate waveform model for the eccentric binary system is needed. Most waveform models for eccentric binary are based on post-Newtonian approximation and are consequently valid only for the inspiral part. Currently, there are three waveform models that can cover the whole inspiral-merger-ringdown process for BBH. One is the Eccentric, Nonspinning, Inspiral, Gaussian-process Merger Approximated waveform model (ENIGMA) and the other two are based on EOB framework including the Effective-One-Body Numerical-Relativity waveform model for Spin-aligned binary black holes along Eccentric orbit (SEOBNRE) and the extended TEOBiResumS_SM model. Among all of these waveform models for eccentric binary, only SEOBNRE and the extended TEOBiResumS_SM model can treat spinning black holes. Such kind of complete waveform model is important to treat parameter degeneracy, especially between the black hole spin and orbit eccentricity.

When one tries to generalize the waveform template of CBC used by ground-based detectors to the waveform template used by space-based detectors, two key issues are involved. One is about the parameter completeness and the other is accuracy. Regarding the parameter completeness, it is the mass ratio of the binary and the eccentricity of the orbit that are involved. For ground-based detectors, only stellar massive black holes are involved. So current waveform template, which is valid from mass ratio 1 to 1 till 1 to 20, is enough. For space-based detectors, since all supermassive black holes, intermediate massive black holes and stellar massive black holes are involved, the mass ratio should cover from 1 to 1 till 1 to 10 million. Regarding the eccentricity, the binary black hole systems may become near-circular when they enter the LIGO frequency band due to the gravitational wave [773]. But when mass ratio increases, such circularization effect becomes less effective and consequently the eccentricity will be significant when the binary enter the detection band.

One may take the binary system with large mass ratio as a perturbation of the big black hole. Consequently the GW problem can be decomposed into a trajectory problem and a related waveform problem. Han [774] used the Teukolsky equation to treat the waveform problem and used the conserved EOB dynamics with numerical energy flux to treat the tra-

jectory [775]. The Teukolsky equation is solved numerically [774, 775]. Teukolsky equation can also be solved through some analytical method [776] or post-Newtonian approximation [777]. The authors of [778] used the geodesic equation to treat the trajectory and used the Teukolsky equation to treat the waveform problem. Geodesic equation indicates that the eccentricity may increase [779, 780]. In contrast post-Newtonian approximation found the eccentricity always decay [773]. Interesting transient resonance phenomena was reported in [781, 782]. When a binary passes through a transient resonance, the radial frequency and polar frequency become commensurate, and the orbital parameters will show a jump behavior. In contrast, the post-Newtonian approximation method has not found the eccentricity increasing and the transient resonance behavior. Possibly this is because the available post-Newtonian result is not accurate enough. But there is also another possibility that the perturbation method breaks down. Ideally, numerical relativity simulation can answer this question. But current numerical relativity techniques can not simulate such large mass ratio systems [730, 731] (but see [783]). Alternatively, the effective-one-body-numerical-relativity (EOBNR) method may also answer this question. On the side of almost equal mass cases, EOBNR framework has been calibrated against numerical relativity; on the side of extreme mass ratio cases, EOB framework can in principle be used to describe the dynamics and the gravitational waveform [784]. We try to use EOBNR framework to aid numerical relativity to solve large mass ratio problem. Based on the above consideration we plan to use EOBNR framework to fill the parameter gap of the current waveform template to let it satisfy the requirement of space-based detectors. During the past years, we have constructed such a waveform model called SEOBNRE [785, 786] where the last letter E represents eccentricity.

The EOB technique is a well known technique to treat the two-body problem in the central force situation of classical mechanics, especially for Newtonian gravity theory [787]. Buonanno and Damour proposed the seminal idea of EOB approach for a two-body problem in GR [788]. EOB approach has adopted many inputs from post-Newtonian approximation, but it is different to the post-Newtonian approximation. Post-Newtonian approximation diverges before the plunge stage. In contrast, the EOB approach works well till the merger. The EOB approach has also adopted the result of perturbation method [784] and the results of numerical relativity. Such a combination results in effective-one-body numerical relativity (EOBNR) model [789]. The EOBNR model family includes version 1 [790], version 2 [791], version 3 [792–794] and version 4 [795].

The EOB approach includes three building blocks: (1) a Hamiltonian describing the conservative part of the dynamics of two compact bodies which is represented by; (2) the radiation-reaction force describing the dissipation force; and (3) the asymptotic gravitational waveform. The first part has nothing to do with the involved orbit. That is to say the first part is valid no matter the orbit is circular or eccentric. Since the radiation-reaction force can be related to energy and angular momentum carried away by GW, the second part is closely related to the third part. So the key issue of SEOBNRE model is the construction of the waveform for eccentric orbit.

The EOB approach describes the conservative dynamics of the two-body problem in GR as a geodesic motion (more precisely Mathisson-Papapetrou-Dixon equation [796]) on the top of an effective spacetime of the reduced one body. The Finsler-type term may possibly be involved besides the geodesic motion [797, 798]. The reduced one body spacetime is a deformed Kerr black hole [799].

The Hamiltonian of the geodesic motion can be written as [790, 798, 800]

$$H = M\sqrt{1 + 2\eta\left(\frac{H_{eff}}{M\eta} - 1\right)}, \quad (4.10)$$

$$H_{eff} = H_{NS} + H_S + H_{SC}. \quad (4.11)$$

The equation of motion corresponding to the conservative part can be written as

$$\dot{\vec{r}} = \frac{\partial H}{\partial \vec{p}}, \quad (4.12)$$

$$\dot{\vec{p}} = -\frac{\partial H}{\partial \vec{r}}. \quad (4.13)$$

Since the part 2 is related to the part 3, we describe our waveform formula first, and introduce the back reaction force afterwards. The gravitational waveform can be decomposed as spin-weighted -2 spherical harmonic modes. This kind of decomposition has been widely used in numerical relativity [801]. Only the dominate modes $(l, m) = (2, \pm 2)$ are available in [785, 786]. Later [802] we rebuild the waveform modes for $(l, m) = (2, \pm 2), (2, \pm 1), (3, \pm 3), (4, \pm 4)$. Only the positive m modes are needed and the negative m modes can be got through relation $h_{lm} = (-1)^l \bar{h}_{l, -m}$ [785, 803]. Here the over bar means the complex conjugate.

When constructing the eccentric waveform, we divide the waveform into quasi-circular part and eccentric part. Following [804] we treat the eccentric part as a perturbation. We borrow the the quasi-circular part from SEOBNR models. In [785, 786], SEOBNRv1 was used. In [802] SEOBNRv4 was used. The waveform is divided into two segments including quasi-normal modes and inspiral-plunge waveform. The inspiral-plunge waveform is written as [803]

$$h_{lm}^{(C)} = h_{lm}^{(N, \epsilon)} \hat{S}_{eff}^{(\epsilon)} T_{lm} e^{i\delta_{lm}} (\rho_{lm})^l N_{lm}, \quad (4.14)$$

$$h_{lm}^{(N, \epsilon)} = \frac{M\eta}{R} n_{lm}^{(\epsilon)} c_{l+\epsilon} V_{\Phi}^l Y^{l-\epsilon, -m}\left(\frac{\pi}{2}, \Phi\right), \quad (4.15)$$

where R is the luminosity distance of the source; Φ denotes the orbital phase; $Y^{lm}(\Theta, \Phi)$ are the usual spherical harmonics. In the non-quasi-circular correction term N_{lm} [785, 786] depends on the parameters $a_1^{h_{lm}}, a_2^{h_{lm}}, a_3^{h_{lm}}, b_1^{h_{lm}}, b_2^{h_{lm}}$ and $a_{3S}^{h_{lm}}, a_4^{h_{lm}}, a_5^{h_{lm}}, b_3^{h_{lm}}, b_4^{h_{lm}}$. These parameters depend on a and η . Following SEOBNRv1, we construct data tables for $a_i^{h_{lm}}, a_{3S}^{h_{lm}}, b_1^{h_{lm}}$ and $b_2^{h_{lm}}$. Then we get the wanted values for the a and η through interpolation. Then we solve the conditions (21)-(25) of [790] for $b_3^{h_{lm}}$ and $b_4^{h_{lm}}$. In [802] a completely different scheme was taken to treat the non-quasi-circular correction term N_{lm} which follows closely the SEOBNRv4 model.

The post-Newtonian (PN) result is valid till second PN order for the eccentric part [805]. We refer our reader to [785] for detailed eccentric part waveforms. The eccentric correction means

$$h_{22}^{(PNE)} = h_{22} - h_{22}|_{\dot{r}=0}. \quad (4.16)$$

Then our inspiral-plunge waveform reads

$$h_{22}^{insp-plun} = h_{22}^{(C)} + h_{22}^{(PNE)}, \quad (4.17)$$

where $h_{22}^{(C)}$ is given in Eq. (4.14).

In [785, 786] we took the above (4.16) directly as the eccentric waveform part. In [802] we borrow the factorization and resummation skills developed in SEOBNR quasi-circular waveform models to treat (4.16). If we denote the resulted eccentric part waveform $h_{22}^{(\text{FPNE})}$, the waveform used in [802] can be written as

$$h_{22}^{\text{insp-plun}} = h_{22}^{(C)} + h_{22}^{(\text{FPNE})}. \quad (4.18)$$

The idea to construct the other modes than (2, 2) is similar. We refer our reader to [802] for details. Based on these waveforms, we have the energy flux $\frac{dE}{dt}$ of GW [806]

$$-\frac{dE}{dt} = \frac{1}{16\pi} \sum_l \sum_{m=-l}^l |\dot{h}_{lm}|^2. \quad (4.19)$$

We assume that h_{lm} behaves as a harmonic oscillation. Consequently $\dot{h}_{lm} \approx m\Omega h_{lm}$ and Ω is the orbital frequency. Then

$$-\frac{dE}{dt} = \frac{1}{16\pi} \sum_l \sum_{m=-l}^l (m\Omega)^2 |h_{lm}|^2 \quad (4.20)$$

$$= \frac{1}{8\pi} \sum_l \sum_{m=1}^l (m\Omega)^2 |h_{lm}|^2. \quad (4.21)$$

Then, the radiation-reaction force $\vec{\mathcal{F}}$ can be written as [790]

$$\vec{\mathcal{F}} = \frac{1}{M\eta\omega_\Phi |\vec{r} \times \vec{p}|} \frac{dE}{dt} \vec{p}, \quad (4.22)$$

$$\omega_\Phi = \frac{|\vec{r} \times \dot{\vec{r}}|}{r^2}. \quad (4.23)$$

E here means the energy of the binary system. E decreases due to the gravitational wave, $\frac{dE}{dt} < 0$. The negative sign corresponds to dissipation. For quasi-circular cases without precession, since $|\vec{r} \times \dot{\vec{r}}| \approx \dot{p}_\phi$ our above relation reduces to

$$\vec{\mathcal{F}} = \frac{1}{M\eta\omega_\Phi} \frac{dE}{dt} \frac{\vec{p}}{\dot{p}_\phi}, \quad (4.24)$$

which is used by SEOBNR series waveform models.

Together with the force $\vec{\mathcal{F}}$, the whole EOB dynamics becomes

$$\dot{\vec{r}} = \frac{\partial H}{\partial \vec{p}}, \quad (4.25)$$

$$\dot{\vec{p}} = -\frac{\partial H}{\partial \vec{r}} + \vec{\mathcal{F}}. \quad (4.26)$$

So the above dynamical equations coupled to waveform are self-contained. Along the evolution of the dynamics, the waveform in time can be constructed. This is the basic strategy of our SEOBNRE waveform models. Through comparing to numerical relativity simulations, we find that our SEOBNRE waveform model works well for highly spinning ($\chi = 0.99$), highly eccentric (e_0 at $Mf_0 = 0.02$ can reach 0.7) and large mass ratio ($q \leq 10$) BBH. In the near future, we will use more numerical relativity simulations to test even larger mass ratio. Especially we expect our SEOBNRE model can work for the whole mass ratio range [784].

4.3 GW memory models for compact binaries

The same as other waveform models, our SEOBNRE described in the last section does not include $m = 0$ modes. Such modes are closely related to the GW memory. GW memory is an interesting prediction of GR. The detection of the GW memory can be used to test GR and to recover the property of the GW source. A quantitative model is needed for such detection and parameters reconstruction.

In [807] we borrowed the idea of SEOBNR waveform models for the non-memory mode to divide the $(2, 0)$ waveform mode into three segments including inspiral, merger, and ringdown. The inspiral part uses the PN approximation. The ringdown part uses the quasi-normal modes. Due to the memory effect, the quasi-normal modes oscillate around a final memory value instead of 0. The merger part is the most difficult part to model. Not like the non-memory modes, the inspiral waveform can join the ringdown waveform perfectly. For $(2, 0)$ mode, there is a jump between the inspiral waveform and the final ringdown waveform. This is why we introduce a stand-alone merger segment in [807].

The post-Newtonian approximation for GW memory reads [808, 809]

$$\begin{aligned}
 h^{(\text{mem})} &= \sum_{l=2}^{\infty} \sum_{m=-l}^l h_{(\text{mem})-2}^{lm} Y_{lm}(\theta, \phi), \\
 h_{(\text{mem})}^{lm} &= R \sqrt{\frac{(l-2)!}{(l+2)!}} \sum_{l'=2}^{\infty} \sum_{l''=2}^{\infty} \sum_{m'=-l'}^{l'} \sum_{m''=-l''}^{l''} (-1)^{m+m''} \\
 &\times \int_{-\infty}^t \langle \dot{h}_{l'm'} \dot{\bar{h}}_{l''m''} \rangle dt' \int {}_2Y_{l'm'-2} \bar{Y}_{l''m''} \bar{Y}_{lm} d\Omega.
 \end{aligned} \tag{4.27}$$

$$\tag{4.28}$$

The angle-bracket $\langle \dots \rangle$ in the above equation means the average over several wavelengths. Here θ and ϕ are the angular coordinates of the detector. R is the luminosity distance of the GW source. Y_{lm} and ${}_2Y_{lm}$ are the usual spherical harmonic function and the spin weighted spherical harmonic function with spin-weight -2 , respectively. h_{lm} are the spin weighted spherical harmonic modes of the non-memory part of the GW. The dot means the time derivative. The overbar means the complex conjugate. Note that h_{lm} is proportional to $\frac{1}{R}$. Therefore $h_{(\text{mem})}^{lm}$ behaves as $\frac{1}{R}$ also.

The non-memory part of PN waveform can be written as [the Eq. (B1) of [808]]

$$h_{lm} = 8 \sqrt{\frac{\pi}{5}} \frac{\eta M x}{R} e^{-im\psi} \hat{h}_{lm}. \tag{4.29}$$

Here $x = (M\omega)^{2/3}$ is the PN parameter with ω the orbital frequency. The phase variable ψ is related to orbital phase φ through [the Eq. (B2) of [808]]

$$\psi = \varphi - 3x^{3/2} \left[1 - \frac{\eta}{2} x \right] \ln\left(\frac{x}{x_0}\right), \tag{4.30}$$

$$\ln x_0 = \frac{11}{18} - \frac{2}{3} \gamma_E - \frac{4}{3} \ln 2, \tag{4.31}$$

where γ_E is Euler's constant with approximated value 0.577216. The time t and the PN parameter x can be related through

$$\frac{dx}{dt} = \frac{-\mathcal{F}}{dE/dx}, \tag{4.32}$$

where \mathcal{F} is the GW luminosity and E the orbital energy. Then we can reduce Eq. (4.28) to

$$h_{(\text{mem})}^{lm} = R \sqrt{\frac{(l-2)!}{(l+2)!}} \sum_{l'=2}^{\infty} \sum_{l''=2}^{\infty} \sum_{m'=-l'}^{l'} \sum_{m''=-l''}^{l''} (-1)^{m+m''} \int_0^x \left\langle \frac{dh_{l'm'}}{dx'} \frac{d\bar{h}_{l''m''}}{dx'} \right\rangle > \frac{dx'}{dt} dx' \int {}_2Y_{l'm'-2} \bar{Y}_{l''m''} \bar{Y}_{lm} d\Omega, \quad (4.33)$$

where we have used x' to denote the dummy integration variable.

Combining all above results we achieve

$$\begin{aligned} \frac{R}{M} h_{20}^{(\text{mem})} = & \frac{4}{7} \sqrt{\frac{5\pi}{6}} \eta x \left\{ 1 + x \left(-\frac{4075}{4032} + \frac{67}{48} \eta \right) \right. \\ & \left. + x^{3/2} \left(\frac{-2813 + 756\eta}{2400} \chi_S + \frac{3187}{2400} \delta\chi_A \right) \right\}. \end{aligned} \quad (4.34)$$

This is the inspiral segment of the memory waveform model we constructed in [807].

Now we come to the quasi-normal segment of the memory waveform. Respect to time we identify this part as the one after the peak of the (2,2) mode. Different to the $m \neq 0$ quasi-normal modes model, the QNM oscillates around a nonzero value due to the “memory” effect. This nonzero “memory” value h_{20}^{∞} (corresponding to the notation h_{20}^{tot} of [810, 811]) has been investigated in [810] for equal mass non-precession binary black hole mergers

$$\begin{aligned} \frac{R}{M} h_{20}^{\infty} = & 0.0996 + 0.0562\chi_S + 0.0340\chi_S^2 \\ & + 0.0296\chi_S^3 + 0.0206\chi_S^4. \end{aligned} \quad (4.35)$$

One caution is in order for the above equation. The numerical relativity results in [810] only include equal mass BBH. So the above equation is only valid for equal mass BBH cases. We have extended the above results to general spin-aligned binary black hole mergers in [811]

$$\begin{aligned} \frac{D}{M} h_{20}^{\infty} = & [0.0969 + 0.0562\chi_{\text{up}} + 0.0340\chi_{\text{up}}^2 \\ & + 0.0296\chi_{\text{up}}^3 + 0.0206\chi_{\text{up}}^4] (4\eta)^{1.65}. \end{aligned} \quad (4.36)$$

$$\chi_{\text{up}} \equiv \chi_{\text{eff}} + \frac{3}{8} \sqrt{1 - 4\eta\chi_A}. \quad (4.37)$$

The above result only considers the asymptotic memory value. Respect to time, the center value of the QNM oscillation increases gradually. In order to find out this gradual increasing behavior, we first construct a simple QNM model for (2, 0) as following

$$\frac{R}{M} h_{20, QNM} = \frac{R}{M} h_{20}^{\infty} - \rho e^{-\frac{t-T_R}{\tau_{200}}} \cos[\omega_{200}(t - T_R)], \quad (4.38)$$

where T_R describes the time when the ringdown waveform begins, ρ describes the amplitude of the QNM. $\sigma_{200} = \frac{1}{\tau_{200}} + i\omega_{200}$ corresponds to the complex frequency of the quasi-normal mode $l = 2, m = 0, n = 0$. The final mass and the final spin of the binary black hole merger can be determined by the initial parameters of the two black holes.

We have fine tuned the parameters h_{20}^∞ , ρ and T_R in Eq. (4.38) to best fit the numerical relativity results of [810]

$$\begin{aligned} \rho = & 0.41667\chi_S^4 - 0.52083\chi_S^3 \\ & + 0.19583\chi_S^2 - 0.036667\chi_S + 0.015, \end{aligned} \quad (4.39)$$

$$\begin{aligned} T_R = & 528.65\chi_S^4 - 751.04\chi_S^3 \\ & + 326.35\chi_S^2 - 42.958\chi_S + 2.5. \end{aligned} \quad (4.40)$$

It is interesting to ask whether these fitted parameters work for the numerical relativity results of [812, 813]. That's our future work.

Although we have constructed a simple model for the merger part of memory waveform, it's not good enough we think. So we do not describe that part in detail here. The interesting readers can refer [807] for the detail.

In [811] we designed a new method to accurately calculate the memory. Our method does not need slow motion and weak field approximations of GW sources. Our method can accurately calculate memory based on non-memory waveform. Many work including [808, 814–818] applied the above PN results (4.28) to binary black hole merger to get the gravitational waveform of memory. And later this GW memory waveform was used to analyze LIGO data [819–822]. In [811] we use our accurate calculation method to confirm that this naive approximated waveform for memory is quite accurate till merger actually.

Using Bondi-Sachs (BS) coordinate (u, r, θ, ϕ) , Bondi-Metzner-Sachs (BMS) theory describes gravitational radiation with the concept of null infinity. Here u corresponds to the time of observer very far away from the GW source. In BMS theory, the GW source is looked as an isolated spacetime. The gravitational waveform depends only on (u, θ, ϕ) . And more the waveform is proportional to $\frac{1}{D}$ where D is the luminosity distance. For simplicity we use notation ' t ' for the Bondi time $t = u$. Aided with some mathematical skills and after a tedious calculation, we get for $l \geq 2$

$$\begin{aligned} h_{lm} \Big|_{t_1}^{t_2} = & -\sqrt{\frac{(l-2)!}{(l+2)!}} \left[\frac{4}{D} \int \Psi_2^\circ [{}^0Y_{lm}] \sin \theta d\theta d\phi \Big|_{t_1}^{t_2} - \right. \\ & D \sum_{l'=2}^{\infty} \sum_{l''=2}^{\infty} \sum_{m'=-l'}^{l'} \sum_{m''=-l''}^{l''} \Gamma_{l'l''lm'-m''-m} \times \\ & \left. \left(\int_{t_1}^{t_2} \dot{h}_{l'm'} \dot{\bar{h}}_{l''m''} dt - \dot{h}_{l'm'}(t_2) \bar{h}_{l''m''}(t_2) + \dot{h}_{l'm'}(t_1) \bar{h}_{l''m''}(t_1) \right) \right], \end{aligned} \quad (4.41)$$

This set of coupled equations can be looked as unknowns h_{l0} respect to $h_{lm}, m \neq 0$. The GW memory is dominated by modes h_{l0} for non-precession binary black holes. That is why h_{l0} are called GW memory modes and $h_{lm}, m \neq 0$ are called non-memory modes.

Because $\dot{h}_{l0} \approx 0$ [808], we get

$$\begin{aligned}
h_{l0} \Big|_{t_1}^{t_2} &= -\sqrt{\frac{(l-2)!}{(l+2)!}} \Re \left[\frac{4}{D} \int \Psi_2^\circ[{}^0Y_{l0}] \sin \theta d\theta d\phi \Big|_{t_1}^{t_2} - \right. \\
D \sum_{l'=2}^{\infty} \sum_{l''=2}^{\infty} \sum_{\substack{m'=-l', \\ m' \neq 0}}^{l'} \sum_{\substack{m''=-l'', \\ m'' \neq 0}}^{l''} \Gamma_{l'l''lm'-m''0} \times \\
&\left. \left(\int_{t_1}^{t_2} \dot{h}_{l'm'} \dot{\bar{h}}_{l''m''} dt - \dot{h}_{l'm'}(t_2) \bar{h}_{l''m''}(t_2) + \right. \right. \\
&\quad \left. \left. \dot{h}_{l'm'}(t_1) \bar{h}_{l''m''}(t_1) \right) \right]. \tag{4.42}
\end{aligned}$$

In the mass center frame of the whole system, we have $\Psi_2^\circ(-\infty, \theta, \phi) = M_0$. Here M_0 corresponds to the Bondi mass and also ADM mass [823]. Later, the Bondi mass M decreases because the GW carries out some energy E_{GW} , $M = M_0 - E_{\text{GW}}$. The spacetime will at last become a Kerr black hole with mass \tilde{M} . But the mass center frame of the Kerr black hole is different from the mass center frame at beginning due to the kick velocity. These two asymptotic inertial frames are related by a boost transformation. So we have $\tilde{M} = M/\gamma$, where γ is the Lorentz factor.

Since the kick velocity is small $v \ll c$, the contribution $\dot{h}_{l'm'} \bar{h}_{l''m''} \Big|_{t_1}^{t_2}$ is small, our Eq. (4.42) recovers the PN approximation result (4.28). Detail investigations done in [811] the corrections introduced by kick velocity \vec{v} are negligible for the whole inspiral-merger-ringdown process. Such corrections contribute between 0.01% and 1% for all kinds of spin-aligned binary black holes.

But we need to note that the accurately calculated waveform for memory (4.42) can not capture the behavior of quasi-normal ringing. So it is interesting to combine the above results (4.38) and (4.42) together to construct a complete waveform for memory. After that add these $m = 0$ modes into our SEOBNRE waveform model to get a most general waveform model for binary black hole systems. When such tasks are done, the waveform of binary black holes with arbitrary mass ratio, arbitrary spin, and arbitrary orbit shape can be described by our SEOBNRE waveform model. Then naturally it can work for GW data analysis for space detectors.

5 Conclusions

In this brief review, we have summarized the important progress of GW studies over the past five years but with a special focus on some of our own work within a key project supported by the National Natural Science Foundation of China, due to the limited time and space, compared to the massive literature in this field, for which we should apologize sincerely here if we have missed any such important papers. The main results we achieved are summarized below:

(1) We have carried out a 3D numerical simulation for the phase transition involving a gauge field to account for the primordial magnetic field. We have found a new GW generation mechanism from preheating with a cuspy potential. We have studied the induced GWs from non-Gaussian curvature perturbations. We have found large anisotropies in the stochastic GW background from cosmic domain walls. We have proposed LISA-Taiji network for a joint

detection and fast and accurate localization of GW events, which also doubles the number of EM counterparts compared to a single Taiji mission so as to provide much tighter constraints on cosmological parameters.

(2) We have obtained strong constraints on the neutron star maximum mass by using the GW and electromagnetic observations of GW170817 with consideration of different EOSs. We have also helped to organize the Chinese-PTA collaboration to search for nano-Hertz GW radiation and investigated the detection of individual SMBBHs by current and future PTAs.

(3) We have developed finite element numerical relativity algorithm and a waveform model SEOBNRE for binary black hole coalescence along an eccentric orbit.

As the flourishing progress has been made from the scientific side, the engineering side has also achieved significant progress. In 2015 the LISA pathfinder was launched with great success. In 2019, two Chinese space-borne GW detector projects, Taiji and TianQin, also launched Taiji-1 and TianQin-1 separately, going the first step to GW detection in space. By the time of the 2030s, it is expected that the space-based GW detectors will run in space. Certainly, updated ground-based GW detectors, PTA measurements and even B-mode polarization measurements of CMB will give us unexpected surprises in a near future. By the time, one is able to resolve those important theoretical issues in GW cosmology and GW astrophysics from the possible detections of massive binary coalescence events, EMRIs events, SMBBHs event, GWs from preheating and first-order phase transition, induced GWs background, and more GW events with EM counterparts.

Acknowledgments

This review is a status progress report supported by the National Natural Science Foundation of China Grants No.11690021, No.11690022, No.11690023, No.11690024.

References

- [1] LIGO SCIENTIFIC, VIRGO collaboration, B. P. Abbott et al., *Observation of Gravitational Waves from a Binary Black Hole Merger*, *Phys. Rev. Lett.* **116** (2016) 061102, [[1602.03837](#)].
- [2] LIGO SCIENTIFIC, VIRGO collaboration, B. P. Abbott et al., *GW170817: Observation of Gravitational Waves from a Binary Neutron Star Inspiral*, *Phys. Rev. Lett.* **119** (2017) 161101, [[1710.05832](#)].
- [3] LIGO SCIENTIFIC, VIRGO collaboration, B. P. Abbott et al., *GWTC-1: A Gravitational-Wave Transient Catalog of Compact Binary Mergers Observed by LIGO and Virgo during the First and Second Observing Runs*, *Phys. Rev. X* **9** (2019) 031040, [[1811.12907](#)].
- [4] LIGO SCIENTIFIC, VIRGO collaboration, R. Abbott et al., *GWTC-2: Compact Binary Coalescences Observed by LIGO and Virgo During the First Half of the Third Observing Run*, [2010.14527](#).
- [5] R. Nan, D. Li, C. Jin, Q. Wang, L. Zhu, W. Zhu et al., *The Five-Hundred Aperture Spherical Radio Telescope (fast) Project*, *Int. J. Mod. Phys. D* **20** (Jan., 2011) 989–1024, [[1105.3794](#)].
- [6] D. Li, P. Wang, L. Qian, M. Krco, P. Jiang, Y. Yue et al., *FAST in Space: Considerations for a Multibeam, Multipurpose Survey Using China’s 500-m Aperture Spherical Radio Telescope (FAST)*, *IEEE Microwave Magazine* **19** (Apr., 2018) 112–119, [[1802.03709](#)].
- [7] M. Punturo et al., *The Einstein Telescope: A third-generation gravitational wave observatory*, *Class. Quant. Grav.* **27** (2010) 194002.

- [8] LIGO SCIENTIFIC collaboration, B. P. Abbott et al., *Exploring the Sensitivity of Next Generation Gravitational Wave Detectors*, *Class. Quant. Grav.* **34** (2017) 044001, [[1607.08697](#)].
- [9] M. Armano et al., *Sub-Femto- g Free Fall for Space-Based Gravitational Wave Observatories: LISA Pathfinder Results*, *Phys. Rev. Lett.* **116** (2016) 231101.
- [10] LISA collaboration, P. Amaro-Seoane et al., *Laser Interferometer Space Antenna*, [1702.00786](#).
- [11] W.-R. Hu and Y.-L. Wu, *The Taiji Program in Space for gravitational wave physics and the nature of gravity*, *Natl. Sci. Rev.* **4** (2017) 685–686.
- [12] W.-H. Ruan, Z.-K. Guo, R.-G. Cai and Y.-Z. Zhang, *Taiji program: Gravitational-wave sources*, *Int. J. Mod. Phys. A* **35** (2020) 2050075, [[1807.09495](#)].
- [13] TAIJI SCI COLLABORATION collaboration, Y.-L. Wu, Z.-R. Luo, J.-Y. Wang et al., *China’s first step towards probing the expanding universe and the nature of gravity using a space borne gravitational wave antenna*, *COMMUNICATIONS PHYSICS* **4** (2021) 34.
- [14] X.-F. Gong et al., *A scientific case study of an advanced LISA mission*, *Class. Quant. Grav.* **28** (2011) 094012.
- [15] X. Gong et al., *Descope of the ALIA mission*, *J. Phys. Conf. Ser.* **610** (2015) 012011, [[1410.7296](#)].
- [16] X. Gong, S. Xu, S. Gui, S. Huang and Y.-K. Lau, *Mission Design for the TAIJI mission and Structure Formation in Early Universe*, [2104.05033](#).
- [17] TIANQIN collaboration, J. Luo et al., *TianQin: a space-borne gravitational wave detector*, *Class. Quant. Grav.* **33** (2016) 035010, [[1512.02076](#)].
- [18] J. Luo et al., *The first round result from the TianQin-1 satellite*, *Class. Quant. Grav.* **37** (2020) 185013, [[2008.09534](#)].
- [19] TIANQIN collaboration, J. Mei et al., *The TianQin project: current progress on science and technology*, *Progress of Theoretical and Experimental Physics* **2021** (5, 2021) , [[2008.10332](#)].
- [20] S. Kawamura et al., *The Japanese space gravitational wave antenna DECIGO*, *Class. Quant. Grav.* **23** (2006) S125–S132.
- [21] S. Kawamura et al., *The Japanese space gravitational wave antenna: DECIGO*, *Class. Quant. Grav.* **28** (2011) 094011.
- [22] J. Crowder and N. J. Cornish, *Beyond LISA: Exploring future gravitational wave missions*, *Phys. Rev. D* **72** (2005) 083005, [[gr-qc/0506015](#)].
- [23] R.-G. Cai, Z. Cao, Z.-K. Guo, S.-J. Wang and T. Yang, *The Gravitational-Wave Physics*, *Natl. Sci. Rev.* **4** (2017) 687–706, [[1703.00187](#)].
- [24] LIGO SCIENTIFIC, KAGRA, VIRGO collaboration, R. Abbott et al., *Observation of Gravitational Waves from Two Neutron Star–Black Hole Coalescences*, *Astrophys. J. Lett.* **915** (2021) L5, [[2106.15163](#)].
- [25] NANOGrav collaboration, Z. Arzoumanian et al., *The NANOGrav 12.5 yr Data Set: Search for an Isotropic Stochastic Gravitational-wave Background*, *Astrophys. J. Lett.* **905** (2020) L34, [[2009.04496](#)].
- [26] LIGO SCIENTIFIC, VIRGO collaboration, B. P. Abbott et al., *Tests of general relativity with GW150914*, *Phys. Rev. Lett.* **116** (2016) 221101, [[1602.03841](#)].
- [27] LIGO SCIENTIFIC, VIRGO collaboration, B. P. Abbott et al., *Astrophysical Implications of the Binary Black-Hole Merger GW150914*, *Astrophys. J. Lett.* **818** (2016) L22, [[1602.03846](#)].

- [28] LIGO SCIENTIFIC, VIRGO collaboration, B. P. Abbott et al., *GW150914: Implications for the stochastic gravitational wave background from binary black holes*, *Phys. Rev. Lett.* **116** (2016) 131102, [[1602.03847](#)].
- [29] LIGO SCIENTIFIC, VIRGO, FERMI GBM, INTEGRAL, ICECUBE, ASTROSAT CADMIUM ZINC TELLURIDE IMAGER TEAM, IPN, INSIGHT-HXMT, ANTARES, SWIFT, AGILE TEAM, 1M2H TEAM, DARK ENERGY CAMERA GW-EM, DES, DLT40, GRAWITA, FERMI-LAT, ATCA, ASKAP, LAS CUMBRES OBSERVATORY GROUP, OzGRAV, DWF (DEEPER WIDER FASTER PROGRAM), AST3, CAASTRO, VINROUGE, MASTER, J-GEM, GROWTH, JAGWAR, CALTECHNRAO, TTU-NRAO, NUSTAR, PAN-STARRS, MAXI TEAM, TZAC CONSORTIUM, KU, NORDIC OPTICAL TELESCOPE, EPESSTO, GROND, TEXAS TECH UNIVERSITY, SALT GROUP, TOROS, BOOTES, MWA, CALET, IKI-GW FOLLOW-UP, H.E.S.S., LOFAR, LWA, HAWC, PIERRE AUGER, ALMA, EURO VLBI TEAM, PI OF SKY, CHANDRA TEAM AT MCGILL UNIVERSITY, DFN, ATLAS TELESCOPES, HIGH TIME RESOLUTION UNIVERSE SURVEY, RIMAS, RATIR, SKA SOUTH AFRICA/MEERKAT collaboration, B. P. Abbott et al., *Multi-messenger Observations of a Binary Neutron Star Merger*, *Astrophys. J. Lett.* **848** (2017) L12, [[1710.05833](#)].
- [30] LIGO SCIENTIFIC, VIRGO, FERMI-GBM, INTEGRAL collaboration, B. P. Abbott et al., *Gravitational Waves and Gamma-rays from a Binary Neutron Star Merger: GW170817 and GRB 170817A*, *Astrophys. J. Lett.* **848** (2017) L13, [[1710.05834](#)].
- [31] LIGO SCIENTIFIC, VIRGO, 1M2H, DARK ENERGY CAMERA GW-E, DES, DLT40, LAS CUMBRES OBSERVATORY, VINROUGE, MASTER collaboration, B. P. Abbott et al., *A gravitational-wave standard siren measurement of the Hubble constant*, *Nature* **551** (2017) 85–88, [[1710.05835](#)].
- [32] LIGO SCIENTIFIC, VIRGO collaboration, B. P. Abbott et al., *GW170817: Measurements of neutron star radii and equation of state*, *Phys. Rev. Lett.* **121** (2018) 161101, [[1805.11581](#)].
- [33] LIGO SCIENTIFIC, VIRGO collaboration, B. P. Abbott et al., *Tests of General Relativity with GW170817*, *Phys. Rev. Lett.* **123** (2019) 011102, [[1811.00364](#)].
- [34] LIGO SCIENTIFIC, VIRGO collaboration, B. P. Abbott et al., *GW170817: Implications for the Stochastic Gravitational-Wave Background from Compact Binary Coalescences*, *Phys. Rev. Lett.* **120** (2018) 091101, [[1710.05837](#)].
- [35] NANOGrav collaboration, Z. Arzoumanian et al., *The NANOGrav 12.5 yr Data Set: Search for an Isotropic Stochastic Gravitational-wave Background*, *Astrophys. J. Lett.* **905** (2020) L34, [[2009.04496](#)].
- [36] A. Mazumdar and G. White, *Review of cosmic phase transitions: their significance and experimental signatures*, *Rept. Prog. Phys.* **82** (2019) 076901, [[1811.01948](#)].
- [37] M. B. Hindmarsh, M. Lüben, J. Lumma and M. Pauly, *Phase transitions in the early universe*, *SciPost Phys. Lect. Notes* **24** (2021) 1, [[2008.09136](#)].
- [38] P. Binetruy, A. Bohe, C. Caprini and J.-F. Dufaux, *Cosmological Backgrounds of Gravitational Waves and eLISA/NGO: Phase Transitions, Cosmic Strings and Other Sources*, *JCAP* **1206** (2012) 027, [[1201.0983](#)].
- [39] P. Amaro-Seoane et al., *Low-frequency gravitational-wave science with eLISA/NGO*, *Class. Quant. Grav.* **29** (2012) 124016, [[1202.0839](#)].
- [40] P. Amaro-Seoane et al., *eLISA/NGO: Astrophysics and cosmology in the gravitational-wave millihertz regime*, *GW Notes* **6** (2013) 4–110, [[1201.3621](#)].
- [41] C. Caprini et al., *Science with the space-based interferometer eLISA. II: Gravitational waves from cosmological phase transitions*, *JCAP* **1604** (2016) 001, [[1512.06239](#)].

- [42] C. Caprini et al., *Detecting gravitational waves from cosmological phase transitions with LISA: an update*, *JCAP* **2003** (2020) 024, [[1910.13125](#)].
- [43] D. J. Weir, *Gravitational waves from a first order electroweak phase transition: a brief review*, *Phil. Trans. Roy. Soc. Lond.* **A376** (2018) 20170126, [[1705.01783](#)].
- [44] R.-G. Cai and S.-J. Wang, *Effective picture of bubble expansion*, *JCAP* **2021** (2021) 096, [[2011.11451](#)].
- [45] Y. Di, J. Wang, R. Zhou, L. Bian, R.-G. Cai and J. Liu, *Magnetic field and gravitational waves from the first-order Phase Transition*, *Phys. Rev. Lett.* *accepted* (2020) , [[2012.15625](#)].
- [46] J. Liu, R.-G. Cai and Z.-K. Guo, *Large Anisotropies of the Stochastic Gravitational Wave Background from Cosmic Domain Walls*, *Phys. Rev. Lett.* **126** (2021) 141303, [[2010.03225](#)].
- [47] S. R. Coleman, *The Fate of the False Vacuum. 1. Semiclassical Theory*, *Phys. Rev.* **D15** (1977) 2929–2936.
- [48] C. G. Callan, Jr. and S. R. Coleman, *The Fate of the False Vacuum. 2. First Quantum Corrections*, *Phys. Rev.* **D16** (1977) 1762–1768.
- [49] A. D. Linde, *Fate of the False Vacuum at Finite Temperature: Theory and Applications*, *Phys. Lett.* **100B** (1981) 37–40.
- [50] A. D. Linde, *Decay of the False Vacuum at Finite Temperature*, *Nucl. Phys.* **B216** (1983) 421.
- [51] D. Cutting, M. Hindmarsh and D. J. Weir, *Gravitational waves from vacuum first-order phase transitions: from the envelope to the lattice*, *Phys. Rev.* **D97** (2018) 123513, [[1802.05712](#)].
- [52] L. Leitao and A. Megevand, *Gravitational waves from a very strong electroweak phase transition*, *JCAP* **1605** (2016) 037, [[1512.08962](#)].
- [53] A. Megevand and S. Ramirez, *Bubble nucleation and growth in very strong cosmological phase transitions*, *Nucl. Phys. B* **919** (2017) 74–109, [[1611.05853](#)].
- [54] R. Jinno, S. Lee, H. Seong and M. Takimoto, *Gravitational waves from first-order phase transitions: Towards model separation by bubble nucleation rate*, *JCAP* **1711** (2017) 050, [[1708.01253](#)].
- [55] L. Leitao, A. Megevand and A. D. Sanchez, *Gravitational waves from the electroweak phase transition*, *JCAP* **1210** (2012) 024, [[1205.3070](#)].
- [56] J. Ellis, M. Lewicki and J. M. No, *On the Maximal Strength of a First-Order Electroweak Phase Transition and its Gravitational Wave Signal*, *JCAP* **04** (2019) 003, [[1809.08242](#)].
- [57] J. Ellis, M. Lewicki and J. M. No, *Gravitational waves from first-order cosmological phase transitions: lifetime of the sound wave source*, *JCAP* **2007** (2020) 050, [[2003.07360](#)].
- [58] X. Wang, F. P. Huang and X. Zhang, *Phase transition dynamics and gravitational wave spectra of strong first-order phase transition in supercooled universe*, *JCAP* **2005** (2020) 045, [[2003.08892](#)].
- [59] A. Kobakhidze, C. Lagger, A. Manning and J. Yue, *Gravitational waves from a supercooled electroweak phase transition and their detection with pulsar timing arrays*, *Eur. Phys. J.* **C77** (2017) 570, [[1703.06552](#)].
- [60] R.-G. Cai, M. Sasaki and S.-J. Wang, *The gravitational waves from the first-order phase transition with a dimension-six operator*, *JCAP* **1708** (2017) 004, [[1707.03001](#)].
- [61] A. H. Guth and E. J. Weinberg, *Could the Universe Have Recovered from a Slow First Order Phase Transition?*, *Nucl. Phys. B* **212** (1983) 321–364.
- [62] M. S. Turner, E. J. Weinberg and L. M. Widrow, *Bubble nucleation in first order inflation and other cosmological phase transitions*, *Phys. Rev. D* **46** (1992) 2384–2403.

- [63] M. J. Baker, M. Breitbach, J. Kopp and L. Mittnacht, *Primordial Black Holes from First-Order Cosmological Phase Transitions*, [2105.07481](#).
- [64] K. Kawana and K.-P. Xie, *Primordial black holes from a cosmic phase transition: The collapse of Fermi-balls*, [2106.00111](#).
- [65] J. Liu, L. Bian, R.-G. Cai, Z.-K. Guo and S.-J. Wang, *Primordial black hole production during first-order phase transitions*, [2106.05637](#).
- [66] S. R. Coleman and F. De Luccia, *Gravitational Effects on and of Vacuum Decay*, *Phys. Rev. D* **21** (1980) 3305.
- [67] B.-H. Lee, W. Lee, D.-h. Yeom and L. Yin, *Gravitational waves from the vacuum decay with eLISA*, [2106.07430](#).
- [68] C. Baccigalupi, L. Amendola, P. Fortini and F. Occhionero, *The Stochastic gravitational background from inflationary phase transitions*, *Phys. Rev. D* **56** (1997) 4610–4617, [[gr-qc/9709044](#)].
- [69] D. Chialva, *Gravitational waves from first order phase transitions during inflation*, *Phys. Rev. D* **83** (2011) 023512, [[1004.2051](#)].
- [70] H. Jiang, T. Liu, S. Sun and Y. Wang, *Echoes of Inflationary First-Order Phase Transitions in the CMB*, *Phys. Lett. B* **765** (2017) 339–343, [[1512.07538](#)].
- [71] H. An, K.-F. Lyu, L.-T. Wang and S. Zhou, *A unique gravitational wave signal from phase transition during inflation*, [2009.12381](#).
- [72] G. Barenboim and W.-I. Park, *Gravitational waves from first order phase transitions as a probe of an early matter domination era and its inverse problem*, *Phys. Lett. B* **759** (2016) 430–438, [[1605.03781](#)].
- [73] J. Ellis, M. Lewicki and V. Vaskonen, *Updated predictions for gravitational waves produced in a strongly supercooled phase transition*, *JCAP* **2011** (2020) 020, [[2007.15586](#)].
- [74] M. Artymowski, M. Lewicki and J. D. Wells, *Gravitational wave and collider implications of electroweak baryogenesis aided by non-standard cosmology*, *JHEP* **03** (2017) 066, [[1609.07143](#)].
- [75] J. R. Espinosa, T. Konstandin, J. M. No and G. Servant, *Energy Budget of Cosmological First-order Phase Transitions*, *JCAP* **1006** (2010) 028, [[1004.4187](#)].
- [76] J. Ellis, M. Lewicki, J. M. No and V. Vaskonen, *Gravitational wave energy budget in strongly supercooled phase transitions*, *JCAP* **1906** (2019) 024, [[1903.09642](#)].
- [77] H.-K. Guo, K. Sinha, D. Vagie and G. White, *Phase Transitions in an Expanding Universe: Stochastic Gravitational Waves in Standard and Non-Standard Histories*, *JCAP* **01** (2021) 001, [[2007.08537](#)].
- [78] R.-G. Cai and S.-J. Wang, *Energy budget of cosmological first-order phase transition in FLRW background*, *Sci. China Phys. Mech. Astron.* **61** (2018) 080411, [[1803.03002](#)].
- [79] L. Leitao and A. Megevand, *Hydrodynamics of phase transition fronts and the speed of sound in the plasma*, *Nucl. Phys. B* **891** (2015) 159–199, [[1410.3875](#)].
- [80] F. Giese, T. Konstandin and J. van de Vis, *Model-independent energy budget of cosmological first-order phase transitions: A sound argument to go beyond the bag model*, *JCAP* **2007** (2020) 057, [[2004.06995](#)].
- [81] F. Giese, T. Konstandin, K. Schmitz and J. Van De Vis, *Model-independent energy budget for LISA*, *JCAP* **01** (2021) 072, [[2010.09744](#)].
- [82] X. Wang, F. P. Huang and X. Zhang, *Energy budget and the gravitational wave spectra beyond the bag model*, *Phys. Rev. D* **103** (2021) 103520, [[2010.13770](#)].

- [83] N. Turok, *Electroweak bubbles: Nucleation and growth*, *Phys. Rev. Lett.* **68** (1992) 1803–1806.
- [84] M. Dine, R. G. Leigh, P. Y. Huet, A. D. Linde and D. A. Linde, *Towards the theory of the electroweak phase transition*, *Phys. Rev.* **D46** (1992) 550–571, [[hep-ph/9203203](#)].
- [85] B.-H. Liu, L. D. McLerran and N. Turok, *Bubble nucleation and growth at a baryon number producing electroweak phase transition*, *Phys. Rev.* **D46** (1992) 2668–2688.
- [86] G. D. Moore and T. Prokopec, *Bubble wall velocity in a first order electroweak phase transition*, *Phys. Rev. Lett.* **75** (1995) 777–780, [[hep-ph/9503296](#)].
- [87] G. D. Moore and T. Prokopec, *How fast can the wall move? A Study of the electroweak phase transition dynamics*, *Phys. Rev.* **D52** (1995) 7182–7204, [[hep-ph/9506475](#)].
- [88] G. D. Moore, *Electroweak bubble wall friction: Analytic results*, *JHEP* **03** (2000) 006, [[hep-ph/0001274](#)].
- [89] T. Konstandin, G. Nardini and I. Rues, *From Boltzmann equations to steady wall velocities*, *JCAP* **1409** (2014) 028, [[1407.3132](#)].
- [90] P. John and M. G. Schmidt, *Do stops slow down electroweak bubble walls?*, *Nucl. Phys.* **B598** (2001) 291–305, [[hep-ph/0002050](#)].
- [91] J. M. Cline, M. Joyce and K. Kainulainen, *Supersymmetric electroweak baryogenesis*, *JHEP* **07** (2000) 018, [[hep-ph/0006119](#)].
- [92] M. Carena, J. M. Moreno, M. Quiros, M. Seco and C. E. M. Wagner, *Supersymmetric CP violating currents and electroweak baryogenesis*, *Nucl. Phys.* **B599** (2001) 158–184, [[hep-ph/0011055](#)].
- [93] M. Carena, M. Quiros, M. Seco and C. E. M. Wagner, *Improved Results in Supersymmetric Electroweak Baryogenesis*, *Nucl. Phys.* **B650** (2003) 24–42, [[hep-ph/0208043](#)].
- [94] T. Konstandin, T. Prokopec, M. G. Schmidt and M. Seco, *MSSM electroweak baryogenesis and flavor mixing in transport equations*, *Nucl. Phys.* **B738** (2006) 1–22, [[hep-ph/0505103](#)].
- [95] V. Cirigliano, S. Profumo and M. J. Ramsey-Musolf, *Baryogenesis, Electric Dipole Moments and Dark Matter in the MSSM*, *JHEP* **07** (2006) 002, [[hep-ph/0603246](#)].
- [96] J. Kozaczuk, *Bubble Expansion and the Viability of Singlet-Driven Electroweak Baryogenesis*, *JHEP* **10** (2015) 135, [[1506.04741](#)].
- [97] G. C. Dorsch, S. J. Huber and T. Konstandin, *Bubble wall velocities in the Standard Model and beyond*, *JCAP* **1812** (2018) 034, [[1809.04907](#)].
- [98] B. Laurent and J. M. Cline, *Fluid equations for fast-moving electroweak bubble walls*, *Phys. Rev.* **D102** (2020) 063516, [[2007.10935](#)].
- [99] A. Friedlander, I. Banta, J. M. Cline and D. Tucker-Smith, *Wall speed and shape in singlet-assisted strong electroweak phase transitions*, *Phys. Rev. D* **103** (2021) 055020, [[2009.14295](#)].
- [100] X. Wang, F. P. Huang and X. Zhang, *Bubble wall velocity beyond leading-log approximation in electroweak phase transition*, [2011.12903](#).
- [101] Y. Bea, J. Casalderrey-Solana, T. Giannakopoulos, D. Mateos, M. Sanchez-Garitaonandia and M. Zilhao, *Bubble Wall Velocity from Holography*, [2104.05708](#).
- [102] F. Bigazzi, A. Caddeo, T. Canneti and A. L. Cotrone, *Bubble Wall Velocity at Strong Coupling*, [2104.12817](#).
- [103] J. Ignatius, K. Kajantie, H. Kurki-Suonio and M. Laine, *The growth of bubbles in cosmological phase transitions*, *Phys. Rev.* **D49** (1994) 3854–3868, [[astro-ph/9309059](#)].
- [104] H. Kurki-Suonio and M. Laine, *Real time history of the cosmological electroweak phase transition*, *Phys. Rev. Lett.* **77** (1996) 3951–3954, [[hep-ph/9607382](#)].

- [105] A. Megevand and A. D. Sanchez, *Detonations and deflagrations in cosmological phase transitions*, *Nucl. Phys.* **B820** (2009) 47–74, [[0904.1753](#)].
- [106] A. Megevand and A. D. Sanchez, *Velocity of electroweak bubble walls*, *Nucl. Phys.* **B825** (2010) 151–176, [[0908.3663](#)].
- [107] S. J. Huber and M. Sopena, *The bubble wall velocity in the minimal supersymmetric light stop scenario*, *Phys. Rev.* **D85** (2012) 103507, [[1112.1888](#)].
- [108] A. Megevand and A. D. Sanchez, *Analytic approach to the motion of cosmological phase transition fronts*, *Nucl. Phys. B* **865** (2012) 217–237, [[1206.2339](#)].
- [109] A. Megevand, *Friction forces on phase transition fronts*, *JCAP* **1307** (2013) 045, [[1303.4233](#)].
- [110] S. J. Huber and M. Sopena, *An efficient approach to electroweak bubble velocities*, [1302.1044](#).
- [111] D. Bodeker and G. D. Moore, *Can electroweak bubble walls run away?*, *JCAP* **0905** (2009) 009, [[0903.4099](#)].
- [112] D. Bodeker and G. D. Moore, *Electroweak Bubble Wall Speed Limit*, *JCAP* **1705** (2017) 025, [[1703.08215](#)].
- [113] M. Barroso Mancha, T. Prokopec and B. Swiezevska, *Field-theoretic derivation of bubble-wall force*, *JHEP* **01** (2021) 070, [[2005.10875](#)].
- [114] S. Höche, J. Kozaczuk, A. J. Long, J. Turner and Y. Wang, *Towards an all-orders calculation of the electroweak bubble wall velocity*, *JCAP* **03** (2021) 009, [[2007.10343](#)].
- [115] A. Azatov and M. Vanvlasselaer, *Bubble wall velocity: heavy physics effects*, *JCAP* **01** (2021) 058, [[2010.02590](#)].
- [116] A. Kosowsky, M. S. Turner and R. Watkins, *Gravitational radiation from colliding vacuum bubbles*, *Phys. Rev.* **D45** (1992) 4514–4535.
- [117] A. Kosowsky, M. S. Turner and R. Watkins, *Gravitational waves from first order cosmological phase transitions*, *Phys. Rev. Lett.* **69** (1992) 2026–2029.
- [118] A. Kosowsky and M. S. Turner, *Gravitational radiation from colliding vacuum bubbles: envelope approximation to many bubble collisions*, *Phys. Rev.* **D47** (1993) 4372–4391, [[astro-ph/9211004](#)].
- [119] M. Kamionkowski, A. Kosowsky and M. S. Turner, *Gravitational radiation from first order phase transitions*, *Phys. Rev.* **D49** (1994) 2837–2851, [[astro-ph/9310044](#)].
- [120] S. J. Huber and T. Konstandin, *Gravitational Wave Production by Collisions: More Bubbles*, *JCAP* **0809** (2008) 022, [[0806.1828](#)].
- [121] M. Hindmarsh, S. J. Huber, K. Rummukainen and D. J. Weir, *Gravitational waves from the sound of a first order phase transition*, *Phys. Rev. Lett.* **112** (2014) 041301, [[1304.2433](#)].
- [122] M. Hindmarsh, S. J. Huber, K. Rummukainen and D. J. Weir, *Numerical simulations of acoustically generated gravitational waves at a first order phase transition*, *Phys. Rev.* **D92** (2015) 123009, [[1504.03291](#)].
- [123] M. Hindmarsh, S. J. Huber, K. Rummukainen and D. J. Weir, *Shape of the acoustic gravitational wave power spectrum from a first order phase transition*, *Phys. Rev.* **D96** (2017) 103520, [[1704.05871](#)].
- [124] D. Cutting, M. Hindmarsh and D. J. Weir, *Vorticity, kinetic energy, and suppressed gravitational wave production in strong first order phase transitions*, *Phys. Rev. Lett.* **125** (2020) 021302, [[1906.00480](#)].
- [125] C. J. Hogan, *Gravitational radiation from cosmological phase transitions*, *Mon. Not. Roy. Astron. Soc.* **218** (1986) 629–636.

- [126] D. J. Weir, *Revisiting the envelope approximation: gravitational waves from bubble collisions*, *Phys. Rev.* **D93** (2016) 124037, [[1604.08429](#)].
- [127] E. Witten, *Cosmic Separation of Phases*, *Phys. Rev.* **D30** (1984) 272–285.
- [128] D. Cutting, E. G. Escartin, M. Hindmarsh and D. J. Weir, *Gravitational waves from vacuum first order phase transitions II: from thin to thick walls*, *Phys. Rev. D* **103** (2021) 023531, [[2005.13537](#)].
- [129] M. Lewicki and V. Vaskonen, *On bubble collisions in strongly supercooled phase transitions*, *Phys. Dark Univ.* **30** (2020) 100672, [[1912.00997](#)].
- [130] M. Lewicki and V. Vaskonen, *Gravitational wave spectra from strongly supercooled phase transitions*, *Eur. Phys. J.* **C80** (2020) 1003, [[2007.04967](#)].
- [131] P. Niksa, M. Schlexer and G. Sigl, *Gravitational Waves produced by Compressible MHD Turbulence from Cosmological Phase Transitions*, *Class. Quant. Grav.* **35** (2018) 144001, [[1803.02271](#)].
- [132] A. Roper Pol, S. Mandal, A. Brandenburg, T. Kahniashvili and A. Kosowsky, *Numerical simulations of gravitational waves from early-universe turbulence*, *Phys. Rev.* **D102** (2020) 083512, [[1903.08585](#)].
- [133] A. Brandenburg, E. Clarke, Y. He and T. Kahniashvili, *Can we observe the QCD phase transition-generated gravitational waves through pulsar timing arrays?*, [2102.12428](#).
- [134] A. Brandenburg, G. Gogoberidze, T. Kahniashvili, S. Mandal, A. Roper Pol and N. Shenoy, *The scalar, vector, and tensor modes in gravitational wave turbulence simulations*, [2103.01140](#).
- [135] T. Kahniashvili, G. Gogoberidze and B. Ratra, *Polarized cosmological gravitational waves from primordial helical turbulence*, *Phys. Rev. Lett.* **95** (2005) 151301, [[astro-ph/0505628](#)].
- [136] T. Kahniashvili, G. Gogoberidze and B. Ratra, *Gravitational Radiation from Primordial Helical MHD Turbulence*, *Phys. Rev. Lett.* **100** (2008) 231301, [[0802.3524](#)].
- [137] T. Kahniashvili, A. Kosowsky, G. Gogoberidze and Y. Maravin, *Detectability of Gravitational Waves from Phase Transitions*, *Phys. Rev.* **D78** (2008) 043003, [[0806.0293](#)].
- [138] T. Kahniashvili, L. Campanelli, G. Gogoberidze, Y. Maravin and B. Ratra, *Gravitational Radiation from Primordial Helical Inverse Cascade MHD Turbulence*, *Phys. Rev.* **D78** (2008) 123006, [[0809.1899](#)].
- [139] C. Caprini, R. Durrer and E. Fenu, *Can the observed large scale magnetic fields be seeded by helical primordial fields?*, *JCAP* **0911** (2009) 001, [[0906.4976](#)].
- [140] T. Kahniashvili, A. G. Tevzadze and B. Ratra, *Phase Transition Generated Cosmological Magnetic Field at Large Scales*, *Astrophys. J.* **726** (2011) 78, [[0907.0197](#)].
- [141] L. Kisslinger and T. Kahniashvili, *Polarized Gravitational Waves from Cosmological Phase Transitions*, *Phys. Rev.* **D92** (2015) 043006, [[1505.03680](#)].
- [142] A. Brandenburg, T. Kahniashvili, S. Mandal, A. Roper Pol, A. G. Tevzadze and T. Vachaspati, *Evolution of hydromagnetic turbulence from the electroweak phase transition*, *Phys. Rev.* **D96** (2017) 123528, [[1711.03804](#)].
- [143] T. Kahniashvili, A. Brandenburg, G. Gogoberidze, S. Mandal and A. Roper Pol, *Circular polarization of gravitational waves from early-Universe helical turbulence*, *Phys. Rev. Res.* **3** (2021) 013193, [[2011.05556](#)].
- [144] J. Ellis, M. Fairbairn, M. Lewicki, V. Vaskonen and A. Wickens, *Detecting circular polarisation in the stochastic gravitational-wave background from a first-order cosmological phase transition*, *JCAP* **2010** (2020) 032, [[2005.05278](#)].

- [145] C. Caprini, R. Durrer and G. Servant, *Gravitational wave generation from bubble collisions in first-order phase transitions: An analytic approach*, *Phys. Rev.* **D77** (2008) 124015, [[0711.2593](#)].
- [146] C. Caprini, R. Durrer, T. Konstandin and G. Servant, *General Properties of the Gravitational Wave Spectrum from Phase Transitions*, *Phys. Rev.* **D79** (2009) 083519, [[0901.1661](#)].
- [147] R. Jinno and M. Takimoto, *Gravitational waves from bubble collisions: An analytic derivation*, *Phys. Rev.* **D95** (2017) 024009, [[1605.01403](#)].
- [148] R. Jinno and M. Takimoto, *Gravitational waves from bubble dynamics: Beyond the Envelope*, *JCAP* **1901** (2019) 060, [[1707.03111](#)].
- [149] M. Hindmarsh, *Sound shell model for acoustic gravitational wave production at a first-order phase transition in the early Universe*, *Phys. Rev. Lett.* **120** (2018) 071301, [[1608.04735](#)].
- [150] M. Hindmarsh and M. Hijazi, *Gravitational waves from first order cosmological phase transitions in the Sound Shell Model*, *JCAP* **1912** (2019) 062, [[1909.10040](#)].
- [151] T. Konstandin, *Gravitational radiation from a bulk flow model*, *JCAP* **1803** (2018) 047, [[1712.06869](#)].
- [152] R. Jinno, H. Seong, M. Takimoto and C. M. Um, *Gravitational waves from first-order phase transitions: Ultra-supercooled transitions and the fate of relativistic shocks*, *JCAP* **1910** (2019) 033, [[1905.00899](#)].
- [153] R. Jinno, T. Konstandin and M. Takimoto, *Relativistic bubble collisions: a closer look*, *JCAP* **1909** (2019) 035, [[1906.02588](#)].
- [154] R. Jinno, T. Konstandin and H. Rubira, *A hybrid simulation of gravitational wave production in first-order phase transitions*, *JCAP* **04** (2021) 014, [[2010.00971](#)].
- [155] A. Kosowsky, A. Mack and T. Kahniashvili, *Gravitational radiation from cosmological turbulence*, *Phys. Rev.* **D66** (2002) 024030, [[astro-ph/0111483](#)].
- [156] A. D. Dolgov, D. Grasso and A. Nicolis, *Relic backgrounds of gravitational waves from cosmic turbulence*, *Phys. Rev.* **D66** (2002) 103505, [[astro-ph/0206461](#)].
- [157] A. Nicolis, *Relic gravitational waves from colliding bubbles and cosmic turbulence*, *Class. Quant. Grav.* **21** (2004) L27, [[gr-qc/0303084](#)].
- [158] C. Caprini and R. Durrer, *Gravitational waves from stochastic relativistic sources: Primordial turbulence and magnetic fields*, *Phys. Rev.* **D74** (2006) 063521, [[astro-ph/0603476](#)].
- [159] G. Gogoberidze, T. Kahniashvili and A. Kosowsky, *The Spectrum of Gravitational Radiation from Primordial Turbulence*, *Phys. Rev.* **D76** (2007) 083002, [[0705.1733](#)].
- [160] C. Caprini, R. Durrer and G. Servant, *The stochastic gravitational wave background from turbulence and magnetic fields generated by a first-order phase transition*, *JCAP* **0912** (2009) 024, [[0909.0622](#)].
- [161] T. Vachaspati, *Estimate of the primordial magnetic field helicity*, *Phys. Rev. Lett.* **87** (2001) 251302, [[astro-ph/0101261](#)].
- [162] R. Durrer and A. Neronov, *Cosmological Magnetic Fields: Their Generation, Evolution and Observation*, *Astron. Astrophys. Rev.* **21** (2013) 62, [[1303.7121](#)].
- [163] D. Grasso and H. R. Rubinstein, *Magnetic fields in the early universe*, *Phys. Rept.* **348** (2001) 163–266, [[astro-ph/0009061](#)].
- [164] K. Subramanian, *The origin, evolution and signatures of primordial magnetic fields*, *Rept. Prog. Phys.* **79** (2016) 076901, [[1504.02311](#)].
- [165] J. Garcia-Bellido, D. G. Figueroa and A. Sastre, *A Gravitational Wave Background from Reheating after Hybrid Inflation*, *Phys. Rev. D* **77** (2008) 043517, [[0707.0839](#)].

- [166] D. Croon, O. Gould, P. Schicho, T. V. I. Tenkanen and G. White, *Theoretical uncertainties for cosmological first-order phase transitions*, *JHEP* **04** (2021) 055, [[2009.10080](#)].
- [167] O. Gould and T. V. I. Tenkanen, *On the perturbative expansion at high temperature and implications for cosmological phase transitions*, [2104.04399](#).
- [168] A. Ekstedt and J. Lafgren, *A Critical Look at the Electroweak Phase Transition*, *JHEP* **12** (2020) 136, [[2006.12614](#)].
- [169] H.-K. Guo, K. Sinha, D. Vagie and G. White, *The Benefits of Diligence: How Precise are Predicted Gravitational Wave Spectra in Models with Phase Transitions?*, [2103.06933](#).
- [170] M. Losada, *High temperature dimensional reduction of the MSSM and other multiscalar models*, *Phys. Rev.* **D56** (1997) 2893–2913, [[hep-ph/9605266](#)].
- [171] J. M. Cline and P.-A. Lemieux, *Electroweak phase transition in two Higgs doublet models*, *Phys. Rev.* **D55** (1997) 3873–3881, [[hep-ph/9609240](#)].
- [172] M. Laine, *Effective theories of MSSM at high temperature*, *Nucl. Phys.* **B481** (1996) 43–84, [[hep-ph/9605283](#)].
- [173] D. Bodeker, P. John, M. Laine and M. G. Schmidt, *The Two loop MSSM finite temperature effective potential with stop condensation*, *Nucl. Phys.* **B497** (1997) 387–414, [[hep-ph/9612364](#)].
- [174] M. Laine and K. Rummukainen, *The MSSM electroweak phase transition on the lattice*, *Nucl. Phys.* **B535** (1998) 423–457, [[hep-lat/9804019](#)].
- [175] M. Laine, G. Nardini and K. Rummukainen, *Lattice study of an electroweak phase transition at $m_h \simeq 126$ GeV*, *JCAP* **1301** (2013) 011, [[1211.7344](#)].
- [176] M. Carena, G. Nardini, M. Quiros and C. E. M. Wagner, *MSSM Electroweak Baryogenesis and LHC Data*, *JHEP* **02** (2013) 001, [[1207.6330](#)].
- [177] T. Brauner, T. V. I. Tenkanen, A. Tranberg, A. Vuorinen and D. J. Weir, *Dimensional reduction of the Standard Model coupled to a new singlet scalar field*, *JHEP* **03** (2017) 007, [[1609.06230](#)].
- [178] J. O. Andersen, T. Gorda, A. Helset, L. Niemi, T. V. I. Tenkanen, A. Tranberg et al., *Nonperturbative Analysis of the Electroweak Phase Transition in the Two Higgs Doublet Model*, *Phys. Rev. Lett.* **121** (2018) 191802, [[1711.09849](#)].
- [179] L. Niemi, H. H. Patel, M. J. Ramsey-Musolf, T. V. I. Tenkanen and D. J. Weir, *Electroweak phase transition in the real triplet extension of the SM: Dimensional reduction*, *Phys. Rev.* **D100** (2019) 035002, [[1802.10500](#)].
- [180] T. Gorda, A. Helset, L. Niemi, T. V. I. Tenkanen and D. J. Weir, *Three-dimensional effective theories for the two Higgs doublet model at high temperature*, *JHEP* **02** (2019) 081, [[1802.05056](#)].
- [181] K. Kainulainen, V. Keus, L. Niemi, K. Rummukainen, T. V. I. Tenkanen and V. Vaskonen, *On the validity of perturbative studies of the electroweak phase transition in the Two Higgs Doublet model*, *JHEP* **06** (2019) 075, [[1904.01329](#)].
- [182] O. Gould, J. Kozaczuk, L. Niemi, M. J. Ramsey-Musolf, T. V. I. Tenkanen and D. J. Weir, *Nonperturbative analysis of the gravitational waves from a first-order electroweak phase transition*, *Phys. Rev.* **D100** (2019) 115024, [[1903.11604](#)].
- [183] P. M. Schicho, T. V. I. Tenkanen and J. Osterman, *Robust approach to thermal resummation: Standard Model meets a singlet*, [2102.11145](#).
- [184] T. Alanne, T. Hogle, M. Platscher and K. Schmitz, *A fresh look at the gravitational-wave signal from cosmological phase transitions*, *JHEP* **03** (2020) 004, [[1909.11356](#)].

- [185] K. Schmitz, *New Sensitivity Curves for Gravitational-Wave Signals from Cosmological Phase Transitions*, *JHEP* **01** (2021) 097, [2002.04615].
- [186] K. Schmitz, *LISA Sensitivity to Gravitational Waves from Sound Waves*, *Symmetry* **12** (2020) 1477, [2005.10789].
- [187] Y. Nakai, M. Suzuki, F. Takahashi and M. Yamada, *Gravitational Waves and Dark Radiation from Dark Phase Transition: Connecting NANOGrav Pulsar Timing Data and Hubble Tension*, *Phys. Lett. B* **816** (2021) 136238, [2009.09754].
- [188] A. Addazi, Y.-F. Cai, Q. Gan, A. Marciano and K. Zeng, *NANOGrav results and Dark First Order Phase Transitions*, 2009.10327.
- [189] W. Ratzinger and P. Schwaller, *Whispers from the dark side: Confronting light new physics with NANOGrav data*, *SciPost Phys.* **10** (2021) 047, [2009.11875].
- [190] L. Bian, R.-G. Cai, J. Liu, X.-Y. Yang and R. Zhou, *Evidence for different gravitational-wave sources in the NANOGrav dataset*, *Phys. Rev. D* **103** (2021) L081301, [2009.13893].
- [191] A. Neronov, A. Roper Pol, C. Caprini and D. Semikoz, *NANOGrav signal from magnetohydrodynamic turbulence at the QCD phase transition in the early Universe*, *Phys. Rev. D* **103** (2021) 041302, [2009.14174].
- [192] B. Barman, A. Dutta Banik and A. Paul, *Implications of NANOGrav results and UV freeze-in in a fast-expanding Universe*, 2012.11969.
- [193] C.-W. Chiang and B.-Q. Lu, *Testing clockwork axion with gravitational waves*, *JCAP* **05** (2021) 049, [2012.14071].
- [194] A. Romero, K. Martinovic, T. A. Callister, H.-K. Guo, M. Martínez, M. Sakellariadou et al., *Implications for First-Order Cosmological Phase Transitions from the Third LIGO-Virgo Observing Run*, *Phys. Rev. Lett.* **126** (2021) 151301, [2102.01714].
- [195] F. Huang, V. Sanz, J. Shu and X. Xue, *LIGO as a probe of Dark Sectors*, 2102.03155.
- [196] M. Geller, A. Hook, R. Sundrum and Y. Tsai, *Primordial Anisotropies in the Gravitational Wave Background from Cosmological Phase Transitions*, *Phys. Rev. Lett.* **121** (2018) 201303, [1803.10780].
- [197] S. Kumar, R. Sundrum and Y. Tsai, *Non-Gaussian Stochastic Gravitational Waves from Phase Transitions*, 2102.05665.
- [198] T. W. B. Kibble, *Topology of Cosmic Domains and Strings*, *J. Phys.* **A9** (1976) 1387–1398.
- [199] A. Vilenkin, *Cosmic Strings and Domain Walls*, *Phys. Rept.* **121** (1985) 263–315.
- [200] P. Auclair et al., *Probing the gravitational wave background from cosmic strings with LISA*, *JCAP* **2004** (2020) 034, [1909.00819].
- [201] K. Saikawa, *A review of gravitational waves from cosmic domain walls*, *Universe* **3** (2017) 40, [1703.02576].
- [202] S. A. Sanidas, R. A. Battye and B. W. Stappers, *Constraints on cosmic string tension imposed by the limit on the stochastic gravitational wave background from the European Pulsar Timing Array*, *Phys. Rev. D* **85** (2012) 122003, [1201.2419].
- [203] LIGO SCIENTIFIC, VIRGO collaboration, B. P. Abbott et al., *Constraints on cosmic strings using data from the first Advanced LIGO observing run*, *Phys. Rev. D* **97** (2018) 102002, [1712.01168].
- [204] J. Ellis and M. Lewicki, *Cosmic String Interpretation of NANOGrav Pulsar Timing Data*, *Phys. Rev. Lett.* **126** (2021) 041304, [2009.06555].
- [205] S. Blasi, V. Brdar and K. Schmitz, *Has NANOGrav found first evidence for cosmic strings?*, *Phys. Rev. Lett.* **126** (2021) 041305, [2009.06607].

- [206] S. Vagnozzi, *Implications of the NANOGrav results for inflation*, *Mon. Not. Roy. Astron. Soc.* **502** (2021) L11, [[2009.13432](#)].
- [207] K. Yagi and N. Seto, *Detector configuration of DECIGO/BBO and identification of cosmological neutron-star binaries*, *Phys. Rev.* **D83** (2011) 044011, [[1101.3940](#)].
- [208] D. Reitze et al., *Cosmic Explorer: The U.S. Contribution to Gravitational-Wave Astronomy beyond LIGO*, *Bull. Am. Astron. Soc.* **51** (2019) 035, [[1907.04833](#)].
- [209] L. Bethke, D. G. Figueroa and A. Rajantie, *Anisotropies in the Gravitational Wave Background from Preheating*, *Phys. Rev. Lett.* **111** (2013) 011301, [[1304.2657](#)].
- [210] L. Bethke, D. G. Figueroa and A. Rajantie, *On the Anisotropy of the Gravitational Wave Background from Massless Preheating*, *JCAP* **1406** (2014) 047, [[1309.1148](#)].
- [211] A. C. Jenkins and M. Sakellariadou, *Anisotropies in the stochastic gravitational-wave background: Formalism and the cosmic string case*, *Phys. Rev.* **D98** (2018) 063509, [[1802.06046](#)].
- [212] C. R. Contaldi, *Anisotropies of Gravitational Wave Backgrounds: A Line Of Sight Approach*, *Phys. Lett.* **B771** (2017) 9–12, [[1609.08168](#)].
- [213] N. Bartolo, D. Bertacca, S. Matarrese, M. Peloso, A. Ricciardone, A. Riotto et al., *Anisotropies and non-Gaussianity of the Cosmological Gravitational Wave Background*, *Phys. Rev.* **D100** (2019) 121501, [[1908.00527](#)].
- [214] N. Bartolo, D. Bertacca, S. Matarrese, M. Peloso, A. Ricciardone, A. Riotto et al., *Characterizing the cosmological gravitational wave background: Anisotropies and non-Gaussianity*, *Phys. Rev.* **D102** (2020) 023527, [[1912.09433](#)].
- [215] L. Valbusa Dall’Armi, A. Ricciardone, N. Bartolo, D. Bertacca and S. Matarrese, *Imprint of relativistic particles on the anisotropies of the stochastic gravitational-wave background*, *Phys. Rev. D* **103** (2021) 023522, [[2007.01215](#)].
- [216] B. Allen and A. C. Ottewill, *Detection of anisotropies in the gravitational wave stochastic background*, *Phys. Rev. D* **56** (1997) 545–563, [[gr-qc/9607068](#)].
- [217] N. Seto and A. Cooray, *LISA measurement of gravitational wave background anisotropy: Hexadecapole moment via a correlation analysis*, *Phys. Rev. D* **70** (2004) 123005, [[astro-ph/0403259](#)].
- [218] S. C. Hotinli, M. Kamionkowski and A. H. Jaffe, *The search for anisotropy in the gravitational-wave background with pulsar-timing arrays*, *Open J. Astrophys.* **2** (2019) 8, [[1904.05348](#)].
- [219] Y.-K. Chu, G.-C. Liu and K.-W. Ng, *Spherical harmonic analysis of anisotropies in polarized stochastic gravitational wave background with interferometry experiments*, *Phys. Rev. D* **103** (2021) 063528, [[2002.01606](#)].
- [220] G. Mentasti and M. Peloso, *ET sensitivity to the anisotropic Stochastic Gravitational Wave Background*, *JCAP* **03** (2021) 080, [[2010.00486](#)].
- [221] D. Alonso, C. R. Contaldi, G. Cusin, P. G. Ferreira and A. I. Renzini, *Noise angular power spectrum of gravitational wave background experiments*, *Phys. Rev. D* **101** (2020) 124048, [[2005.03001](#)].
- [222] A. Vilenkin, *Gravitational Field of Vacuum Domain Walls and Strings*, *Phys. Rev.* **D23** (1981) 852–857.
- [223] G. B. Gelmini, M. Gleiser and E. W. Kolb, *Cosmology of Biased Discrete Symmetry Breaking*, *Phys. Rev.* **D39** (1989) 1558.
- [224] J. R. Espinosa, G. F. Giudice, E. Morgante, A. Riotto, L. Senatore, A. Strumia et al., *The cosmological Higgstory of the vacuum instability*, *JHEP* **09** (2015) 174, [[1505.04825](#)].

- [225] J.-C. Hwang, D. Jeong and H. Noh, *Gauge dependence of gravitational waves generated from scalar perturbations*, *Astrophys. J.* **842** (2017) 46, [[1704.03500](#)].
- [226] B. Wang and Y. Zhang, *Second-order cosmological perturbations IV. Produced by scalar-tensor and tensor-tensor couplings during the radiation dominated stage*, *Phys. Rev. D* **99** (2019) 123008, [[1905.03272](#)].
- [227] J.-O. Gong, *Analytic integral solutions for induced gravitational waves*, [1909.12708](#).
- [228] K. Tomikawa and T. Kobayashi, *Gauge dependence of gravitational waves generated at second order from scalar perturbations*, *Phys. Rev. D* **101** (2020) 083529, [[1910.01880](#)].
- [229] V. De Luca, G. Franciolini, A. Kehagias and A. Riotto, *On the Gauge Invariance of Cosmological Gravitational Waves*, *JCAP* **03** (2020) 014, [[1911.09689](#)].
- [230] K. Inomata and T. Terada, *Gauge Independence of Induced Gravitational Waves*, *Phys. Rev. D* **101** (2020) 023523, [[1912.00785](#)].
- [231] C. Yuan, Z.-C. Chen and Q.-G. Huang, *Scalar induced gravitational waves in different gauges*, *Phys. Rev. D* **101** (2020) 063018, [[1912.00885](#)].
- [232] K. Nakamura, *Second-order Gauge-invariant Cosmological Perturbation Theory: Current Status updated in 2019*, [1912.12805](#).
- [233] Y. Lu, A. Ali, Y. Gong, J. Lin and F. Zhang, *Gauge transformation of scalar induced gravitational waves*, *Phys. Rev. D* **102** (2020) 083503, [[2006.03450](#)].
- [234] A. Ali, Y. Gong and Y. Lu, *Gauge transformation of scalar induced tensor perturbation during matter domination*, *Phys. Rev. D* **103** (2021) 043516, [[2009.11081](#)].
- [235] M. Giovannini, *Spurious gauge-invariance of higher-order contributions to the spectral energy density of the relic gravitons*, *Int. J. Mod. Phys. A* **35** (2020) 2050165, [[2005.04962](#)].
- [236] M. Giovannini, *Effective anisotropic stresses of the relic gravitons*, *Int. J. Mod. Phys. D* **29** (2020) 2050112, [[2007.14956](#)].
- [237] Z. Chang, S. Wang and Q.-H. Zhu, *Gauge invariance of the second order cosmological perturbations*, [2009.11025](#).
- [238] Z. Chang, S. Wang and Q.-H. Zhu, *Gauge Invariant Second Order Gravitational Waves*, [2009.11994](#).
- [239] Z. Chang, S. Wang and Q.-H. Zhu, *On the Gauge Invariance of Scalar Induced Gravitational Waves: Gauge Fixings Considered*, [2010.01487](#).
- [240] G. Domènech and M. Sasaki, *Approximate gauge independence of the induced gravitational wave spectrum*, *Phys. Rev. D* **103** (2021) 063531, [[2012.14016](#)].
- [241] PLANCK collaboration, N. Aghanim et al., *Planck 2018 results. VI. Cosmological parameters*, *Astron. Astrophys.* **641** (2020) A6, [[1807.06209](#)].
- [242] S. Matarrese, O. Pantano and D. Saez, *A General relativistic approach to the nonlinear evolution of collisionless matter*, *Phys. Rev. D* **47** (1993) 1311–1323.
- [243] S. Matarrese, O. Pantano and D. Saez, *General relativistic dynamics of irrotational dust: Cosmological implications*, *Phys. Rev. Lett.* **72** (1994) 320–323, [[astro-ph/9310036](#)].
- [244] S. Matarrese, S. Mollerach and M. Bruni, *Second order perturbations of the Einstein-de Sitter universe*, *Phys. Rev. D* **58** (1998) 043504, [[astro-ph/9707278](#)].
- [245] H. Noh and J.-c. Hwang, *Second-order perturbations of the Friedmann world model*, *Phys. Rev. D* **69** (2004) 104011.
- [246] C. Carbone and S. Matarrese, *A Unified treatment of cosmological perturbations from super-horizon to small scales*, *Phys. Rev. D* **71** (2005) 043508, [[astro-ph/0407611](#)].

- [247] K. Nakamura, *Second-order gauge invariant cosmological perturbation theory: Einstein equations in terms of gauge invariant variables*, *Prog. Theor. Phys.* **117** (2007) 17–74, [[gr-qc/0605108](#)].
- [248] K. N. Ananda, C. Clarkson and D. Wands, *The Cosmological gravitational wave background from primordial density perturbations*, *Phys. Rev. D* **75** (2007) 123518, [[gr-qc/0612013](#)].
- [249] B. Osano, C. Pitrou, P. Dunsby, J.-P. Uzan and C. Clarkson, *Gravitational waves generated by second order effects during inflation*, *JCAP* **04** (2007) 003, [[gr-qc/0612108](#)].
- [250] S. Pi, Y.-l. Zhang, Q.-G. Huang and M. Sasaki, *Scalaron from R^2 -gravity as a heavy field*, *JCAP* **05** (2018) 042, [[1712.09896](#)].
- [251] R.-G. Cai, Z.-K. Guo, J. Liu, L. Liu and X.-Y. Yang, *Primordial black holes and gravitational waves from parametric amplification of curvature perturbations*, *JCAP* **06** (2020) 013, [[1912.10437](#)].
- [252] I. D. Zel'dovich, Ya.B.; Novikov, *The Hypothesis of Cores Retarded during Expansion and the Hot Cosmological Model*, *Soviet Astron. AJ (Engl. Transl.)*, **10** (1967) 602.
- [253] S. Hawking, *Gravitationally collapsed objects of very low mass*, *Mon. Not. Roy. Astron. Soc.* **152** (1971) 75.
- [254] B. J. Carr and S. Hawking, *Black holes in the early Universe*, *Mon. Not. Roy. Astron. Soc.* **168** (1974) 399–415.
- [255] P. Meszaros, *The behaviour of point masses in an expanding cosmological substratum*, *Astron. Astrophys.* **37** (1974) 225–228.
- [256] B. J. Carr, *The Primordial black hole mass spectrum*, *Astrophys. J.* **201** (1975) 1–19.
- [257] M. Khlopov, B. Malomed and I. Zeldovich, *Gravitational instability of scalar fields and formation of primordial black holes*, *Mon. Not. Roy. Astron. Soc.* **215** (1985) 575–589.
- [258] S. Young, C. T. Byrnes and M. Sasaki, *Calculating the mass fraction of primordial black holes*, *JCAP* **07** (2014) 045, [[1405.7023](#)].
- [259] C. Germani and I. Musco, *Abundance of Primordial Black Holes Depends on the Shape of the Inflationary Power Spectrum*, *Phys. Rev. Lett.* **122** (2019) 141302, [[1805.04087](#)].
- [260] Y.-P. Wu, *Peak statistics for the primordial black hole abundance*, *Phys. Dark Univ.* **30** (2020) 100654, [[2005.00441](#)].
- [261] V. De Luca, G. Franciolini, A. Kehagias, M. Peloso, A. Riotto and C. Ünal, *The Ineludible non-Gaussianity of the Primordial Black Hole Abundance*, *JCAP* **07** (2019) 048, [[1904.00970](#)].
- [262] J. M. Ezquiaga, J. García-Bellido and V. Vennin, *The exponential tail of inflationary fluctuations: consequences for primordial black holes*, *JCAP* **03** (2020) 029, [[1912.05399](#)].
- [263] M. He and T. Suyama, *Formation threshold of rotating primordial black holes*, *Phys. Rev. D* **100** (2019) 063520, [[1906.10987](#)].
- [264] I. Musco, V. De Luca, G. Franciolini and A. Riotto, *Threshold for primordial black holes. II. A simple analytic prescription*, *Phys. Rev. D* **103** (2021) 063538, [[2011.03014](#)].
- [265] M. Taoso and A. Urbano, *Non-gaussianities for primordial black hole formation*, [2102.03610](#).
- [266] F. Ricciardi, M. Taoso and A. Urbano, *Solving peak theory in the presence of local non-gaussianities*, [2102.04084](#).
- [267] J. Yokoyama, *Chaotic new inflation and formation of primordial black holes*, *Phys. Rev. D* **58** (1998) 083510, [[astro-ph/9802357](#)].
- [268] J. Garcia-Bellido, M. Peloso and C. Unal, *Gravitational waves at interferometer scales and primordial black holes in axion inflation*, *JCAP* **12** (2016) 031, [[1610.03763](#)].

- [269] S.-L. Cheng, W. Lee and K.-W. Ng, *Production of high stellar-mass primordial black holes in trapped inflation*, *JHEP* **02** (2017) 008, [[1606.00206](#)].
- [270] J. Garcia-Bellido and E. Ruiz Morales, *Primordial black holes from single field models of inflation*, *Phys. Dark Univ.* **18** (2017) 47–54, [[1702.03901](#)].
- [271] S.-L. Cheng, W. Lee and K.-W. Ng, *Primordial black holes and associated gravitational waves in axion monodromy inflation*, *JCAP* **07** (2018) 001, [[1801.09050](#)].
- [272] I. Dalianis, A. Kehagias and G. Tringas, *Primordial black holes from α -attractors*, *JCAP* **01** (2019) 037, [[1805.09483](#)].
- [273] Y. Tada and S. Yokoyama, *Primordial black hole tower: Dark matter, earth-mass, and LIGO black holes*, *Phys. Rev. D* **100** (2019) 023537, [[1904.10298](#)].
- [274] W.-T. Xu, J. Liu, T.-J. Gao and Z.-K. Guo, *Gravitational waves from double-inflection-point inflation*, *Phys. Rev. D* **101** (2020) 023505, [[1907.05213](#)].
- [275] S. S. Mishra and V. Sahni, *Primordial Black Holes from a tiny bump/dip in the Inflaton potential*, *JCAP* **04** (2020) 007, [[1911.00057](#)].
- [276] N. Bhaumik and R. K. Jain, *Primordial black holes dark matter from inflection point models of inflation and the effects of reheating*, *JCAP* **01** (2020) 037, [[1907.04125](#)].
- [277] J. Liu, Z.-K. Guo and R.-G. Cai, *Analytical approximation of the scalar spectrum in the ultraslow-roll inflationary models*, *Phys. Rev. D* **101** (2020) 083535, [[2003.02075](#)].
- [278] V. Atal, J. Cid, A. Escrivà and J. Garriga, *PBH in single field inflation: the effect of shape dispersion and non-Gaussianities*, *JCAP* **05** (2020) 022, [[1908.11357](#)].
- [279] C. Fu, P. Wu and H. Yu, *Primordial black holes and oscillating gravitational waves in slow-roll and slow-climb inflation with an intermediate noninflationary phase*, *Phys. Rev. D* **102** (2020) 043527, [[2006.03768](#)].
- [280] V. Vennin, *Stochastic inflation and primordial black holes*. PhD thesis, U. Paris-Saclay, 2020. [[2009.08715](#)].
- [281] H. V. Ragavendra, P. Saha, L. Sriramkumar and J. Silk, *Primordial black holes and secondary gravitational waves from ultraslow roll and punctuated inflation*, *Phys. Rev. D* **103** (2021) 083510, [[2008.12202](#)].
- [282] T.-J. Gao and X.-Y. Yang, *Double peaks of gravitational wave spectrum induced from inflection point inflation*, [2101.07616](#).
- [283] J. Garcia-Bellido, A. D. Linde and D. Wands, *Density perturbations and black hole formation in hybrid inflation*, *Phys. Rev. D* **54** (1996) 6040–6058, [[astro-ph/9605094](#)].
- [284] M. Kawasaki, N. Sugiyama and T. Yanagida, *Primordial black hole formation in a double inflation model in supergravity*, *Phys. Rev. D* **57** (1998) 6050–6056, [[hep-ph/9710259](#)].
- [285] P. H. Frampton, M. Kawasaki, F. Takahashi and T. T. Yanagida, *Primordial Black Holes as All Dark Matter*, *JCAP* **04** (2010) 023, [[1001.2308](#)].
- [286] M. Giovannini, *Secondary graviton spectra and waterfall-like fields*, *Phys. Rev. D* **82** (2010) 083523, [[1008.1164](#)].
- [287] S. Clesse and J. García-Bellido, *Massive Primordial Black Holes from Hybrid Inflation as Dark Matter and the seeds of Galaxies*, *Phys. Rev. D* **92** (2015) 023524, [[1501.07565](#)].
- [288] K. Inomata, M. Kawasaki, K. Mukaida, Y. Tada and T. T. Yanagida, *Inflationary Primordial Black Holes as All Dark Matter*, *Phys. Rev. D* **96** (2017) 043504, [[1701.02544](#)].
- [289] H. Di and Y. Gong, *Primordial black holes and second order gravitational waves from ultra-slow-roll inflation*, *JCAP* **07** (2018) 007, [[1707.09578](#)].

- [290] K. Inomata, M. Kawasaki, K. Mukaida and T. T. Yanagida, *Double inflation as a single origin of primordial black holes for all dark matter and LIGO observations*, *Phys. Rev. D* **97** (2018) 043514, [[1711.06129](#)].
- [291] J. Espinosa, D. Racco and A. Riotto, *Cosmological Signature of the Standard Model Higgs Vacuum Instability: Primordial Black Holes as Dark Matter*, *Phys. Rev. Lett.* **120** (2018) 121301, [[1710.11196](#)].
- [292] M. Kawasaki, H. Nakatsuka and I. Obata, *Generation of Primordial Black Holes and Gravitational Waves from Dilaton-Gauge Field Dynamics*, *JCAP* **05** (2020) 007, [[1912.09111](#)].
- [293] G. A. Palma, S. Sypsas and C. Zenteno, *Seeding primordial black holes in multifield inflation*, *Phys. Rev. Lett.* **125** (2020) 121301, [[2004.06106](#)].
- [294] J. Fumagalli, S. Renaux-Petel, J. W. Ronayne and L. T. Witkowski, *Turning in the landscape: a new mechanism for generating Primordial Black Holes*, [2004.08369](#).
- [295] M. Braglia, D. K. Hazra, F. Finelli, G. F. Smoot, L. Sriramkumar and A. A. Starobinsky, *Generating PBHs and small-scale GWs in two-field models of inflation*, *JCAP* **08** (2020) 001, [[2005.02895](#)].
- [296] L. Anguelova, *On Primordial Black Holes from Rapid Turns in Two-field Models*, *JCAP* **06** (2021) 004, [[2012.03705](#)].
- [297] A. E. Romano, *Sound speed induced production of primordial black holes*, [2006.07321](#).
- [298] A. Gundhi and C. F. Steinwachs, *Scalaron–Higgs inflation reloaded: Higgs-dependent scalaron mass and primordial black hole dark matter*, *Eur. Phys. J. C* **81** (2021) 460, [[2011.09485](#)].
- [299] A. Gundhi, S. V. Ketov and C. F. Steinwachs, *Primordial black hole dark matter in dilaton-extended two-field Starobinsky inflation*, *Phys. Rev. D* **103** (2021) 083518, [[2011.05999](#)].
- [300] K. Kannike, L. Marzola, M. Raidal and H. Veermäe, *Single Field Double Inflation and Primordial Black Holes*, *JCAP* **09** (2017) 020, [[1705.06225](#)].
- [301] T.-J. Gao and Z.-K. Guo, *Primordial Black Hole Production in Inflationary Models of Supergravity with a Single Chiral Superfield*, *Phys. Rev. D* **98** (2018) 063526, [[1806.09320](#)].
- [302] D. Y. Cheong, S. M. Lee and S. C. Park, *Primordial black holes in Higgs- R^2 inflation as the whole of dark matter*, *JCAP* **01** (2021) 032, [[1912.12032](#)].
- [303] D. Y. Cheong, H. M. Lee and S. C. Park, *Beyond the Starobinsky model for inflation*, *Phys. Lett. B* **805** (2020) 135453, [[2002.07981](#)].
- [304] C. Fu, P. Wu and H. Yu, *Primordial Black Holes from Inflation with Nonminimal Derivative Coupling*, *Phys. Rev. D* **100** (2019) 063532, [[1907.05042](#)].
- [305] I. Dalianis, S. Karydas and E. Papantonopoulos, *Generalized Non-Minimal Derivative Coupling: Application to Inflation and Primordial Black Hole Production*, *JCAP* **06** (2020) 040, [[1910.00622](#)].
- [306] J. Lin, Q. Gao, Y. Gong, Y. Lu, C. Zhang and F. Zhang, *Primordial black holes and secondary gravitational waves from k and G inflation*, *Phys. Rev.* **D101** (2020) 103515, [[2001.05909](#)].
- [307] C. Fu, P. Wu and H. Yu, *Scalar induced gravitational waves in inflation with gravitationally enhanced friction*, *Phys. Rev. D* **101** (2020) 023529, [[1912.05927](#)].
- [308] Y. Aldabergenov, A. Addazi and S. V. Ketov, *Primordial black holes from modified supergravity*, *Eur. Phys. J. C* **80** (2020) 917, [[2006.16641](#)].
- [309] Y. Aldabergenov, A. Addazi and S. V. Ketov, *Testing Primordial Black Holes as Dark Matter in Supergravity from Gravitational Waves*, *Phys. Lett. B* **814** (2021) 136069, [[2008.10476](#)].

- [310] Z. Yi, Q. Gao, Y. Gong and Z.-h. Zhu, *Primordial black holes and scalar-induced secondary gravitational waves from inflationary models with a noncanonical kinetic term*, *Phys. Rev. D* **103** (2021) 063534, [2011.10606].
- [311] Q. Gao, Y. Gong and Z. Yi, *Primordial black holes and secondary gravitational waves from natural inflation*, 2012.03856.
- [312] I. Dalianis and K. Kritos, *Exploring the Spectral Shape of Gravitational Waves Induced by Primordial Scalar Perturbations and Connection with the Primordial Black Hole Scenarios*, *Phys. Rev. D* **103** (2021) 023505, [2007.07915].
- [313] M. Kawasaki, N. Kitajima and T. T. Yanagida, *Primordial black hole formation from an axionlike curvaton model*, *Phys. Rev. D* **87** (2013) 063519, [1207.2550].
- [314] K. Kohri, C.-M. Lin and T. Matsuda, *Primordial black holes from the inflating curvaton*, *Phys. Rev. D* **87** (2013) 103527, [1211.2371].
- [315] K. Ando, K. Inomata, M. Kawasaki, K. Mukaida and T. T. Yanagida, *Primordial black holes for the LIGO events in the axionlike curvaton model*, *Phys. Rev. D* **97** (2018) 123512, [1711.08956].
- [316] K. Ando, M. Kawasaki and H. Nakatsuka, *Formation of primordial black holes in an axionlike curvaton model*, *Phys. Rev. D* **98** (2018) 083508, [1805.07757].
- [317] C. Chen and Y.-F. Cai, *Primordial black holes from sound speed resonance in the inflaton-curvaton mixed scenario*, *JCAP* **10** (2019) 068, [1908.03942].
- [318] Y.-F. Cai, X. Tong, D.-G. Wang and S.-F. Yan, *Primordial Black Holes from Sound Speed Resonance during Inflation*, *Phys. Rev. Lett.* **121** (2018) 081306, [1805.03639].
- [319] C. Chen, X.-H. Ma and Y.-F. Cai, *Dirac-Born-Infeld realization of sound speed resonance mechanism for primordial black holes*, *Phys. Rev. D* **102** (2020) 063526, [2003.03821].
- [320] Y.-F. Cai, C. Chen, X. Tong, D.-G. Wang and S.-F. Yan, *When Primordial Black Holes from Sound Speed Resonance Meet a Stochastic Background of Gravitational Waves*, *Phys. Rev. D* **100** (2019) 043518, [1902.08187].
- [321] A. Kusenko, M. Sasaki, S. Sugiyama, M. Takada, V. Takhistov and E. Vitagliano, *Exploring Primordial Black Holes from the Multiverse with Optical Telescopes*, *Phys. Rev. Lett.* **125** (2020) 18, [2001.09160].
- [322] E. Cotner and A. Kusenko, *Primordial black holes from supersymmetry in the early universe*, *Phys. Rev. Lett.* **119** (2017) 031103, [1612.02529].
- [323] E. Cotner and A. Kusenko, *Primordial black holes from scalar field evolution in the early universe*, *Phys. Rev. D* **96** (2017) 103002, [1706.09003].
- [324] E. Cotner, A. Kusenko and V. Takhistov, *Primordial Black Holes from Inflaton Fragmentation into Oscillons*, *Phys. Rev. D* **98** (2018) 083513, [1801.03321].
- [325] E. Cotner, A. Kusenko, M. Sasaki and V. Takhistov, *Analytic Description of Primordial Black Hole Formation from Scalar Field Fragmentation*, *JCAP* **10** (2019) 077, [1907.10613].
- [326] Q. Gao, *Primordial black holes and secondary gravitational waves from chaotic inflation*, 2102.07369.
- [327] M. Solbi and K. Karami, *Primordial black holes and induced gravitational waves in Galileon inflation*, 2102.05651.
- [328] M. Kawasaki and H. Nakatsuka, *Gravitational waves from type II axion-like curvaton model and its implication for NANOGrav result*, 2101.11244.
- [329] K.-W. Ng and Y.-P. Wu, *Constant-rate inflation: primordial black holes from conformal weight transitions*, 2102.05620.

- [330] A. M. Green, A. R. Liddle, K. A. Malik and M. Sasaki, *A New calculation of the mass fraction of primordial black holes*, *Phys. Rev. D* **70** (2004) 041502, [[astro-ph/0403181](#)].
- [331] P. H. Frampton, *Identification of All Dark Matter as Black Holes*, *JCAP* **10** (2009) 016, [[0905.3632](#)].
- [332] B. Carr, K. Kohri, Y. Sendouda and J. Yokoyama, *New cosmological constraints on primordial black holes*, *Phys. Rev. D* **81** (2010) 104019, [[0912.5297](#)].
- [333] B. Carr, K. Kohri, Y. Sendouda and J. Yokoyama, *Constraints on primordial black holes from the Galactic gamma-ray background*, *Phys. Rev. D* **94** (2016) 044029, [[1604.05349](#)].
- [334] B. Carr, F. Kuhnel and M. Sandstad, *Primordial Black Holes as Dark Matter*, *Phys. Rev. D* **94** (2016) 083504, [[1607.06077](#)].
- [335] H. Poulter, Y. Ali-Haïmoud, J. Hamann, M. White and A. G. Williams, *CMB constraints on ultra-light primordial black holes with extended mass distributions*, [1907.06485](#).
- [336] S. Wang, T. Terada and K. Kohri, *Prospective constraints on the primordial black hole abundance from the stochastic gravitational-wave backgrounds produced by coalescing events and curvature perturbations*, *Phys. Rev. D* **99** (2019) 103531, [[1903.05924](#)].
- [337] EROS-2 collaboration, P. Tisserand et al., *Limits on the Macho Content of the Galactic Halo from the EROS-2 Survey of the Magellanic Clouds*, *Astron. Astrophys.* **469** (2007) 387–404, [[astro-ph/0607207](#)].
- [338] P. W. Graham, S. Rajendran and J. Varela, *Dark Matter Triggers of Supernovae*, *Phys. Rev. D* **92** (2015) 063007, [[1505.04444](#)].
- [339] S. M. Koushiappas and A. Loeb, *Dynamics of Dwarf Galaxies Disfavor Stellar-Mass Black Holes as Dark Matter*, *Phys. Rev. Lett.* **119** (2017) 041102, [[1704.01668](#)].
- [340] LIGO SCIENTIFIC, VIRGO collaboration, B. Abbott et al., *Search for Subsolar Mass Ultracompact Binaries in Advanced LIGO’s Second Observing Run*, *Phys. Rev. Lett.* **123** (2019) 161102, [[1904.08976](#)].
- [341] V. De Luca, G. Franciolini, P. Pani and A. Riotto, *Primordial Black Holes Confront LIGO/Virgo data: Current situation*, *JCAP* **06** (2020) 044, [[2005.05641](#)].
- [342] P. D. Serpico, V. Poulin, D. Inman and K. Kohri, *Cosmic microwave background bounds on primordial black holes including dark matter halo accretion*, *Phys. Rev. Res.* **2** (2020) 023204, [[2002.10771](#)].
- [343] O. Mena, S. Palomares-Ruiz, P. Villanueva-Domingo and S. J. Witte, *Constraining the primordial black hole abundance with 21-cm cosmology*, *Phys. Rev. D* **100** (2019) 043540, [[1906.07735](#)].
- [344] R. Murgia, G. Scelfo, M. Viel and A. Raccanelli, *Lyman- α Forest Constraints on Primordial Black Holes as Dark Matter*, *Phys. Rev. Lett.* **123** (2019) 071102, [[1903.10509](#)].
- [345] R.-G. Cai, Y.-C. Ding, X.-Y. Yang and Y.-F. Zhou, *Constraints on a mixed model of dark matter particles and primordial black holes from the galactic 511 keV line*, *JCAP* **2103** (2021) 057, [[2007.11804](#)].
- [346] LIGO SCIENTIFIC, VIRGO collaboration, R. Abbott et al., *Population Properties of Compact Objects from the Second LIGO-Virgo Gravitational-Wave Transient Catalog*, *Astrophys. J. Lett.* **913** (2021) L7, [[2010.14533](#)].
- [347] K. W. K. Wong, G. Franciolini, V. De Luca, V. Baibhav, E. Berti, P. Pani et al., *Constraining the primordial black hole scenario with Bayesian inference and machine learning: the GWTC-2 gravitational wave catalog*, *Phys. Rev. D* **103** (2021) 023026, [[2011.01865](#)].
- [348] G. Hütsi, M. Raidal, V. Vaskonen and H. Veermäe, *Two populations of LIGO-Virgo black holes*, *JCAP* **03** (2021) 068, [[2012.02786](#)].

- [349] V. De Luca, G. Franciolini, P. Pani and A. Riotto, *Bayesian Evidence for Both Astrophysical and Primordial Black Holes: Mapping the GWTC-2 Catalog to Third-Generation Detectors*, *JCAP* **05** (2021) 003, [[2102.03809](#)].
- [350] R. Bean and J. Magueijo, *Could supermassive black holes be quintessential primordial black holes?*, *Phys. Rev. D* **66** (2002) 063505, [[astro-ph/0204486](#)].
- [351] M. Kawasaki, A. Kusenko and T. T. Yanagida, *Primordial seeds of supermassive black holes*, *Phys. Lett. B* **711** (2012) 1–5, [[1202.3848](#)].
- [352] T. Nakama, B. Carr and J. Silk, *Limits on primordial black holes from μ distortions in cosmic microwave background*, *Phys. Rev. D* **97** (2018) 043525, [[1710.06945](#)].
- [353] B. Carr and J. Silk, *Primordial Black Holes as Generators of Cosmic Structures*, *Mon. Not. Roy. Astron. Soc.* **478** (2018) 3756–3775, [[1801.00672](#)].
- [354] T. Nakama, K. Kohri and J. Silk, *Ultracompact minihalos associated with stellar-mass primordial black holes*, *Phys. Rev. D* **99** (2019) 123530, [[1905.04477](#)].
- [355] B. Carr, F. Kuhnel and L. Visinelli, *Constraints on Stupendously Large Black Holes*, *Mon. Not. Roy. Astron. Soc.* **501** (2021) 2, [[2008.08077](#)].
- [356] V. Atal, A. Sanglas and N. Triantafyllou, *NANOGrav signal as mergers of Stupendously Large Primordial Black Holes*, [2012.14721](#).
- [357] P. Mróz, A. Udalski, J. Skowron, R. Poleski, S. Kozłowski, M. K. Szymański et al., *No large population of unbound or wide-orbit Jupiter-mass planets*, *Nature* **548** (Aug., 2017) 183–186, [[1707.07634](#)].
- [358] H. Niikura, M. Takada, S. Yokoyama, T. Sumi and S. Masaki, *Constraints on Earth-mass primordial black holes from OGLE 5-year microlensing events*, *Phys. Rev. D* **99** (2019) 083503, [[1901.07120](#)].
- [359] G. Domènech and S. Pi, *NANOGrav Hints on Planet-Mass Primordial Black Holes*, [2010.03976](#).
- [360] S. Bhattacharya, S. Mohanty and P. Parashari, *Implications of the NANOGrav result on primordial gravitational waves in nonstandard cosmologies*, *Phys. Rev. D* **103** (2021) 063532, [[2010.05071](#)].
- [361] J. Scholtz and J. Unwin, *What if Planet 9 is a Primordial Black Hole?*, *Phys. Rev. Lett.* **125** (2020) 051103, [[1909.11090](#)].
- [362] C. T. Byrnes, M. Hindmarsh, S. Young and M. R. S. Hawkins, *Primordial black holes with an accurate QCD equation of state*, *JCAP* **08** (2018) 041, [[1801.06138](#)].
- [363] B. Carr, S. Clesse, J. Garcia-Bellido and F. Kuhnel, *Cosmic Conundra Explained by Thermal History and Primordial Black Holes*, [1906.08217](#).
- [364] B. Carr, S. Clesse and J. García-Bellido, *Primordial black holes from the QCD epoch: Linking dark matter, baryogenesis and anthropic selection*, *Mon. Not. Roy. Astron. Soc.* **501** (2021) 1426–1439, [[1904.02129](#)].
- [365] J. García-Bellido, B. Carr and S. Clesse, *A common origin for baryons and dark matter*, [1904.11482](#).
- [366] M. Sasaki, T. Suyama, T. Tanaka and S. Yokoyama, *Primordial black holes—perspectives in gravitational wave astronomy*, *Class. Quant. Grav.* **35** (2018) 063001, [[1801.05235](#)].
- [367] B. Carr, K. Kohri, Y. Sendouda and J. Yokoyama, *Constraints on Primordial Black Holes*, [2002.12778](#).
- [368] A. M. Green and B. J. Kavanagh, *Primordial Black Holes as a dark matter candidate*, *J. Phys. G* **48** (2021) 4, [[2007.10722](#)].

- [369] B. Carr and F. Kuhnel, *Primordial Black Holes as Dark Matter: Recent Developments*, *Ann. Rev. Nucl. Part. Sci.* **70** (2020) 355–394, [2006.02838].
- [370] H. Niikura et al., *Microlensing constraints on primordial black holes with Subaru/HSC Andromeda observations*, *Nature Astron.* **3** (2019) 524–534, [1701.02151].
- [371] A. Katz, J. Kopp, S. Sibiryakov and W. Xue, *Femtolensing by Dark Matter Revisited*, *JCAP* **12** (2018) 005, [1807.11495].
- [372] P. Montero-Camacho, X. Fang, G. Vasquez, M. Silva and C. M. Hirata, *Revisiting constraints on asteroid-mass primordial black holes as dark matter candidates*, *JCAP* **08** (2019) 031, [1906.05950].
- [373] S. Sugiyama, T. Kurita and M. Takada, *On the wave optics effect on primordial black hole constraints from optical microlensing search*, *Mon. Not. Roy. Astron. Soc.* **493** (2020) 3632–3641, [1905.06066].
- [374] R. Laha, *Primordial Black Holes as a Dark Matter Candidate Are Severely Constrained by the Galactic Center 511 keV γ -Ray Line*, *Phys. Rev. Lett.* **123** (2019) 251101, [1906.09994].
- [375] W. DeRocco and P. W. Graham, *Constraining Primordial Black Hole Abundance with the Galactic 511 keV Line*, *Phys. Rev. Lett.* **123** (2019) 251102, [1906.07740].
- [376] B. Dasgupta, R. Laha and A. Ray, *Neutrino and positron constraints on spinning primordial black hole dark matter*, *Phys. Rev. Lett.* **125** (2020) 101101, [1912.01014].
- [377] A. Ray, R. Laha, J. B. Muñoz and R. Caputo, *Closing the gap: Near future MeV telescopes can discover asteroid-mass primordial black hole dark matter*, **2102.06714**.
- [378] X.-c. Luo and D. N. Schramm, *Kurtosis, skewness, and nonGaussian cosmological density perturbations*, *Astrophys. J.* **408** (1993) 33–42.
- [379] L. Verde, L.-M. Wang, A. Heavens and M. Kamionkowski, *Large scale structure, the cosmic microwave background, and primordial non-gaussianity*, *Mon. Not. Roy. Astron. Soc.* **313** (2000) L141–L147, [astro-ph/9906301].
- [380] L. Verde, R. Jimenez, M. Kamionkowski and S. Matarrese, *Tests for primordial nonGaussianity*, *Mon. Not. Roy. Astron. Soc.* **325** (2001) 412, [astro-ph/0011180].
- [381] E. Komatsu and D. N. Spergel, *Acoustic signatures in the primary microwave background bispectrum*, *Phys. Rev. D* **63** (2001) 063002, [astro-ph/0005036].
- [382] N. Bartolo, E. Komatsu, S. Matarrese and A. Riotto, *Non-Gaussianity from inflation: Theory and observations*, *Phys. Rept.* **402** (2004) 103–266, [astro-ph/0406398].
- [383] L. Boubekeur and D. H. Lyth, *Detecting a small perturbation through its non-Gaussianity*, *Phys. Rev. D* **73** (2006) 021301, [astro-ph/0504046].
- [384] C. T. Byrnes, K. Koyama, M. Sasaki and D. Wands, *Diagrammatic approach to non-Gaussianity from inflation*, *JCAP* **11** (2007) 027, [0705.4096].
- [385] S. Young and C. T. Byrnes, *Primordial black holes in non-Gaussian regimes*, *JCAP* **08** (2013) 052, [1307.4995].
- [386] R.-g. Cai, S. Pi and M. Sasaki, *Gravitational Waves Induced by non-Gaussian Scalar Perturbations*, *Phys. Rev. Lett.* **122** (2019) 201101, [1810.11000].
- [387] P. Bender, A. Brilliet, I. Ciufolini, A. Cruise, C. Cutler, K. Danzmann et al., *Lisa. laser interferometer space antenna for the detection and observation of gravitational waves. an international project in the field of fundamental physics in space*, .
- [388] A. Kalaja, N. Bellomo, N. Bartolo, D. Bertacca, S. Matarrese, I. Musco et al., *From Primordial Black Holes Abundance to Primordial Curvature Power Spectrum (and back)*, *JCAP* **10** (2019) 031, [1908.03596].

- [389] G. Sato-Polito, E. D. Kovetz and M. Kamionkowski, *Constraints on the primordial curvature power spectrum from primordial black holes*, *Phys. Rev. D* **100** (2019) 063521, [[1904.10971](#)].
- [390] A. D. Gow, C. T. Byrnes, P. S. Cole and S. Young, *The power spectrum on small scales: Robust constraints and comparing PBH methodologies*, *JCAP* **02** (2021) 002, [[2008.03289](#)].
- [391] C. Ünal, E. D. Kovetz and S. P. Patil, *Multimessenger probes of inflationary fluctuations and primordial black holes*, *Phys. Rev. D* **103** (2021) 063519, [[2008.11184](#)].
- [392] N. Bartolo, V. De Luca, G. Franciolini, M. Peloso, D. Racco and A. Riotto, *Testing primordial black holes as dark matter with LISA*, *Phys. Rev. D* **99** (2019) 103521, [[1810.12224](#)].
- [393] R. Caldwell et al., *Astro2020 Science White Paper: Cosmology with a Space-Based Gravitational Wave Observatory*, [1903.04657](#).
- [394] E. Barausse et al., *Prospects for Fundamental Physics with LISA*, *Gen. Rel. Grav.* **52** (2020) 81, [[2001.09793](#)].
- [395] Y.-L. Wu et al., *Taiji White Paper*, [to appear](#).
- [396] E. Thrane and J. D. Romano, *Sensitivity curves for searches for gravitational-wave backgrounds*, *Phys. Rev. D* **88** (2013) 124032, [[1310.5300](#)].
- [397] R.-G. Cai, S. Pi and M. Sasaki, *Universal infrared scaling of gravitational wave background spectra*, *Phys. Rev. D* **102** (2020) 083528, [[1909.13728](#)].
- [398] G. Domènech, *Induced gravitational waves in a general cosmological background*, *Int. J. Mod. Phys. D* **29** (2020) 2050028, [[1912.05583](#)].
- [399] G. Domènech, S. Pi and M. Sasaki, *Induced gravitational waves as a probe of thermal history of the universe*, *JCAP* **08** (2020) 017, [[2005.12314](#)].
- [400] S. Pi and M. Sasaki, *Gravitational Waves Induced by Scalar Perturbations with a Lognormal Peak*, *JCAP* **09** (2020) 037, [[2005.12306](#)].
- [401] K. Kohri and T. Terada, *Semianalytic calculation of gravitational wave spectrum nonlinearly induced from primordial curvature perturbations*, *Phys. Rev. D* **97** (2018) 123532, [[1804.08577](#)].
- [402] A. Achúcarro, J.-O. Gong, S. Hardeman, G. A. Palma and S. P. Patil, *Features of heavy physics in the CMB power spectrum*, *JCAP* **01** (2011) 030, [[1010.3693](#)].
- [403] X. Chen, *Primordial Features as Evidence for Inflation*, *JCAP* **01** (2012) 038, [[1104.1323](#)].
- [404] X. Gao, D. Langlois and S. Mizuno, *Influence of heavy modes on perturbations in multiple field inflation*, *JCAP* **10** (2012) 040, [[1205.5275](#)].
- [405] Q.-G. Huang and S. Pi, *Power-law modulation of the scalar power spectrum from a heavy field with a monomial potential*, *JCAP* **04** (2018) 001, [[1610.00115](#)].
- [406] G. Domènech, J. Rubio and J. Wons, *Mimicking features in alternatives to inflation with interacting spectator fields*, *Phys. Lett. B* **790** (2019) 263–269, [[1811.08224](#)].
- [407] J. Fan, M. Reece and Y. Wang, *An Inflationary Probe of Cosmic Higgs Switching*, *JHEP* **05** (2020) 042, [[1905.05764](#)].
- [408] R.-G. Cai, S. Pi, S.-J. Wang and X.-Y. Yang, *Resonant multiple peaks in the induced gravitational waves*, *JCAP* **1905** (2019) 013, [[1901.10152](#)].
- [409] J. Fumagalli, S. Renaux-Petel and L. T. Witkowski, *Oscillations in the stochastic gravitational wave background from sharp features and particle production during inflation*, [2012.02761](#).
- [410] M. Braglia, X. Chen and D. K. Hazra, *Probing Primordial Features with the Stochastic Gravitational Wave Background*, [2012.05821](#).

- [411] J. Fumagalli, S. Renaux-Petel and L. T. Witkowski, *Resonant features in the stochastic gravitational wave background*, [2105.06481](#).
- [412] I. Dalianis, G. P. Kodaxis, I. D. Stamou, N. Tetradis and A. Tsigkas-Kouvelis, *Spectrum oscillations from features in the potential of single-field inflation*, [2106.02467](#).
- [413] S. Bird, I. Cholis, J. B. Muñoz, Y. Ali-Haïmoud, M. Kamionkowski, E. D. Kovetz et al., *Did LIGO detect dark matter?*, *Phys. Rev. Lett.* **116** (2016) 201301, [[1603.00464](#)].
- [414] M. Sasaki, T. Suyama, T. Tanaka and S. Yokoyama, *Primordial Black Hole Scenario for the Gravitational-Wave Event GW150914*, *Phys. Rev. Lett.* **117** (2016) 061101, [[1603.08338](#)].
- [415] R.-G. Cai, S. Pi, S.-J. Wang and X.-Y. Yang, *Pulsar Timing Array Constraints on the Induced Gravitational Waves*, *JCAP* **10** (2019) 059, [[1907.06372](#)].
- [416] G. Franciolini, V. Baibhav, V. De Luca, K. K. Y. Ng, K. W. K. Wong, E. Berti et al., *Evidence for primordial black holes in LIGO/Virgo gravitational-wave data*, [2105.03349](#).
- [417] K. Inomata, M. Kawasaki, K. Mukaida and T. T. Yanagida, *NANOGrav results and LIGO-Virgo primordial black holes in axion-like curvaton model*, [2011.01270](#).
- [418] K. Kohri and T. Terada, *Solar-Mass Primordial Black Holes Explain NANOGrav Hint of Gravitational Waves*, *Phys. Lett.* **B813** (2021) 136040, [[2009.11853](#)].
- [419] L. Lentati et al., *European Pulsar Timing Array Limits On An Isotropic Stochastic Gravitational-Wave Background*, *Mon. Not. Roy. Astron. Soc.* **453** (2015) 2576–2598, [[1504.03692](#)].
- [420] R. M. Shannon et al., *Gravitational waves from binary supermassive black holes missing in pulsar observations*, *Science* **349** (2015) 1522–1525, [[1509.07320](#)].
- [421] NANOGrav collaboration, Z. Arzoumanian et al., *The NANOGrav 11-year Data Set: Pulsar-timing Constraints On The Stochastic Gravitational-wave Background*, *Astrophys. J.* **859** (2018) 47, [[1801.02617](#)].
- [422] C. J. Moore, R. H. Cole and C. P. L. Berry, *Gravitational-wave sensitivity curves*, *Class. Quant. Grav.* **32** (2015) 015014, [[1408.0740](#)].
- [423] A. Albrecht, P. J. Steinhardt, M. S. Turner and F. Wilczek, *Reheating an Inflationary Universe*, *Phys. Rev. Lett.* **48** (1982) 1437.
- [424] Y. Shtanov, J. H. Traschen and R. H. Brandenberger, *Universe reheating after inflation*, *Phys. Rev.* **D51** (1995) 5438–5455, [[hep-ph/9407247](#)].
- [425] L. Kofman, A. D. Linde and A. A. Starobinsky, *Reheating after inflation*, *Phys. Rev. Lett.* **73** (1994) 3195–3198, [[hep-th/9405187](#)].
- [426] L. Kofman, A. D. Linde and A. A. Starobinsky, *Towards the theory of reheating after inflation*, *Phys. Rev.* **D56** (1997) 3258–3295, [[hep-ph/9704452](#)].
- [427] D. Huang and L. Yin, *Stochastic Gravitational Waves from Inflaton Decays*, *Phys. Rev. D* **100** (2019) 043538, [[1905.08510](#)].
- [428] J.-F. Dufaux, G. Felder, L. Kofman and O. Navros, *Gravity Waves from Tachyonic Preheating after Hybrid Inflation*, *JCAP* **0903** (2009) 001, [[0812.2917](#)].
- [429] P. Adshead, J. T. Giblin and Z. J. Weiner, *Gravitational waves from gauge preheating*, *Phys. Rev.* **D98** (2018) 043525, [[1805.04550](#)].
- [430] J. R. C. Cuissa and D. G. Figueroa, *Lattice formulation of axion inflation. Application to preheating*, *JCAP* **1906** (2019) 002, [[1812.03132](#)].
- [431] P. Adshead, J. T. Giblin, M. Pieroni and Z. J. Weiner, *Constraining axion inflation with gravitational waves from preheating*, *Phys. Rev.* **D101** (2020) 083534, [[1909.12842](#)].

- [432] C. Fu, P. Wu and H. Yu, *Production of gravitational waves during preheating with nonminimal coupling*, *Phys. Rev. D* **97** (2018) 081303, [[1711.10888](#)].
- [433] J. Garcia-Bellido, D. G. Figueroa and J. Rubio, *Preheating in the Standard Model with the Higgs-Inflaton coupled to gravity*, *Phys. Rev.* **D79** (2009) 063531, [[0812.4624](#)].
- [434] G. Jin, C. Fu, P. Wu and H. Yu, *Production of gravitational waves during preheating in the Starobinsky inflationary model*, *Eur. Phys. J.* **C80** (2020) 491, [[2007.02225](#)].
- [435] T. Zhu, Q. Wu and A. Wang, *An analytical approach to the field amplification and particle production by parametric resonance during inflation and reheating*, *Phys. Dark Univ.* **26** (2019) 100373, [[1811.12612](#)].
- [436] S. Y. Khlebnikov and I. I. Tkachev, *Relic gravitational waves produced after preheating*, *Phys. Rev. D* **56** (1997) 653–660, [[hep-ph/9701423](#)].
- [437] A. A. Starobinsky, *A New Type of Isotropic Cosmological Models Without Singularity*, *Phys. Lett.* **91B** (1980) 99–102.
- [438] V. F. Mukhanov and G. V. Chibisov, *Quantum Fluctuations and a Nonsingular Universe*, *JETP Lett.* **33** (1981) 532–535.
- [439] A. D. Linde, *Chaotic Inflation*, *Phys. Lett.* **129B** (1983) 177–181.
- [440] K. D. Lozanov and M. A. Amin, *Equation of State and Duration to Radiation Domination after Inflation*, *Phys. Rev. Lett.* **119** (2017) 061301, [[1608.01213](#)].
- [441] K. D. Lozanov and M. A. Amin, *Self-resonance after inflation: oscillons, transients and radiation domination*, *Phys. Rev.* **D97** (2018) 023533, [[1710.06851](#)].
- [442] I. Tkachev, S. Khlebnikov, L. Kofman and A. D. Linde, *Cosmic strings from preheating*, *Phys. Lett.* **B440** (1998) 262–268, [[hep-ph/9805209](#)].
- [443] J.-F. Dufaux, D. G. Figueroa and J. Garcia-Bellido, *Gravitational Waves from Abelian Gauge Fields and Cosmic Strings at Preheating*, *Phys. Rev.* **D82** (2010) 083518, [[1006.0217](#)].
- [444] A. Diaz-Gil, J. Garcia-Bellido, M. Garcia Perez and A. Gonzalez-Arroyo, *Magnetic field production during preheating at the electroweak scale*, *Phys. Rev. Lett.* **100** (2008) 241301, [[0712.4263](#)].
- [445] A. Diaz-Gil, J. Garcia-Bellido, M. Garcia Perez and A. Gonzalez-Arroyo, *Primordial magnetic fields from preheating at the electroweak scale*, *JHEP* **07** (2008) 043, [[0805.4159](#)].
- [446] B. A. Bassett and S. Tsujikawa, *Inflationary preheating and primordial black holes*, *Phys. Rev.* **D63** (2001) 123503, [[hep-ph/0008328](#)].
- [447] A. M. Green and K. A. Malik, *Primordial black hole production due to preheating*, *Phys. Rev.* **D64** (2001) 021301, [[hep-ph/0008113](#)].
- [448] X.-X. Kou, C. Tian and S.-Y. Zhou, *Oscillon Preheating in Full General Relativity*, *Class. Quant. Grav.* **38** (2021) 045005, [[1912.09658](#)].
- [449] P. Auclair and V. Vennin, *Primordial black holes from metric preheating: mass fraction in the excursion-set approach*, *JCAP* **2102** (2021) 038, [[2011.05633](#)].
- [450] Z. Nazari, M. Cicoli, K. Clough and F. Muia, *Oscillon collapse to black holes*, *JCAP* **2105** (2021) 027, [[2010.05933](#)].
- [451] R. Easther and E. A. Lim, *Stochastic gravitational wave production after inflation*, *JCAP* **04** (2006) 010, [[astro-ph/0601617](#)].
- [452] R. Easther, J. T. Giblin, Jr. and E. A. Lim, *Gravitational Wave Production At The End Of Inflation*, *Phys. Rev. Lett.* **99** (2007) 221301, [[astro-ph/0612294](#)].
- [453] R.-G. Cai, Z.-K. Guo, P.-Z. Ding, C.-J. Fu and J. Liu, *Dependence of the amplitude of gravitational waves from preheating on the inflationary energy scale*, [2105.00427](#).

- [454] J. Garcia-Bellido and D. G. Figueroa, *A stochastic background of gravitational waves from hybrid preheating*, *Phys. Rev. Lett.* **98** (2007) 061302, [[astro-ph/0701014](#)].
- [455] M. A. Amin and D. Shirokoff, *Flat-top oscillons in an expanding universe*, *Phys. Rev. D* **81** (2010) 085045, [[1002.3380](#)].
- [456] S.-Y. Zhou, E. J. Copeland, R. Easther, H. Finkel, Z.-G. Mou and P. M. Saffin, *Gravitational Waves from Oscillon Preheating*, *JHEP* **10** (2013) 026, [[1304.6094](#)].
- [457] S. Antusch, F. Cefala and S. Orani, *Gravitational waves from oscillons after inflation*, *Phys. Rev. Lett.* **118** (2017) 011303, [[1607.01314](#)].
- [458] S. Antusch, F. Cefala, S. Krippendorff, F. Muia, S. Orani and F. Quevedo, *Oscillons from String Moduli*, *JHEP* **01** (2018) 083, [[1708.08922](#)].
- [459] S. Antusch, F. Cefala and S. Orani, *What can we learn from the stochastic gravitational wave background produced by oscillons?*, *JCAP* **03** (2018) 032, [[1712.03231](#)].
- [460] M. A. Amin, J. Braden, E. J. Copeland, J. T. Giblin, C. Solorio, Z. J. Weiner et al., *Gravitational waves from asymmetric oscillon dynamics?*, *Phys. Rev. D* **98** (2018) 024040, [[1803.08047](#)].
- [461] J. Liu, Z.-K. Guo, R.-G. Cai and G. Shiu, *Gravitational Waves from Oscillons with Cuspy Potentials*, *Phys. Rev. Lett.* **120** (2018) 031301, [[1707.09841](#)].
- [462] J. Liu, Z.-K. Guo, R.-G. Cai and G. Shiu, *Gravitational wave production after inflation with cuspy potentials*, *Phys. Rev. D* **99** (2019) 103506, [[1812.09235](#)].
- [463] T. Liu, S. Cao, J. Zhang, S. Geng, Y. Liu, X. Ji et al., *Implications from Simulated Strong Gravitational Lensing Systems: Constraining Cosmological Parameters Using Gaussian Processes*, *Astrophysical Journal* **886** (Dec., 2019) 94, [[1910.02592](#)].
- [464] T. Liu, S. Cao, J. Zhang, M. Biesiada, Y. Liu and Y. Lian, *Testing the cosmic curvature at high redshifts: the combination of LSST strong lensing systems and quasars as new standard candles*, *Mon. Not. Roy. Astron. Soc.* **496** (July, 2020) 708–717, [[2005.13990](#)].
- [465] S. Geng, S. Cao, Y. Liu, T. Liu, M. Biesiada and Y. Lian, *The velocity dispersion function of early-type galaxies and its redshift evolution: the newest results from lens redshift test*, *Mon. Not. Roy. Astron. Soc.* **503** (May, 2021) 1319–1326, [[2102.12140](#)].
- [466] J.-Z. Qi, J.-W. Zhao, S. Cao, M. Biesiada and Y. Liu, *Measurements of the Hubble constant and cosmic curvature with quasars: ultracompact radio structure and strong gravitational lensing*, *Mon. Not. Roy. Astron. Soc.* **503** (May, 2021) 2179–2186, [[2011.00713](#)].
- [467] M. Sereno, P. Jetzer, A. Sesana and M. Volonteri, *Cosmography with strong lensing of LISA gravitational wave sources*, *Mon. Not. Roy. Astron. Soc.* **415** (2011) 2773, [[1104.1977](#)].
- [468] X. Ding, M. Biesiada and Z.-H. Zhu, *Strongly lensed gravitational waves from intrinsically faint double compact binaries—prediction for the Einstein Telescope*, *JCAP* **12** (2015) 006, [[1508.05000](#)].
- [469] T. E. Collett and D. Bacon, *Testing the speed of gravitational waves over cosmological distances with strong gravitational lensing*, *Phys. Rev. Lett.* **118** (2017) 091101, [[1602.05882](#)].
- [470] X.-L. Fan, K. Liao, M. Biesiada, A. Piorkowska-Kurpas and Z.-H. Zhu, *Speed of Gravitational Waves from Strongly Lensed Gravitational Waves and Electromagnetic Signals*, *Phys. Rev. Lett.* **118** (2017) 091102, [[1612.04095](#)].
- [471] K. Liao, X.-L. Fan, X.-H. Ding, M. Biesiada and Z.-H. Zhu, *Precision cosmology from future lensed gravitational wave and electromagnetic signals*, *Nature Commun.* **8** (2017) 1148, [[1703.04151](#)].
- [472] T. Yang, B. Hu, R.-G. Cai and B. Wang, *New probe of gravity: strongly lensed gravitational wave multi-messenger approach*, *Astrophys. J.* **880** (2019) 50, [[1810.00164](#)].

- [473] O. A. Hannuksela, T. E. Collett, M. Calzavara and T. G. F. Li, *Localizing merging black holes with sub-arcsecond precision using gravitational-wave lensing*, *Mon. Not. Roy. Astron. Soc.* **498** (2020) 3395–3402, [[2004.13811](#)].
- [474] H. Yu, P. Zhang and F.-Y. Wang, *Strong lensing as a giant telescope to localize the host galaxy of gravitational wave event*, *Mon. Not. Roy. Astron. Soc.* **497** (2020) 204–209, [[2007.00828](#)].
- [475] S. Cao, J. Qi, M. Biesiada, T. Liu, J. Li and Z.-H. Zhu, *Measuring the viscosity of dark matter with strongly lensed gravitational waves*, *Mon. Not. Roy. Astron. Soc.* **502** (2021) L16–L20, [[2012.12462](#)].
- [476] F. Xu, J. M. Ezquiaga and D. E. Holz, *Please repeat: Strong lensing of gravitational waves as a probe of compact binary and galaxy populations*, [2105.14390](#).
- [477] O. A. Hannuksela, K. Haris, K. K. Y. Ng, S. Kumar, A. K. Mehta, D. Keitel et al., *Search for gravitational lensing signatures in LIGO-Virgo binary black hole events*, *Astrophys. J. Lett.* **874** (2019) L2, [[1901.02674](#)].
- [478] LIGO SCIENTIFIC, VIRGO collaboration, R. Abbott et al., *Search for lensing signatures in the gravitational-wave observations from the first half of LIGO-Virgo’s third observing run*, [2105.06384](#).
- [479] B. Bertotti, L. Iess and P. Tortora, *A test of general relativity using radio links with the Cassini spacecraft*, *Nature* **425** (2003) 374–376.
- [480] S. S. Shapiro, J. L. Davis, D. E. Lebach and J. S. Gregory, *Measurement of the Solar Gravitational Deflection of Radio Waves using Geodetic Very-Long-Baseline Interferometry Data, 1979-1999*, *Phys. Rev. Lett.* **92** (2004) 121101.
- [481] K. S. Thorne and C. M. Will, *Theoretical Frameworks for Testing Relativistic Gravity. I. Foundations*, *Astrophys. J.* **163** (1971) 595–610.
- [482] A. S. Bolton, S. Rappaport and S. Burles, *Constraint on the Post-Newtonian Parameter γ on Galactic Size Scales*, *Phys. Rev.* **D74** (2006) 061501, [[astro-ph/0607657](#)].
- [483] T. L. Smith, *Testing gravity on kiloparsec scales with strong gravitational lenses*, [0907.4829](#).
- [484] J. Schwab, A. S. Bolton and S. A. Rappaport, *Galaxy-Scale Strong Lensing Tests of Gravity and Geometric Cosmology: Constraints and Systematic Limitations*, *Astrophys. J.* **708** (2010) 750–757, [[0907.4992](#)].
- [485] S. Cao, X. Li, M. Biesiada, T. Xu, Y. Cai and Z.-H. Zhu, *Test of parametrized post-Newtonian gravity with galaxy-scale strong lensing systems*, *Astrophys. J.* **835** (2017) 92, [[1701.00357](#)].
- [486] T. E. Collett, L. J. Oldham, R. J. Smith, M. W. Auger, K. B. Westfall, D. Bacon et al., *A precise extragalactic test of General Relativity*, *Science* **360** (2018) 1342, [[1806.08300](#)].
- [487] J. Ehlers and A. R. Prasanna, *A WKB formalism for multicomponent fields and its application to gravitational and sound waves in perfect fluids*, *Class. Quant. Grav.* **13** (aug, 1996) 2231–2240.
- [488] J.-Z. Qi, S. Cao, C. Zheng, Y. Pan, Z. Li, J. Li et al., *Testing the Etherington distance duality relation at higher redshifts: Combined radio quasar and gravitational wave data*, *Phys. Rev.* **D99** (2019) 063507, [[1902.01988](#)].
- [489] J.-Z. Qi, S. Cao, Y. Pan and J. Li, *Cosmic opacity: cosmological-model-independent tests from gravitational waves and Type Ia Supernova*, *Phys. Dark Univ.* **26** (2019) 100338, [[1902.01702](#)].
- [490] W. Zimdahl, D. J. Schwarz, A. B. Balakin and D. Pavon, *Cosmic anti-friction and accelerated expansion*, *Phys. Rev. D* **64** (2001) 063501, [[astro-ph/0009353](#)].
- [491] S. Cao, Z.-H. Zhu and N. Liang, *Observational Constraints on Interacting Dark Matter Model Without Dark Energy*, *Astron. Astrophys.* **529** (2011) A61, [[1011.4848](#)].

- [492] S. W. Hawking, *Perturbations of an expanding universe*, *Astrophys. J.* **145** (1966) 544–554.
- [493] G. Baym, S. P. Patil and C. J. Pethick, *Damping of gravitational waves by matter*, *Phys. Rev. D* **96** (Oct, 2017) 084033.
- [494] N. Mirón-Granese, *Relativistic viscous effects on the primordial gravitational waves spectrum*, *Journal of Cosmology and Astroparticle Physics* **2021** (jun, 2021) 008.
- [495] B.-Q. Lu, D. Huang, Y.-L. Wu and Y.-F. Zhou, *Damping of gravitational waves in a viscous Universe and its implication for dark matter self-interactions*, [1803.11397](#).
- [496] S. Cao, Y. Pan, M. Biesiada, W. Godłowski and Z.-H. Zhu, *Constraints on cosmological models from strong gravitational lensing systems*, *Journal of Cosmology and Astroparticle Physics* **2012** (Mar., 2012) 016, [[1105.6226](#)].
- [497] S. Cao, G. Covone and Z.-H. Zhu, *Testing the Dark Energy with Gravitational Lensing Statistics*, *Astrophysical Journal* **755** (Aug., 2012) 31, [[1206.4948](#)].
- [498] S. Cao, M. Biesiada, R. Gavazzi, A. Piórkowska and Z.-H. Zhu, *Cosmology with Strong-lensing Systems*, *Astrophysical Journal* **806** (June, 2015) 185, [[1509.07649](#)].
- [499] S. Cao, J. Qi, Z. Cao, M. Biesiada, J. Li, Y. Pan et al., *Direct test of the FLRW metric from strongly lensed gravitational wave observations*, *Sci. Rep.* **9** (2019) 11608, [[1910.10365](#)].
- [500] K. Liao, X. Ding, M. Biesiada, X.-L. Fan and Z.-H. Zhu, *Anomalies in Time Delays of Lensed Gravitational Waves and Dark Matter Substructures*, *Astrophys. J.* **867** (2018) 69, [[1809.07079](#)].
- [501] S. R. Taylor and J. R. Gair, *Cosmology with the lights off: standard sirens in the Einstein Telescope era*, *Phys. Rev. D* **86** (2012) 023502, [[1204.6739](#)].
- [502] C. Cutler and D. E. Holz, *Ultra-high precision cosmology from gravitational waves*, *Phys. Rev. D* **80** (2009) 104009, [[0906.3752](#)].
- [503] S. Kawamura et al., *Space gravitational-wave antennas DECIGO and B-DECIGO*, *Int. J. Mod. Phys. D* **28** (2019) 1845001.
- [504] T. E. Collett, *The population of galaxy-galaxy strong lenses in forthcoming optical imaging surveys*, *Astrophys. J.* **811** (2015) 20, [[1507.02657](#)].
- [505] M. Dominik, K. Belczynski, C. Fryer, D. E. Holz, E. Berti, T. Bulik et al., *Double Compact Objects II: Cosmological Merger Rates*, *Astrophys. J.* **779** (2013) 72, [[1308.1546](#)].
- [506] A. Piórkowska-Kurpas, S. Hou, M. Biesiada, X. Ding, S. Cao, X. Fan et al., *Inspiraling double compact object detection and lensing rate: Forecast for DECIGO and b-DECIGO*, *The Astrophysical Journal* **908** (feb, 2021) 196.
- [507] M. Kaplinghat, S. Tulin and H.-B. Yu, *Dark Matter Halos as Particle Colliders: Unified Solution to Small-Scale Structure Puzzles from Dwarfs to Clusters*, *Phys. Rev. Lett.* **116** (2016) 041302, [[1508.03339](#)].
- [508] S. Tulin and H.-B. Yu, *Dark Matter Self-interactions and Small Scale Structure*, *Phys. Rept.* **730** (2018) 1–57, [[1705.02358](#)].
- [509] D. N. Spergel and P. J. Steinhardt, *Observational evidence for self-interacting cold dark matter*, *Phys. Rev. Lett.* **84** (2000) 3760–3763, [[astro-ph/9909386](#)].
- [510] B. F. Schutz, *Determining the Hubble Constant from Gravitational Wave Observations*, *Nature* **323** (1986) 310–311.
- [511] S. A. Hughes, *Listening to the universe with gravitational-wave astronomy*, *Annals Phys.* **303** (2003) 142–178, [[astro-ph/0210481](#)].
- [512] L. Blanchet, *Gravitational Radiation from Post-Newtonian Sources and Inspiralling Compact Binaries*, *Living Rev. Rel.* **17** (2014) 2, [[1310.1528](#)].

- [513] P. S. Drell, T. J. Loredo and I. Wasserman, *Type Ia supernovae, evolution, and the cosmological constant*, *Astrophys. J.* **530** (2000) 593, [[astro-ph/9905027](#)].
- [514] S. Benetti et al., *The Diversity of type Ia supernovae: Evidence for systematics?*, *Astrophys. J.* **623** (2005) 1011–1016, [[astro-ph/0411059](#)].
- [515] D. Eichler, M. Livio, T. Piran and D. N. Schramm, *Nucleosynthesis, Neutrino Bursts and Gamma-Rays from Coalescing Neutron Stars*, *Nature* **340** (1989) 126–128.
- [516] D. B. Fox et al., *The afterglow of grb050709 and the nature of the short-hard gamma-ray bursts*, *Nature* **437** (2005) 845–850, [[astro-ph/0510110](#)].
- [517] E. Nakar, A. Gal-Yam and D. B. Fox, *The Local Rate and the Progenitor Lifetimes of Short-Hard Gamma-Ray Bursts: Synthesis and Predictions for LIGO*, *Astrophys. J.* **650** (2006) 281–290, [[astro-ph/0511254](#)].
- [518] E. Berger et al., *A New Population of High Redshift Short-Duration Gamma-Ray Bursts*, *Astrophys. J.* **664** (2007) 1000–1010, [[astro-ph/0611128](#)].
- [519] N. Dalal, D. E. Holz, S. A. Hughes and B. Jain, *Short grb and binary black hole standard sirens as a probe of dark energy*, *Phys. Rev.* **D74** (2006) 063006, [[astro-ph/0601275](#)].
- [520] S. Nissanke, D. E. Holz, S. A. Hughes, N. Dalal and J. L. Sievers, *Exploring short gamma-ray bursts as gravitational-wave standard sirens*, *Astrophys. J.* **725** (2010) 496–514, [[0904.1017](#)].
- [521] B. S. Sathyaprakash, B. F. Schutz and C. Van Den Broeck, *Cosmography with the Einstein Telescope*, *Class. Quant. Grav.* **27** (2010) 215006, [[0906.4151](#)].
- [522] W. Zhao, C. Van Den Broeck, D. Baskaran and T. G. F. Li, *Determination of Dark Energy by the Einstein Telescope: Comparing with CMB, BAO and SNIa Observations*, *Phys. Rev.* **D83** (2011) 023005, [[1009.0206](#)].
- [523] R.-G. Cai and T. Yang, *Estimating cosmological parameters by the simulated data of gravitational waves from the Einstein Telescope*, *Phys. Rev.* **D95** (2017) 044024, [[1608.08008](#)].
- [524] LIGO SCIENTIFIC, VIRGO, FERMI GBM, INTEGRAL, ICECUBE, ASTROSAT CADMIUM ZINC TELLURIDE IMAGER TEAM, IPN, INSIGHT-HXMT, ANTARES, SWIFT, AGILE TEAM, 1M2H TEAM, DARK ENERGY CAMERA GW-EM, DES, DLT40, GRAWITA, FERMI-LAT, ATCA, ASKAP, LAS CUMBRES OBSERVATORY GROUP, OzGRAV, DWF (DEEPER WIDER FASTER PROGRAM), AST3, CAASTRO, VINROUGE, MASTER, J-GEM, GROWTH, JAGWAR, CALTECHNRAO, TTU-NRAO, NUSTAR, PAN-STARRS, MAXI TEAM, TZAC CONSORTIUM, KU, NORDIC OPTICAL TELESCOPE, EPESSTO, GROND, TEXAS TECH UNIVERSITY, SALT GROUP, TOROS, BOOTES, MWA, CALET, IKI-GW FOLLOW-UP, H.E.S.S., LOFAR, LWA, HAWC, PIERRE AUGER, ALMA, EURO VLBI TEAM, PI OF SKY, CHANDRA TEAM AT MCGILL UNIVERSITY, DFN, ATLAS TELESCOPES, HIGH TIME RESOLUTION UNIVERSE SURVEY, RIMAS, RATIR, SKA SOUTH AFRICA/MEERKAT collaboration, B. P. Abbott et al., *Multi-messenger Observations of a Binary Neutron Star Merger*, *Astrophys. J. Lett.* **848** (2017) L12, [[1710.05833](#)].
- [525] LIGO SCIENTIFIC, VIRGO, FERMI-GBM, INTEGRAL collaboration, B. P. Abbott et al., *Gravitational Waves and Gamma-rays from a Binary Neutron Star Merger: GW170817 and GRB 170817A*, *Astrophys. J. Lett.* **848** (2017) L13, [[1710.05834](#)].
- [526] LIGO SCIENTIFIC, VIRGO, 1M2H, DARK ENERGY CAMERA GW-E, DES, DLT40, LAS CUMBRES OBSERVATORY, VINROUGE, MASTER collaboration, B. P. Abbott et al., *A gravitational-wave standard siren measurement of the Hubble constant*, *Nature* **551** (2017) 85–88, [[1710.05835](#)].
- [527] M. J. Graham et al., *Candidate Electromagnetic Counterpart to the Binary Black Hole Merger Gravitational Wave Event S190521g*, *Phys. Rev. Lett.* **124** (2020) 251102, [[2006.14122](#)].

- [528] H.-Y. Chen, C.-J. Haster, S. Vitale, W. M. Farr and M. Isi, *A Standard Siren Cosmological Measurement from the Potential GW190521 Electromagnetic Counterpart ZTF19abnrhr*, [2009.14057](#).
- [529] S. Mukherjee, A. Ghosh, M. J. Graham, C. Karathanasis, M. M. Kasliwal, I. Magaña Hernandez et al., *First measurement of the Hubble parameter from bright binary black hole GW190521*, [2009.14199](#).
- [530] H.-Y. Chen, M. Fishbach and D. E. Holz, *A two per cent Hubble constant measurement from standard sirens within five years*, *Nature* **562** (2018) 545–547, [[1712.06531](#)].
- [531] C. Palenzuela, L. Lehner and S. L. Liebling, *Dual Jets from Binary Black Holes*, *Science* **329** (2010) 927, [[1005.1067](#)].
- [532] M. Dotti, A. Sesana and R. Decarli, *Massive black hole binaries: dynamical evolution and observational signatures*, *Adv. Astron.* **2012** (2012) 940568, [[1111.0664](#)].
- [533] B. Giacomazzo, J. G. Baker, M. C. Miller, C. S. Reynolds and J. R. van Meter, *General Relativistic Simulations of Magnetized Plasmas around Merging Supermassive Black Holes*, *Astrophys. J. Lett.* **752** (2012) L15, [[1203.6108](#)].
- [534] B. Kocsis, Z. Haiman and K. Menou, *Pre-Merger Localization of Gravitational-Wave Standard Sirens With LISA: Triggered Search for an Electromagnetic Counterpart*, *Astrophys. J.* **684** (2008) 870–888, [[0712.1144](#)].
- [535] R. O’Shaughnessy, D. L. Kaplan, A. Sesana and A. Kamble, *Blindly detecting orbital modulations of jets from merging supermassive black holes*, *Astrophys. J.* **743** (2011) 136, [[1109.1050](#)].
- [536] D. L. Kaplan, R. O’Shaughnessy, A. Sesana and M. Volonteri, *Blindly Detecting Merging Supermassive Black Holes with Radio Surveys*, *Astrophys. J. Lett.* **734** (2011) L37, [[1105.3653](#)].
- [537] Z. Haiman, *Electromagnetic chirp of a compact binary black hole: A phase template for the gravitational wave inspiral*, *Phys. Rev.* **D96** (2017) 023004, [[1705.06765](#)].
- [538] D. E. Holz and S. A. Hughes, *Using gravitational-wave standard sirens*, *Astrophys. J.* **629** (2005) 15–22, [[astro-ph/0504616](#)].
- [539] A. Klein et al., *Science with the space-based interferometer eLISA: Supermassive black hole binaries*, *Phys. Rev.* **D93** (2016) 024003, [[1511.05581](#)].
- [540] N. Tamanini, C. Caprini, E. Barausse, A. Sesana, A. Klein and A. Petiteau, *Science with the space-based interferometer eLISA. III: Probing the expansion of the Universe using gravitational wave standard sirens*, *JCAP* **1604** (2016) 002, [[1601.07112](#)].
- [541] N. Tamanini, *Late time cosmology with LISA: probing the cosmic expansion with massive black hole binary mergers as standard sirens*, *J. Phys. Conf. Ser.* **840** (2017) 012029, [[1612.02634](#)].
- [542] C. Caprini and N. Tamanini, *Constraining early and interacting dark energy with gravitational wave standard sirens: the potential of the eLISA mission*, *JCAP* **1610** (2016) 006, [[1607.08755](#)].
- [543] R.-G. Cai, N. Tamanini and T. Yang, *Reconstructing the dark sector interaction with LISA*, *JCAP* **1705** (2017) 031, [[1703.07323](#)].
- [544] P. Creminelli and F. Vernizzi, *Dark Energy after GW170817 and GRB170817A*, *Phys. Rev. Lett.* **119** (2017) 251302, [[1710.05877](#)].
- [545] J. M. Ezquiaga and M. Zumalacábarregui, *Dark Energy After GW170817: Dead Ends and the Road Ahead*, *Phys. Rev. Lett.* **119** (2017) 251304, [[1710.05901](#)].

- [546] L. Amendola, M. Kunz, I. D. Saltas and I. Sawicki, *Fate of Large-Scale Structure in Modified Gravity After GW170817 and GRB170817A*, *Phys. Rev. Lett.* **120** (2018) 131101, [[1711.04825](#)].
- [547] D. Langlois, R. Saito, D. Yamauchi and K. Noui, *Scalar-tensor theories and modified gravity in the wake of GW170817*, *Phys. Rev.* **D97** (2018) 061501, [[1711.07403](#)].
- [548] T. Baker, E. Bellini, P. G. Ferreira, M. Lagos, J. Noller and I. Sawicki, *Strong constraints on cosmological gravity from GW170817 and GRB 170817A*, *Phys. Rev. Lett.* **119** (2017) 251301, [[1710.06394](#)].
- [549] R. Kase and S. Tsujikawa, *Dark energy in Horndeski theories after GW170817: A review*, *Int. J. Mod. Phys.* **D28** (2019) 1942005, [[1809.08735](#)].
- [550] E. J. Copeland, M. Kopp, A. Padilla, P. M. Saffin and C. Skordis, *Dark energy after GW170817 revisited*, *Phys. Rev. Lett.* **122** (2019) 061301, [[1810.08239](#)].
- [551] R.-G. Cai, T.-B. Liu and S.-J. Wang, *Gravitational wave as probe of superfluid dark matter*, *Phys. Rev.* **D97** (2018) 023027, [[1710.02425](#)].
- [552] I. D. Saltas, I. Sawicki, L. Amendola and M. Kunz, *Anisotropic Stress as a Signature of Nonstandard Propagation of Gravitational Waves*, *Phys. Rev. Lett.* **113** (2014) 191101, [[1406.7139](#)].
- [553] A. Nishizawa, *Generalized framework for testing gravity with gravitational-wave propagation. I. Formulation*, *Phys. Rev.* **D97** (2018) 104037, [[1710.04825](#)].
- [554] S. Arai and A. Nishizawa, *Generalized framework for testing gravity with gravitational-wave propagation. II. Constraints on Horndeski theory*, *Phys. Rev.* **D97** (2018) 104038, [[1711.03776](#)].
- [555] E. Belgacem, Y. Dirian, S. Foffa and M. Maggiore, *Gravitational-wave luminosity distance in modified gravity theories*, *Phys. Rev.* **D97** (2018) 104066, [[1712.08108](#)].
- [556] L. Amendola, I. Sawicki, M. Kunz and I. D. Saltas, *Direct detection of gravitational waves can measure the time variation of the Planck mass*, *JCAP* **1808** (2018) 030, [[1712.08623](#)].
- [557] E. Belgacem, Y. Dirian, S. Foffa and M. Maggiore, *Modified gravitational-wave propagation and standard sirens*, *Phys. Rev.* **D98** (2018) 023510, [[1805.08731](#)].
- [558] M. Lagos, M. Fishbach, P. Landry and D. E. Holz, *Standard sirens with a running Planck mass*, *Phys. Rev.* **D99** (2019) 083504, [[1901.03321](#)].
- [559] A. Nishizawa and S. Arai, *Generalized framework for testing gravity with gravitational-wave propagation. III. Future prospect*, *Phys. Rev.* **D99** (2019) 104038, [[1901.08249](#)].
- [560] LISA COSMOLOGY WORKING GROUP collaboration, E. Belgacem et al., *Testing modified gravity at cosmological distances with LISA standard sirens*, *JCAP* **1907** (2019) 024, [[1906.01593](#)].
- [561] E. Belgacem, Y. Dirian, S. Foffa, E. J. Howell, M. Maggiore and T. Regimbau, *Cosmology and dark energy from joint gravitational wave-GRB observations*, *JCAP* **1908** (2019) 015, [[1907.01487](#)].
- [562] E. Belgacem, S. Foffa, M. Maggiore and T. Yang, *Gaussian processes reconstruction of modified gravitational wave propagation*, *Phys. Rev.* **D101** (2020) 063505, [[1911.11497](#)].
- [563] W.-H. Ruan, C. Liu, Z.-K. Guo, Y.-L. Wu and R.-G. Cai, *The LISA-Taiji network: precision localization of massive black hole binaries*, *Research* **2021** (10, 2019) 6014164, [[1909.07104](#)].
- [564] W.-H. Ruan, C. Liu, Z.-K. Guo, Y.-L. Wu and R.-G. Cai, *The LISA-Taiji network*, *Nat. Astron.* **4** (2020) 108–109, [[2002.03603](#)].

- [565] R. Wang, W.-H. Ruan, Q. Yang, Z.-K. Guo, R.-G. Cai and B. Hu, *Hubble parameter estimation via dark sirens with the LISA-Taiji network*, *National Science Review* (04, 2021) , [2010.14732].
- [566] G. Orlando, M. Pieroni and A. Ricciardone, *Measuring Parity Violation in the Stochastic Gravitational Wave Background with the LISA-Taiji network*, *JCAP* **03** (2021) 069, [2011.07059].
- [567] L.-F. Wang, S.-J. Jin, J.-F. Zhang and X. Zhang, *Forecast for cosmological parameter estimation with gravitational-wave standard sirens from the LISA-Taiji network*, **2101.11882**.
- [568] T. Yang, *Gravitational-Wave Detector Networks: Standard Sirens on Cosmology and Modified Gravity Theory*, *JCAP* **05** (2021) 044, [2103.01923].
- [569] E. Barausse, *The evolution of massive black holes and their spins in their galactic hosts*, *Mon. Not. Roy. Astron. Soc.* **423** (2012) 2533–2557, [1201.5888].
- [570] PLANCK collaboration, P. A. R. Ade et al., *Planck 2015 results. XVI. Isotropy and statistics of the CMB*, *Astron. Astrophys.* **594** (2016) A16, [1506.07135].
- [571] R.-G. Cai and Z.-L. Tuo, *Direction Dependence of the Deceleration Parameter*, *JCAP* **1202** (2012) 004, [1109.0941].
- [572] R.-G. Cai, Y.-Z. Ma, B. Tang and Z.-L. Tuo, *Constraining the anisotropic expansion of the Universe*, *Phys. Rev.* **D87** (2013) 123522, [1303.0961].
- [573] R. Fernández-Cobos, P. Vielva, D. Pietrobon, A. Balbi, E. Martínez-González and R. B. Barreiro, *Searching for a dipole modulation in the large-scale structure of the Universe*, *Mon. Not. Roy. Astron. Soc.* **441** (2014) 2392–2397, [1312.0275].
- [574] C. A. P. Bengaly, A. Bernui, J. S. Alcaniz, H. S. Xavier and C. P. Novaes, *Is there evidence for anomalous dipole anisotropy in the large-scale structure?*, *Mon. Not. Roy. Astron. Soc.* **464** (2017) 768–774, [1606.06751].
- [575] R.-G. Cai, T.-B. Liu, X.-W. Liu, S.-J. Wang and T. Yang, *Probing cosmic anisotropy with gravitational waves as standard sirens*, *Phys. Rev.* **D97** (2018) 103005, [1712.00952].
- [576] L. Verde, T. Treu and A. G. Riess, *Tensions between the Early and the Late Universe*, *Nature Astron.* **3** (7, 2019) 891, [1907.10625].
- [577] H. Li and X. Zhang, *A novel method of measuring cosmological distances using broad-line regions of quasars*, *Sci. Bull.* **65** (2020) 1419–1421, [2005.10458].
- [578] R.-Y. Guo, J.-F. Zhang and X. Zhang, *Can the H_0 tension be resolved in extensions to Λ CDM cosmology?*, *JCAP* **02** (2019) 054, [1809.02340].
- [579] E. Di Valentino, O. Mena, S. Pan, L. Visinelli, W. Yang, A. Melchiorri et al., *In the Realm of the Hubble tension – a Review of Solutions*, **2103.01183**.
- [580] A. G. Riess, S. Casertano, W. Yuan, J. B. Bowers, L. Macri, J. C. Zinn et al., *Cosmic Distances Calibrated to 1% Precision with Gaia EDR3 Parallaxes and Hubble Space Telescope Photometry of 75 Milky Way Cepheids Confirm Tension with Λ CDM*, *Astrophys. J. Lett.* **908** (2021) L6, [2012.08534].
- [581] M. Zhao, R. Guo, D. He, J. Zhang and X. Zhang, *Dark energy versus modified gravity: Impacts on measuring neutrino mass*, *Sci. China Phys. Mech. Astron.* **63** (2020) 230412, [1810.11658].
- [582] L. Feng, H.-L. Li, J.-F. Zhang and X. Zhang, *Exploring neutrino mass and mass hierarchy in interacting dark energy models*, *Sci. China Phys. Mech. Astron.* **63** (2020) 220401, [1903.08848].

- [583] L. Feng, D.-Z. He, H.-L. Li, J.-F. Zhang and X. Zhang, *Constraints on active and sterile neutrinos in an interacting dark energy cosmology*, *Sci. China Phys. Mech. Astron.* **63** (2020) 290404, [[1910.03872](#)].
- [584] H.-L. Li, L. Feng, J.-F. Zhang and X. Zhang, *Models of vacuum energy interacting with cold dark matter: Constraints and comparison*, *Sci. China Phys. Mech. Astron.* **62** (2019) 120411, [[1812.00319](#)].
- [585] R.-Y. Guo, L. Zhang, J.-F. Zhang and X. Zhang, *Constraints on brane inflation after Planck 2015: Impacts of the latest local measurement of the Hubble constant*, *Sci. China Phys. Mech. Astron.* **62** (2019) 30411, [[1801.02187](#)].
- [586] R.-Y. Guo, J.-F. Zhang and X. Zhang, *Inflation model selection revisited after a 1.91% measurement of the Hubble constant*, *Sci. China Phys. Mech. Astron.* **63** (2020) 290406, [[1910.13944](#)].
- [587] M. Zhang, J.-F. Zhang and X. Zhang, *Impacts of dark energy on constraining neutrino mass after Planck 2018*, *Commun. Theor. Phys.* **72** (2020) 125402, [[2005.04647](#)].
- [588] H.-L. Li, J.-F. Zhang and X. Zhang, *Constraints on neutrino mass in the scenario of vacuum energy interacting with cold dark matter after Planck 2018*, *Commun. Theor. Phys.* **72** (2020) 125401, [[2005.12041](#)].
- [589] J.-F. Zhang, B. Wang and X. Zhang, *Forecast for weighing neutrinos in cosmology with SKA*, *Sci. China Phys. Mech. Astron.* **63** (2020) 280411, [[1907.00179](#)].
- [590] Y. Xu and X. Zhang, *Cosmological parameter measurement and neutral hydrogen 21 cm sky survey with the Square Kilometre Array*, *Sci. China Phys. Mech. Astron.* **63** (2020) 270431, [[2002.00572](#)].
- [591] M. Zhang, B. Wang, J.-Z. Qi, Y. Xu, J.-F. Zhang and X. Zhang, *Prospects for constraining interacting dark energy model with 21 cm intensity mapping experiments*, [2102.03979](#).
- [592] X. Zhang, *Gravitational wave standard sirens and cosmological parameter measurement*, *Sci. China Phys. Mech. Astron.* **62** (2019) 110431, [[1905.11122](#)].
- [593] X.-N. Zhang, L.-F. Wang, J.-F. Zhang and X. Zhang, *Improving cosmological parameter estimation with the future gravitational-wave standard siren observation from the Einstein Telescope*, *Phys. Rev. D* **99** (2019) 063510, [[1804.08379](#)].
- [594] L.-F. Wang, X.-N. Zhang, J.-F. Zhang and X. Zhang, *Impacts of gravitational-wave standard siren observation of the Einstein Telescope on weighing neutrinos in cosmology*, *Phys. Lett. B* **782** (2018) 87–93, [[1802.04720](#)].
- [595] M. Du, W. Yang, L. Xu, S. Pan and D. F. Mota, *Future constraints on dynamical dark-energy using gravitational-wave standard sirens*, *Phys. Rev. D* **100** (2019) 043535, [[1812.01440](#)].
- [596] E. Di Valentino, D. E. Holz, A. Melchiorri and F. Renzi, *The cosmological impact of future constraints on H_0 from gravitational-wave standard sirens*, *Phys. Rev. D* **98** (2018) 083523, [[1806.07463](#)].
- [597] J.-F. Zhang, H.-Y. Dong, J.-Z. Qi and X. Zhang, *Prospect for constraining holographic dark energy with gravitational wave standard sirens from the Einstein Telescope*, *Eur. Phys. J. C* **80** (2020) 217, [[1906.07504](#)].
- [598] J.-F. Zhang, M. Zhang, S.-J. Jin, J.-Z. Qi and X. Zhang, *Cosmological parameter estimation with future gravitational wave standard siren observation from the Einstein Telescope*, *JCAP* **09** (2019) 068, [[1907.03238](#)].
- [599] H.-L. Li, D.-Z. He, J.-F. Zhang and X. Zhang, *Quantifying the impacts of future gravitational-wave data on constraining interacting dark energy*, *JCAP* **06** (2020) 038, [[1908.03098](#)].

- [600] W. Yang, S. Vagnozzi, E. Di Valentino, R. C. Nunes, S. Pan and D. F. Mota, *Listening to the sound of dark sector interactions with gravitational wave standard sirens*, *JCAP* **07** (2019) 037, [[1905.08286](#)].
- [601] W. Yang, S. Pan, E. Di Valentino, B. Wang and A. Wang, *Forecasting interacting vacuum-energy models using gravitational waves*, *JCAP* **05** (2020) 050, [[1904.11980](#)].
- [602] S.-J. Jin, D.-Z. He, Y. Xu, J.-F. Zhang and X. Zhang, *Forecast for cosmological parameter estimation with gravitational-wave standard siren observation from the Cosmic Explorer*, *JCAP* **03** (2020) 051, [[2001.05393](#)].
- [603] Z.-W. Zhao, Z.-X. Li, J.-Z. Qi, H. Gao, J.-F. Zhang and X. Zhang, *Cosmological parameter estimation for dynamical dark energy models with future fast radio burst observations*, *Astrophys. J.* **903** (2020) 83, [[2006.01450](#)].
- [604] R. D. Blandford and R. L. Znajek, *Electromagnetic extractions of energy from Kerr black holes*, *Mon. Not. Roy. Astron. Soc.* **179** (1977) 433–456.
- [605] D. L. Meier, *The association of jet production with geometrically thick accretion flows and black hole rotation*, *Astrophys. J. Lett.* **548** (2001) L9–L12, [[astro-ph/0010231](#)].
- [606] LSST SCIENCE, LSST PROJECT collaboration, P. A. Abell et al., *LSST Science Book, Version 2.0*, [0912.0201](#).
- [607] J. Liske et al., *Cosmic dynamics in the era of Extremely Large Telescopes*, *Mon. Not. Roy. Astron. Soc.* **386** (2008) 1192–1218, [[0802.1532](#)].
- [608] SKA collaboration, D. J. Bacon et al., *Cosmology with Phase 1 of the Square Kilometre Array: Red Book 2018: Technical specifications and performance forecasts*, *Publ. Astron. Soc. Austral.* **37** (2020) e007, [[1811.02743](#)].
- [609] Z.-W. Zhao, L.-F. Wang, J.-F. Zhang and X. Zhang, *Prospects for improving cosmological parameter estimation with gravitational-wave standard sirens from Taiji*, *Sci. Bull.* **65** (2020) 1340–1348, [[1912.11629](#)].
- [610] L.-F. Wang, Z.-W. Zhao, J.-F. Zhang and X. Zhang, *A preliminary forecast for cosmological parameter estimation with gravitational-wave standard sirens from TianQin*, *JCAP* **11** (2020) 012, [[1907.01838](#)].
- [611] J.-Z. Qi, S.-J. Jin, X.-L. Fan, J.-F. Zhang and X. Zhang, *Using a multi-messenger and multi-wavelength observational strategy to probe the nature of dark energy through direct measurements of cosmic expansion history*, [2102.01292](#).
- [612] W. Del Pozzo, *Inference of the cosmological parameters from gravitational waves: application to second generation interferometers*, *Phys. Rev. D* **86** (2012) 043011, [[1108.1317](#)].
- [613] LIGO SCIENTIFIC, VIRGO collaboration, M. Fishbach et al., *A Standard Siren Measurement of the Hubble Constant from GW170817 without the Electromagnetic Counterpart*, *Astrophys. J. Lett.* **871** (2019) L13, [[1807.05667](#)].
- [614] R. Gray et al., *Cosmological inference using gravitational wave standard sirens: A mock data analysis*, *Phys. Rev. D* **101** (2020) 122001, [[1908.06050](#)].
- [615] DES, LIGO SCIENTIFIC, VIRGO collaboration, M. Soares-Santos et al., *First Measurement of the Hubble Constant from a Dark Standard Siren using the Dark Energy Survey Galaxies and the LIGO/Virgo Binary–Black-hole Merger GW170814*, *Astrophys. J. Lett.* **876** (2019) L7, [[1901.01540](#)].
- [616] LIGO SCIENTIFIC, VIRGO collaboration, B. P. Abbott et al., *A Gravitational-wave Measurement of the Hubble Constant Following the Second Observing Run of Advanced LIGO and Virgo*, *Astrophys. J.* **909** (2021) 218, [[1908.06060](#)].

- [617] D. F. Chernoff and L. S. Finn, *Gravitational radiation, inspiraling binaries, and cosmology*, *Astrophys. J. Lett.* **411** (1993) L5–L8, [[gr-qc/9304020](#)].
- [618] S. R. Taylor, J. R. Gair and I. Mandel, *Hubble without the Hubble: Cosmology using advanced gravitational-wave detectors alone*, *Phys. Rev. D* **85** (2012) 023535, [[1108.5161](#)].
- [619] W. M. Farr, M. Fishbach, J. Ye and D. Holz, *A Future Percent-Level Measurement of the Hubble Expansion at Redshift 0.8 With Advanced LIGO*, *Astrophys. J. Lett.* **883** (2019) L42, [[1908.09084](#)].
- [620] Z.-Q. You, X.-J. Zhu, G. Ashton, E. Thrane and Z.-H. Zhu, *Standard-siren cosmology using gravitational waves from binary black holes*, *Astrophys. J.* **908** (2021) 215, [[2004.00036](#)].
- [621] J. M. Ezquiaga and D. E. Holz, *Jumping the Gap: Searching for LIGO’s Biggest Black Holes*, *Astrophys. J. Lett.* **909** (2021) L23, [[2006.02211](#)].
- [622] C. Messenger and J. Read, *Measuring a cosmological distance-redshift relationship using only gravitational wave observations of binary neutron star coalescences*, *Phys. Rev. Lett.* **108** (2012) 091101, [[1107.5725](#)].
- [623] W. Del Pozzo, T. G. F. Li and C. Messenger, *Cosmological inference using only gravitational wave observations of binary neutron stars*, *Phys. Rev. D* **95** (2017) 043502, [[1506.06590](#)].
- [624] B. Wang, Z. Zhu, A. Li and W. Zhao, *Comprehensive analysis of the tidal effect in gravitational waves and implication for cosmology*, *Astrophys. J. Suppl.* **250** (2020) 6, [[2005.12875](#)].
- [625] S. Yu and Y. Lu, *The gravitational wave radiation from ultracompact X-ray binaries*, *Scientia Sinica Physica, Mechanica & Astronomica* **49** (Jan., 2019) 019501.
- [626] S. Yu, Y. Lu and C. S. Jeffery, *Orbital Evolution of Neutron-Star – White-Dwarf Binaries by Roche-Lobe Overflow and Gravitational Wave Radiation*, *Mon. Not. Roy. Astron. Soc.* **503** (2021) 2776–2790, [[2103.01884](#)].
- [627] H. Gao, Z. Cao, S. Ai and B. Zhang, *A more stringent constraint on the mass ratio of binary neutron star merger GW170817*, *Astrophys. J. Lett.* **851** (2017) L45, [[1711.08577](#)].
- [628] H. Gao, *GW170817: The key to the door of multi-messenger astronomy including gravitational waves*, *Sci. China Phys. Mech. Astron.* **61** (2018) 059531.
- [629] S.-B. Ma, W.-H. Lei, H. Gao, W. Xie, W. Chen, B. Zhang et al., *Bright Merger-nova Emission Powered by Magnetic Wind from a Newborn Black Hole*, *Astrophys. J. Lett.* **852** (2018) L5, [[1710.06318](#)].
- [630] S. Ai, H. Gao and B. Zhang, *What constraints on the neutron star maximum mass can one pose from GW170817 observations?*, [1912.06369](#).
- [631] H. Gao, S.-K. Ai, Z.-J. Cao, B. Zhang, Z.-Y. Zhu, A. Li et al., *Relation between gravitational mass and baryonic mass for non-rotating and rapidly rotating neutron stars*, *Front. Phys.(Beijing)* **15** (2020) 24603, [[1905.03784](#)].
- [632] L. Cao, Y. Lu and Y. Zhao, *Host galaxy properties of mergers of stellar binary black holes and their implications for advanced LIGO gravitational wave sources*, *Mon. Not. Roy. Astron. Soc.* **474** (2018) 4997–5007, [[1711.09190](#)].
- [633] Y. Zhao and Y. Lu, *Stochastic Gravitational Wave Background and Eccentric Stellar Compact Binaries*, *Mon. Not. Roy. Astron. Soc.* **500** (2020) 1421–1436, [[2009.01436](#)].
- [634] R. N. Caballero et al., *Studying the solar system with the International Pulsar Timing Array*, *Mon. Not. Roy. Astron. Soc.* **481** (2018) 5501–5516, [[1809.10744](#)].
- [635] Y. J. Guo, G. Y. Li, K. J. Lee and R. N. Caballero, *Studying the Solar system dynamics using pulsar timing arrays and the LINIMOSS dynamical model*, *Mon. Not. Roy. Astron. Soc.* **489** (2019) 5573–5581, [[1909.04507](#)].

- [636] Y. Feng, D. Li, Z. Zheng and C.-W. Tsai, *Supermassive Binary Black Hole Evolution can be traced by a small SKA Pulsar Timing Array*, *Phys. Rev.* **D102** (2020) 023014, [2005.11118].
- [637] Y. Feng, D. Li, Y.-R. Li and J.-M. Wang, *Constraints on individual supermassive binary black holes using observations of PSR J1909-3744*, [1907.03460](#).
- [638] C. Yan, W. Zhao and Y. Lu, *On using inspiralling supermassive binary black holes in the PTA frequency band as standard sirens to constrain dark energy*, *Astrophys. J.* **889** (2020) 79, [1912.04103].
- [639] Y.-R. Li et al., *Spectroscopic Indication of a Centi-parsec Supermassive Black Hole Binary in the Galactic Center of Ngc 5548*, *Astrophys. J.* **822** (2016) 4, [1602.05005].
- [640] Y.-R. Li et al., *A Possible 20 yr Periodicity in Long-term Optical Photometric and Spectral Variations of the Nearby Radio-quiet Active Galactic Nucleus Ark 120*, *Astrophys. J. Suppl.* **241** (2019) 33, [1705.07781].
- [641] Z. Song, J. Ge, Y. Lu and X. Ji, *Testing the relativistic Doppler boost hypothesis for supermassive binary black holes candidates via broad emission line profiles*, *Mon. Not. Roy. Astron. Soc.* **491** (Jan., 2020) 4023–4030, [1912.00560].
- [642] Z. Song, J. Ge, Y. Lu, C. Yan and X. Ji, *Broad-line region configuration of the supermassive binary black hole candidate PG1302-102 in the relativistic Doppler boosting scenario*, *Astron. Astrophys.* **645** (Jan., 2021) A15, [2010.07512].
- [643] Y.-Y. Songsheng, J.-M. Wang, Y.-R. Li and P. Du, *Differential Interferometric Signatures of Close Binaries of Supermassive Black Holes in Active Galactic Nuclei*, *Astrophys. J.* **881** (2019) 140, [1903.08067].
- [644] Y.-Y. Songsheng, M. Xiao, J.-M. Wang and L. C. Ho, *Kinematic Signatures of Reverberation Mapping of Close Binaries of Supermassive Black Holes in Active Galactic Nuclei. II. Atlas of Two-dimensional Transfer Functions*, *Astrophys.J.Suppl.* **247** (Mar., 2020) 3, [1912.12965].
- [645] J.-M. Wang and E. Bon, *Changing-look active galactic nuclei: close binaries of supermassive black holes in action*, *Astron. Astrophys.* **643** (Nov., 2020) L9, [2010.04417].
- [646] X. Ji, Y. Lu, J. Ge, C. Yan and Z. Song, *Variation of Broad Emission Lines from QSOs with Optical/UV Periodicity to Test the Interpretation of Supermassive Binary Black Holes*, *Astrophys. J.* **910** (Apr., 2021) 101, [2103.16448].
- [647] Y. Chen, Q. Yu and Y. Lu, *Dynamical evolution of cosmic supermassive binary black holes and their gravitational wave radiation*, *Astrophys. J.* **897** (2020) 86, [2005.10818].
- [648] G. Nelemans, *The Galactic Gravitational wave foreground*, *Class. Quant. Grav.* **26** (2009) 094030, [0901.1778].
- [649] G. Nelemans and P. G. Jonker, *Ultra-compact (X-ray) binaries*, *New Astron. Rev.* **54** (2010) 87–92, [astro-ph/0605722].
- [650] W.-H. Ruan, Z.-K. Guo, R.-G. Cai and Y.-Z. Zhang, *Taiji program: Gravitational-wave sources*, *Int. J. Mod. Phys. A* **35** (June, 2020) 2050075.
- [651] H.-T. Wang et al., *Science with the TianQin observatory: Preliminary results on massive black hole binaries*, *Phys. Rev.* **D100** (2019) 043003, [1902.04423].
- [652] B. Wang, W. Chen, D. Liu, H. Chen, C. Wu, W. Tang et al., *Ultra-compact X-ray binaries with He star companions*, *arXiv e-prints* (June, 2021) arXiv:2106.01369, [2106.01369].
- [653] T. M. Tauris, *Disentangling Coalescing Neutron-Star–White-Dwarf Binaries for LISA*, *Phys. Rev. Lett.* **121** (2018) 131105, [1809.03504].
- [654] A. G. Suvorov, *Ultra-compact X-ray binaries as dual-line gravitational-wave sources*, *mnras* **503** (June, 2021) 5495–5503, [2103.09858].

- [655] G. Ushomirsky, C. Cutler and L. Bildsten, *Deformations of accreting neutron star crusts and gravitational wave emission*, *Mon. Not. Roy. Astron. Soc.* **319** (2000) 902, [[astro-ph/0001136](#)].
- [656] B. Haskell, M. Priymak, A. Patruno, M. Oppenorth, A. Melatos and P. D. Lasky, *Detecting gravitational waves from mountains on neutron stars in the Advanced Detector Era*, *Mon. Not. Roy. Astron. Soc.* **450** (2015) 2393–2403, [[1501.06039](#)].
- [657] W.-C. Chen, D.-D. Liu and B. Wang, *Detectability of ultra-compact X-ray binaries as LISA sources*, *Astrophys. J. Lett.* **900** (2020) L8, [[2008.05143](#)].
- [658] L. Rezzolla, L. Baiotti, B. Giacomazzo, D. Link and J. A. Font, *Accurate evolutions of unequal-mass neutron-star binaries: properties of the torus and short GRB engines*, *Class. Quant. Grav.* **27** (2010) 114105, [[1001.3074](#)].
- [659] I. Bartos, P. Brady and S. Marka, *How Gravitational-wave Observations Can Shape the Gamma-ray Burst Paradigm*, *Class. Quant. Grav.* **30** (2013) 123001, [[1212.2289](#)].
- [660] P. D. Lasky, B. Haskell, V. Ravi, E. J. Howell and D. M. Coward, *Nuclear Equation of State from Observations of Short Gamma-Ray Burst Remnants*, *Phys. Rev.* **D89** (2014) 047302, [[1311.1352](#)].
- [661] V. Ravi and P. D. Lasky, *The birth of black holes: neutron star collapse times, gamma-ray bursts and fast radio bursts*, *Mon. Not. Roy. Astron. Soc.* **441** (Jul, 2014) 2433–2439, [[1403.6327](#)].
- [662] H. Gao, B. Zhang and H.-J. Lu, *Constraints on binary neutron star merger product from short GRB observations*, *Phys. Rev.* **D93** (2016) 044065, [[1511.00753](#)].
- [663] J. R. Oppenheimer and G. M. Volkoff, *On Massive neutron cores*, *Phys. Rev.* **55** (1939) 374–381.
- [664] F. Douchin and P. Haensel, *A unified equation of state of dense matter and neutron star structure*, *Astron. Astrophys.* **380** (2001) 151, [[astro-ph/0111092](#)].
- [665] R. B. Wiringa, V. Fiks and A. Fabrocini, *Equation of state for dense nucleon matter*, *Phys. Rev.* **C38** (1988) 1010–1037.
- [666] A. Akmal and V. R. Pandharipande, *Spin - isospin structure and pion condensation in nucleon matter*, *Phys. Rev.* **C56** (1997) 2261–2279, [[nucl-th/9705013](#)].
- [667] S. Goriely, N. Chamel and J. M. Pearson, *Further explorations of Skyrme-Hartree-Fock-Bogoliubov mass formulas. XII. Stiffness and stability of neutron-star matter*, *Phys. Rev. C* **82** (Sep, 2010) 035804, [[1009.3840](#)].
- [668] S. Typel, G. Ropke, T. Klahn, D. Blaschke and H. H. Wolter, *Composition and thermodynamics of nuclear matter with light clusters*, *Phys. Rev.* **C81** (2010) 015803, [[0908.2344](#)].
- [669] H. Mütter, M. Prakash and T. L. Ainsworth, *The nuclear symmetry energy in relativistic Brueckner-Hartree-Fock calculations*, *Phys. Lett.* **B199** (1987) 469–474.
- [670] H. Mueller and B. D. Serot, *Relativistic mean field theory and the high density nuclear equation of state*, *Nucl. Phys.* **A606** (1996) 508–537, [[nucl-th/9603037](#)].
- [671] M. J. Graham, S. G. Djorgovski, D. Stern, A. J. Drake, A. A. Mahabal, C. Donalek et al., *A systematic search for close supermassive black hole binaries in the Catalina Real-Time Transient Survey*, *Mon. Not. Roy. Astron. Soc.* **453** (2015) 1562–1576, [[1507.07603](#)].
- [672] M. Charisi, I. Bartos, Z. Haiman, A. M. Price-Whelan, M. J. Graham, E. C. Bellm et al., *A Population of Short-Period Variable Quasars from PTF as Supermassive Black Hole Binary Candidates*, *Mon. Not. Roy. Astron. Soc.* **463** (2016) 2145–2171, [[1604.01020](#)].

- [673] T. Liu et al., *A Systematic Search for Periodically Varying Quasars in Pan-STARRS1: An Extended Baseline Test in Medium Deep Survey Field MD09*, *Astrophys. J.* **833** (2016) 6, [1609.09503].
- [674] M. J. Valtonen et al., *A massive binary black-hole system in OJ 287 and a test of general relativity*, *Nature* **452** (2008) 851–853, [0809.1280].
- [675] E. Bon et al., *Evidence for periodicity in 43 year-long monitoring of NGC 5548*, *Astrophys. J. Suppl.* **225** (2016) 29, [1606.04606].
- [676] F. K. Liu, S. Li and S. Komossa, *A milliparsec supermassive black hole binary candidate in the galaxy SDSS J120136.02+300305.5*, *Astrophys. J.* **786** (2014) 103, [1404.4933].
- [677] C.-S. Yan, Y. Lu, X. Dai and Q. Yu, *A Probable Milli-parsec Supermassive Binary Black Hole in the Nearest Quasar mrk 231*, *Astrophys. J.* **809** (2015) 117, [1508.06292].
- [678] J.-M. Wang and Y.-R. Li, *Observational signatures of close binaries of supermassive black holes in active galactic nuclei*, *Res. Astron. Astrophys.* **20** (Oct., 2020) 160.
- [679] J.-M. Wang, Y.-Y. Songsheng, Y.-R. Li, P. Du and Z. Yu, *Dynamical evidence from the sub-parsec counter-rotating disc for a close binary of supermassive black holes in NGC 1068*, *Mon. Not. Roy. Astron. Soc.* **497** (Sept., 2020) 1020–1028, [2005.01220].
- [680] L. Barack et al., *Black holes, gravitational waves and fundamental physics: a roadmap*, *Class. Quant. Grav.* **36** (2019) 143001, [1806.05195].
- [681] K. Belczynski, V. Kalogera and T. Bulik, *A Comprehensive study of binary compact objects as gravitational wave sources: Evolutionary channels, rates, and physical properties*, *Astrophys. J.* **572** (2001) 407–431, [astro-ph/0111452].
- [682] K. Belczynski, V. Kalogera, F. A. Rasio, R. E. Taam, A. Zezas, T. Bulik et al., *Compact object modeling with the startrack population synthesis code*, *Astrophys. J. Suppl.* **174** (2008) 223, [astro-ph/0511811].
- [683] C. L. Rodriguez, S. Chatterjee and F. A. Rasio, *Binary Black Hole Mergers from Globular Clusters: Masses, Merger Rates, and the Impact of Stellar Evolution*, *Phys. Rev.* **D93** (2016) 084029, [1602.02444].
- [684] I. M. Romero-Shaw, P. D. Lasky, E. Thrane and J. C. Bustillo, *GW190521: orbital eccentricity and signatures of dynamical formation in a binary black hole merger signal*, *Astrophys. J. Lett.* **903** (2020) L5, [2009.04771].
- [685] G. Fragione, A. Loeb and F. A. Rasio, *On the Origin of GW190521-like events from repeated black hole mergers in star clusters*, *Astrophys. J. Lett.* **902** (2020) L26, [2009.05065].
- [686] LIGO SCIENTIFIC, VIRGO collaboration, B. P. Abbott et al., *GW150914: Implications for the stochastic gravitational wave background from binary black holes*, *Phys. Rev. Lett.* **116** (2016) 131102, [1602.03847].
- [687] LIGO SCIENTIFIC, VIRGO collaboration, B. P. Abbott et al., *GW170817: Implications for the Stochastic Gravitational-Wave Background from Compact Binary Coalescences*, *Phys. Rev. Lett.* **120** (2018) 091101, [1710.05837].
- [688] R. W. Hellings and G. S. Downs, *Upper limits on the isotropic gravitational radiation background from pulsar timing analysis*, *Astrophys. J. Lett.* **265** (Feb., 1983) L39–L42.
- [689] G. Hobbs et al., *A pulsar-based time-scale from the International Pulsar Timing Array*, *Mon. Not. Roy. Astron. Soc.* **491** (2020) 5951–5965, [1910.13628].
- [690] D. J. Champion et al., *Measuring the mass of solar system planets using pulsar timing*, *Astrophys. J. Lett.* **720** (2010) L201, [1008.3607].
- [691] R. S. Foster and D. C. Backer, *Constructing a pulsar timing array*, *Astrophys. J.* **361** (Sept., 1990) 300–308.

- [692] Y. J. Guo, K. J. Lee and R. N. Caballero, *A dynamical approach in exploring the unknown mass in the Solar system using pulsar timing arrays*, *Mon. Not. Roy. Astron. Soc.* **475** (2018) 3644–3653, [1802.05452].
- [693] NANOGrav collaboration, M. F. Alam et al., *The NANOGrav 12.5-year Data Set: Wideband Timing of 47 Millisecond Pulsars*, *Astrophys. J. Suppl.* **252** (2021) 5, [2005.06495].
- [694] G. Desvignes et al., *High-precision timing of 42 millisecond pulsars with the European Pulsar Timing Array*, *Mon. Not. Roy. Astron. Soc.* **458** (2016) 3341–3380, [1602.08511].
- [695] M. Kerr et al., *The Parkes Pulsar Timing Array project: second data release*, *Publ. Astron. Soc. Austral.* **37** (2020) e020, [2003.09780].
- [696] B. B. P. Perera et al., *The International Pulsar Timing Array: Second data release*, *Mon. Not. Roy. Astron. Soc.* **490** (2019) 4666–4687, [1909.04534].
- [697] K. J. Lee, *Prospects of Gravitational Wave Detection Using Pulsar Timing Array for Chinese Future Telescopes*, in *Frontiers in Radio Astronomy and FAST Early Sciences Symposium 2015* (L. Qain and D. Li, eds.), vol. 502 of *Astronomical Society of the Pacific Conference Series*, p. 19, Feb., 2016.
- [698] B. C. Joshi et al., *Precision pulsar timing with the ORT and the GMRT and its applications in pulsar astrophysics*, *J. Astrophys. Astron.* **39** (2018) .
- [699] X. J. Zhu et al., *An all-sky search for continuous gravitational waves in the Parkes Pulsar Timing Array data set*, *Mon. Not. Roy. Astron. Soc.* **444** (2014) 3709–3720, [1408.5129].
- [700] S. Babak et al., *European Pulsar Timing Array Limits on Continuous Gravitational Waves from Individual Supermassive Black Hole Binaries*, *Mon. Not. Roy. Astron. Soc.* **455** (2016) 1665–1679, [1509.02165].
- [701] K. Aggarwal et al., *The NANOGrav 11-Year Data Set: Limits on Gravitational Waves from Individual Supermassive Black Hole Binaries*, *Astrophys. J.* **880** (2019) 2, [1812.11585].
- [702] J. B. Wang et al., *Searching for gravitational wave memory bursts with the Parkes Pulsar Timing Array*, *Mon. Not. Roy. Astron. Soc.* **446** (2015) 1657–1671, [1410.3323].
- [703] NANOGrav collaboration, K. Aggarwal et al., *The NANOGrav 11 yr Data Set: Limits on Gravitational Wave Memory*, *Astrophys. J.* **889** (2020) 38, [1911.08488].
- [704] R. Hellings and G. Downs, *UPPER LIMITS ON THE ISOTROPIC GRAVITATIONAL RADIATION BACKGROUND FROM PULSAR TIMING ANALYSIS*, *Astrophys. J. Lett.* **265** (1983) L39–L42.
- [705] G. Hobbs, S. Dai, R. N. Manchester, R. M. Shannon, M. Kerr, K. J. Lee et al., *The Role of FAST in Pulsar Timing Arrays*, *Res. Astron. Astrophys.* **19** (2019) 020, [1407.0435].
- [706] G. Janssen et al., *Gravitational wave astronomy with the SKA*, *PoS AASKA14* (2015) 037, [1501.00127].
- [707] R. Smits, M. Kramer, B. Stappers, D. R. Lorimer, J. Cordes and A. Faulkner, *Pulsar searches and timing with the square kilometre array*, *Astron. Astrophys.* **493** (2009) 1161–1170, [0811.0211].
- [708] S. Burke-Spolaor et al., *The Astrophysics of Nanohertz Gravitational Waves*, *Astron. Astrophys. Rev.* **27** (2019) 5, [1811.08826].
- [709] Y. Wang, S. D. Mohanty and F. A. Jenet, *Coherent network analysis for continuous gravitational wave signals in a pulsar timing array: Pulsar phases as extrinsic parameters*, *Astrophys. J.* **815** (2015) 125, [1506.01526].
- [710] Y. Wang, S. D. Mohanty and Y.-Q. Qian, *Continuous gravitational wave searches with pulsar timing arrays: Maximization versus marginalization over pulsar phase parameters*, *J. Phys. Conf. Ser.* **840** (2017) 012058, [1704.05784].

- [711] Y. Wang and S. D. Mohanty, *Pulsar Timing Array Based Search for Supermassive Black Hole Binaries in the Square Kilometer Array Era*, *Phys. Rev. Lett.* **118** (2017) 151104, [[1611.09440](#)].
- [712] S. Klimenko, S. Mohanty, M. Rakhmanov and G. Mitselmakher, *Constraint likelihood analysis for a network of gravitational wave detectors*, *Phys. Rev. D* **72** (2005) 122002, [[gr-qc/0508068](#)].
- [713] S. D. Mohanty, M. Rakhmanov, S. Klimenko and G. Mitselmakher, *Variability of signal to noise ratio and the network analysis of gravitational wave burst signals*, *Class. Quant. Grav.* **23** (2006) 4799–4810, [[gr-qc/0601076](#)].
- [714] M. Rakhmanov, *Rank deficiency and Tikhonov regularization in the inverse problem for gravitational-wave bursts*, *Class. Quant. Grav.* **23** (2006) S673–S686, [[gr-qc/0604005](#)].
- [715] Y. Wang, S. D. Mohanty and Z. Cao, *Extending the frequency reach of pulsar timing array based gravitational wave search without high cadence observations*, *Astrophys. J. Lett.* **907** (2021) L43, [[2012.04261](#)].
- [716] NANOGrav collaboration, T. Dolch et al., *Single-Source Gravitational Wave Limits from the J1713+0747 24-hr Global Campaign*, *J. Phys. Conf. Ser.* **716** (2016) 012014, [[1509.05446](#)].
- [717] M. Isi, M. Giesler, W. M. Farr, M. A. Scheel and S. A. Teukolsky, *Testing the no-hair theorem with GW150914*, *Phys. Rev. Lett.* **123** (2019) 111102, [[1905.00869](#)].
- [718] D. J. D’Orazio and A. Loeb, *Using Gravitational Wave Parallax to Measure the Hubble Parameter with Pulsar Timing Arrays*, [2009.06084](#).
- [719] Y. Feng, G. Hobbs, D. Li, S. Dai, W. W. Zhu, Y. L. Yue et al., *A Single-pulse Study of PSR J1022+1001 Using the FAST Radio Telescope*, *Astrophys. J.* **908** (Feb., 2021) 105.
- [720] D. Li, J. M. Dickey and S. Liu, *Preface: Planning the scientific applications of the Five-hundred-meter Aperture Spherical radio Telescope*, *Res. Astron. Astrophys.* **19** (Feb., 2019) 016, [[1904.05882](#)].
- [721] M. Chen, Y. Zhong, Y. Feng, D. Li and J. Li, *Machine Learning for Nanohertz Gravitational Wave Detection and Parameter Estimation with Pulsar Timing Array*, *Sci. China Phys. Mech. Astron.* **63** (2020) 129511, [[2003.13928](#)].
- [722] Z. Cao, *Numerical study of binary black hole systems (in chinese)*, in *10000 Science Challenges in Mathematics*, ch. Numerical study of binary black hole systems (in Chinese), pp. 390–392. Science Press, Beijing, 2009.
- [723] F. Pretorius, *Evolution of binary black hole spacetimes*, *Phys. Rev. Lett.* **95** (2005) 121101, [[gr-qc/0507014](#)].
- [724] M. Campanelli, C. O. Lousto, P. Marronetti and Y. Zlochower, *Accurate evolutions of orbiting black-hole binaries without excision*, *Phys. Rev. Lett.* **96** (2006) 111101, [[gr-qc/0511048](#)].
- [725] J. G. Baker, J. Centrella, D.-I. Choi, M. Koppitz and J. van Meter, *Gravitational wave extraction from an inspiraling configuration of merging black holes*, *Phys. Rev. Lett.* **96** (2006) 111102, [[gr-qc/0511103](#)].
- [726] Z.-j. Cao, H.-J. Yo and J.-P. Yu, *A Reinvestigation of Moving Punctured Black Holes with a New Code*, *Phys. Rev.* **D78** (2008) 124011, [[0812.0641](#)].
- [727] Z. Cao and Z. Du, *Numerical relativity and gravitational wave astronomy*, *SCIENTIA SINICA Physica, Mechanica & Astronomica* **47** (dec, 2016) 010405.
- [728] T. W. Baumgarte and S. L. Shapiro, *Numerical Relativity: Solving Einstein’s Equations on the Computer*. Cambridge University Press, 2010, [10.1017/CBO9781139193344](#).
- [729] R.-G. Cai, Z. Cao and W.-B. Han, *The gravitational wave models for binary compact objects*, *Chinese Science Bulletin* **61** (2016) 1525–1535.

- [730] C. O. Lousto and Y. Zlochower, *Orbital Evolution of Extreme-Mass-Ratio Black-Hole Binaries with Numerical Relativity*, *Phys. Rev. Lett.* **106** (2011) 041101, [[1009.0292](#)].
- [731] C. O. Lousto and J. Healy, *Exploring the Small Mass Ratio Binary Black Hole Merger via Zeno's Dichotomy Approach*, *Phys. Rev. Lett.* **125** (2020) 191102, [[2006.04818](#)].
- [732] M. Fernando, D. Neilsen, H. Lim, E. Hirschmann and H. Sundar, *Massively Parallel Simulations of Binary Black Hole Intermediate-Mass-Ratio Inspirals*, *SIAM Journal on Scientific Computing* (7, 2018) , [[1807.06128](#)].
- [733] F. Loffler, Z. Cao, S. R. Brandt and Z. Du, *A new parallelization scheme for adaptive mesh refinement*, *Journal of Computational Science* **16** (2016) 79 – 88.
- [734] M. A. Scheel, M. Boyle, T. Chu, L. E. Kidder, K. D. Matthews and H. P. Pfeiffer, *High-accuracy waveforms for binary black hole inspiral, merger, and ringdown*, *Phys. Rev. D* **79** (2009) 024003, [[0810.1767](#)].
- [735] Z. Cao, *Binary black hole simulation with an adaptive finite element method: Solving the Einstein constraint equations*, *Phys. Rev. D* **91** (2015) 044033.
- [736] S. Brandt and B. Bruegmann, *A Simple construction of initial data for multiple black holes*, *Phys. Rev. Lett.* **78** (1997) 3606–3609, [[gr-qc/9703066](#)].
- [737] Z. Cao, P. Fu, L.-W. Ji and Y. Xia, *Application of local discontinuous Galerkin method to Einstein equations*, *Int. J. Mod. Phys. D* **28** (2018) 1950014.
- [738] J. Yan and S. Osher, *A local discontinuous galerkin method for directly solving hamilton-jacobi equations*, *Journal of Computational Physics* **230** (2011) 232–244.
- [739] D. Hilditch, S. Bernuzzi, M. Thierfelder, Z. Cao, W. Tichy and B. Bruegmann, *Compact binary evolutions with the Z4c formulation*, *Phys. Rev. D* **88** (2013) 084057, [[1212.2901](#)].
- [740] D. Hilditch, A. Weyhausen and B. Brüggmann, *Pseudospectral method for gravitational wave collapse*, *Phys. Rev. D* **93** (2016) 063006, [[1504.04732](#)].
- [741] L.-W. Ji, L. Lindblom and Z. Cao, *Linear Degeneracy of the First-Order Generalized-Harmonic Einstein System*, *Class. Quant. Grav.* **36** (2019) 087001, [[1903.00140](#)].
- [742] L.-B. Zhang, *A parallel algorithm for adaptive local refinement of tetrahedral meshes using bisection*, *Numer. Math.: Theory, Methods and Applications* **2** (2009) 65–89.
- [743] L. Zhang, T. Cui and H. Liu, *A set of symmetric quadrature rules on triangles and tetrahedra*, *Journal of Computational Mathematics* **27** (2009) 89–96.
- [744] L.-W. Ji, R.-G. Cai and Z. Cao, *Binary black hole simulation with an adaptive finite element method III: Evolving a single black hole*, [1805.10642](#).
- [745] P. Fischer and J. Mullen, *Filter-based stabilization of spectral element methods*, *Comptes Rendus de l'Academie des Sciences - Series I - Mathematics* **332** (2001) 265 – 270.
- [746] R. Pasquetti and C. Xu, *Comments on filter-based stabilization of spectral element methods*, *Journal of Computational Physics* **182** (2002) 646 – 650.
- [747] D. Hils and P. L. Bender, *Gradual approach to coalescence for compact stars orbiting massive black holes*, *Astrophys. J. Lett.* **445** (1995) L7–L10.
- [748] M. Shibata, *Gravitational waves by compact stars orbiting around rotating supermassive black holes*, *Phys. Rev. D* **50** (1994) 6297–6311.
- [749] B. Mikoczi, B. Kocsis, P. Forgacs and M. Vasuth, *Parameter estimation for inspiraling eccentric compact binaries including pericenter precession*, *Phys. Rev. D* **86** (2012) 104027, [[1206.5786](#)].
- [750] E. A. Huerta and D. A. Brown, *Effect of eccentricity on binary neutron star searches in Advanced LIGO*, *Phys. Rev. D* **87** (2013) 127501, [[1301.1895](#)].

- [751] N. Loutrel, N. Yunes and F. Pretorius, *Parametrized post-Einsteinian framework for gravitational wave bursts*, *Phys. Rev.* **D90** (2014) 104010, [[1404.0092](#)].
- [752] M. Coughlin, P. Meyers, E. Thrane, J. Luo and N. Christensen, *Detectability of eccentric compact binary coalescences with advanced gravitational-wave detectors*, *Phys. Rev.* **D91** (2015) 063004, [[1412.4665](#)].
- [753] B. Sun, Z. Cao, Y. Wang and H.-C. Yeh, *Parameter estimation of eccentric inspiraling compact binaries using an enhanced post circular model for ground-based detectors*, *Phys. Rev.* **D92** (2015) 044034.
- [754] S. Ma, Z. Cao, C.-Y. Lin, H.-P. Pan and H.-J. Yo, *Gravitational wave source localization for eccentric binary coalesce with a ground-based detector network*, *Phys. Rev.* **D96** (2017) 084046, [[1710.02965](#)].
- [755] S. Tanay, A. Klein, E. Berti and A. Nishizawa, *Convergence of Fourier-domain templates for inspiraling eccentric compact binaries*, *Phys. Rev.* **D100** (2019) 064006, [[1905.08811](#)].
- [756] N. Loutrel, *Analytic Waveforms for Eccentric Gravitational Wave Bursts*, *Class. Quant. Grav.* **37** (2020) 075008, [[1909.02143](#)].
- [757] N. Loutrel and N. Yunes, *Hereditary Effects in Eccentric Compact Binary Inspirals to Third Post-Newtonian Order*, *Class. Quant. Grav.* **34** (2017) 044003, [[1607.05409](#)].
- [758] N. Loutrel and N. Yunes, *Eccentric Gravitational Wave Bursts in the Post-Newtonian Formalism*, *Class. Quant. Grav.* **34** (2017) 135011, [[1702.01818](#)].
- [759] N. Loutrel, S. Liebersbach, N. Yunes and N. Cornish, *Nature Abhors a Circle*, *Class. Quant. Grav.* **36** (2019) 01, [[1801.09009](#)].
- [760] B. Moore, T. Robson, N. Loutrel and N. Yunes, *Towards a Fourier domain waveform for non-spinning binaries with arbitrary eccentricity*, *Class. Quant. Grav.* **35** (2018) 235006, [[1807.07163](#)].
- [761] N. Loutrel, S. Liebersbach, N. Yunes and N. Cornish, *The eccentric behavior of inspiralling compact binaries*, *Class. Quant. Grav.* **36** (2019) 025004, [[1810.03521](#)].
- [762] L. Gondan and B. Kocsis, *Measurement Accuracy of Inspiralng Eccentric Neutron Star and Black Hole Binaries Using Gravitational Waves*, *Astrophys. J.* **871** (2019) 178, [[1809.00672](#)].
- [763] L. Gondan, B. Kocsis, P. Raffai and Z. Frei, *Eccentric Black Hole Gravitational-Wave Capture Sources in Galactic Nuclei: Distribution of Binary Parameters*, *Astrophys. J.* **860** (2018) 5, [[1711.09989](#)].
- [764] B.-M. Hoang, S. Naoz, B. Kocsis, F. A. Rasio and F. Dosopoulou, *Black Hole Mergers in Galactic Nuclei Induced by the Eccentric Kozai-Lidov Effect*, *Astrophys. J.* **856** (2018) 140, [[1706.09896](#)].
- [765] L. Gondan, B. Kocsis, P. Raffai and Z. Frei, *Accuracy of Estimating Highly Eccentric Binary Black Hole Parameters with Gravitational-Wave Detections*, *Astrophys. J.* **855** (2018) 34, [[1705.10781](#)].
- [766] B. Moore and N. Yunes, *A 3PN Fourier Domain Waveform for Non-Spinning Binaries with Moderate Eccentricity*, *Class. Quant. Grav.* **36** (2019) 185003, [[1903.05203](#)].
- [767] B. Moore and N. Yunes, *Data Analysis Implications of Moderately Eccentric Gravitational Waves*, *Class. Quant. Grav.* **37** (2020) 225015, [[1910.01680](#)].
- [768] D. Chiaramello and A. Nagar, *Faithful analytical effective-one-body waveform model for spin-aligned, moderately eccentric, coalescing black hole binaries*, *Phys. Rev.* **D101** (2020) 101501, [[2001.11736](#)].

- [769] A. H. Nitz, A. Lenon and D. A. Brown, *Search for Eccentric Binary Neutron Star Mergers in the first and second observing runs of Advanced LIGO*, *Astrophys. J.* **890** (2019) 1, [[1912.05464](#)].
- [770] A. K. Lenon, A. H. Nitz and D. A. Brown, *Measuring the eccentricity of GW170817 and GW190425*, *Mon. Not. Roy. Astron. Soc.* **497** (2020) 1966–1971, [[2005.14146](#)].
- [771] A. Ramos-Buades, S. Husa, G. Pratten, H. Estellés, C. García-Quirós, M. Mateu-Lucena et al., *First survey of spinning eccentric black hole mergers: Numerical relativity simulations, hybrid waveforms, and parameter estimation*, *Phys. Rev.* **D101** (2020) 083015, [[1909.11011](#)].
- [772] A. Ramos-Buades, S. Tiwari, M. Haney and S. Husa, *Impact of eccentricity on the gravitational wave searches for binary black holes: High mass case*, *Phys. Rev.* **D102** (2020) 043005, [[2005.14016](#)].
- [773] P. C. Peters, *Gravitational Radiation and the Motion of Two Point Masses*, *Phys. Rev.* **136** (1964) B1224–B1232.
- [774] W.-B. Han, *Gravitational waves from extreme-mass-ratio inspirals in equatorially eccentric orbits*, *Int. J. Mod. Phys.* **D23** (2014) 1450064.
- [775] W.-B. Han and Z. Cao, *Constructing EOB dynamics with numerical energy flux for intermediate-mass-ratio inspirals*, *Phys. Rev.* **D84** (2011) 044014, [[1108.0995](#)].
- [776] M. Sasaki and H. Tagoshi, *Analytic black hole perturbation approach to gravitational radiation*, *Living Rev. Rel.* **6** (2003) 6, [[gr-qc/0306120](#)].
- [777] E. Forseth, C. R. Evans and S. Hopper, *Eccentric-orbit extreme-mass-ratio inspiral gravitational wave energy fluxes to 7PN order*, *Phys. Rev.* **D93** (2016) 064058, [[1512.03051](#)].
- [778] S. Drasco and S. A. Hughes, *Gravitational wave snapshots of generic extreme mass ratio inspirals*, *Phys. Rev.* **D73** (2006) 024027, [[gr-qc/0509101](#)].
- [779] T. Apostolatos, D. Kennefick, E. Poisson and A. Ori, *Gravitational radiation from a particle in circular orbit around a black hole. 3: Stability of circular orbits under radiation reaction*, *Phys. Rev.* **D47** (1993) 5376–5388.
- [780] D. Kennefick, *Stability under radiation reaction of circular equatorial orbits around Kerr black holes*, *Phys. Rev.* **D58** (1998) 064012, [[gr-qc/9805102](#)].
- [781] E. E. Flanagan and T. Hinderer, *Transient resonances in the inspirals of point particles into black holes*, *Phys. Rev. Lett.* **109** (2012) 071102, [[1009.4923](#)].
- [782] C. P. L. Berry, R. H. Cole, P. Canizares and J. R. Gair, *Importance of transient resonances in extreme-mass-ratio inspirals*, *Phys. Rev.* **D94** (2016) 124042, [[1608.08951](#)].
- [783] A. G. M. Lewis, A. Zimmerman and H. P. Pfeiffer, *Fundamental frequencies and resonances from eccentric and precessing binary black hole inspirals*, *Class. Quant. Grav.* **34** (2017) 124001, [[1611.03418](#)].
- [784] N. Yunes, A. Buonanno, S. A. Hughes, M. Coleman Miller and Y. Pan, *Modeling Extreme Mass Ratio Inspirals within the Effective-One-Body Approach*, *Phys. Rev. Lett.* **104** (2010) 091102, [[0909.4263](#)].
- [785] Z. Cao and W.-B. Han, *Waveform model for an eccentric binary black hole based on the effective-one-body-numerical-relativity formalism*, *Phys. Rev.* **D96** (2017) 044028, [[1708.00166](#)].
- [786] X. Liu, Z. Cao and L. Shao, *Validating the Effective-One-Body Numerical-Relativity Waveform Models for Spin-aligned Binary Black Holes along Eccentric Orbits*, *Phys. Rev.* **D101** (2020) 044049, [[1910.00784](#)].
- [787] H. Goldstein, C. Poole and J. Safko, *Classical Mechanics*. Addison Wesley, Reading, Massachusetts, 2001.

- [788] A. Buonanno and T. Damour, *Effective one-body approach to general relativistic two-body dynamics*, *Phys. Rev.* **D59** (1999) 084006, [[gr-qc/9811091](#)].
- [789] A. Buonanno, Y. Pan, J. G. Baker, J. Centrella, B. J. Kelly, S. T. McWilliams et al., *Toward faithful templates for non-spinning binary black holes using the effective-one-body approach*, *Phys. Rev.* **D76** (2007) 104049, [[0706.3732](#)].
- [790] A. Taracchini, Y. Pan, A. Buonanno, E. Barausse, M. Boyle, T. Chu et al., *Prototype effective-one-body model for nonprecessing spinning inspiral-merger-ringdown waveforms*, *Phys. Rev.* **D86** (2012) 024011, [[1202.0790](#)].
- [791] A. Taracchini et al., *Effective-one-body model for black-hole binaries with generic mass ratios and spins*, *Phys. Rev.* **D89** (2014) 061502, [[1311.2544](#)].
- [792] LIGO SCIENTIFIC, VIRGO collaboration, T. D. Abbott et al., *Improved analysis of GW150914 using a fully spin-precessing waveform Model*, *Phys. Rev.* **X6** (2016) 041014, [[1606.01210](#)].
- [793] S. Babak, A. Taracchini and A. Buonanno, *Validating the effective-one-body model of spinning, precessing binary black holes against numerical relativity*, *Phys. Rev.* **D95** (2017) 024010, [[1607.05661](#)].
- [794] LIGO SCIENTIFIC, VIRGO collaboration, B. P. Abbott et al., *GW170104: Observation of a 50-Solar-Mass Binary Black Hole Coalescence at Redshift 0.2*, *Phys. Rev. Lett.* **118** (2017) 221101, [[1706.01812](#)].
- [795] A. Bohe et al., *Improved effective-one-body model of spinning, nonprecessing binary black holes for the era of gravitational-wave astrophysics with advanced detectors*, *Phys. Rev.* **D95** (2017) 044028, [[1611.03703](#)].
- [796] E. Barausse, E. Racine and A. Buonanno, *Hamiltonian of a spinning test-particle in curved spacetime*, *Phys. Rev.* **D80** (2009) 104025, [[0907.4745](#)].
- [797] T. Damour, *High-energy gravitational scattering and the general relativistic two-body problem*, *Phys. Rev.* **D97** (2018) 044038, [[1710.10599](#)].
- [798] X. He, M. Sun, J. Jing and Z. Cao, *Energy map and effective metric in an effective-one-body theory based on the second-post-Minkowskian approximation*, *Eur. Phys. J.* **C81** (2021) 97.
- [799] E. Barausse and A. Buonanno, *An Improved effective-one-body Hamiltonian for spinning black-hole binaries*, *Phys. Rev.* **D81** (2010) 084024, [[0912.3517](#)].
- [800] E. Barausse and A. Buonanno, *Extending the effective-one-body Hamiltonian of black-hole binaries to include next-to-next-to-leading spin-orbit couplings*, *Phys. Rev.* **D84** (2011) 104027, [[1107.2904](#)].
- [801] S. Bai, Z.-J. Cao, W.-B. Han, C.-Y. Lin, H.-J. Yo and J.-P. Yu, *From binary black hole simulation to triple black hole simulation*, *J. Phys. Conf. Ser.* **330** (2011) 012016, [[1203.6185](#)].
- [802] X. Liu, Z. Cao and Z.-H. Zhu, *A higher-multipole gravitational waveform model for an eccentric binary black holes based on the effective-one-body-numerical-relativity formalism*, [2102.08614](#).
- [803] Y. Pan, A. Buonanno, M. Boyle, L. T. Buchman, L. E. Kidder, H. P. Pfeiffer et al., *Inspiral-merger-ringdown multipolar waveforms of nonspinning black-hole binaries using the effective-one-body formalism*, *Phys. Rev.* **D84** (2011) 124052, [[1106.1021](#)].
- [804] E. A. Huerta et al., *Complete waveform model for compact binaries on eccentric orbits*, *Phys. Rev.* **D95** (2017) 024038, [[1609.05933](#)].
- [805] C. M. Will and A. G. Wiseman, *Gravitational radiation from compact binary systems: Gravitational wave forms and energy loss to second postNewtonian order*, *Phys. Rev.* **D54** (1996) 4813–4848, [[gr-qc/9608012](#)].

- [806] Y. Pan, A. Buonanno, R. Fujita, E. Racine and H. Tagoshi, *Post-Newtonian factorized multipolar waveforms for spinning, non-precessing black-hole binaries*, *Phys. Rev.* **D83** (2011) 064003, [[1006.0431](#)].
- [807] Z. Cao and W.-B. Han, *Inspiral-merger-ringdown ($2, 0$) mode waveforms for aligned-spin black-hole binaries*, *Class. Quant. Grav.* **33** (2016) 155011.
- [808] M. Favata, *Post-Newtonian corrections to the gravitational-wave memory for quasi-circular, inspiralling compact binaries*, *Phys. Rev.* **D80** (2009) 024002, [[0812.0069](#)].
- [809] L. Blanchet and T. Damour, *Hereditary effects in gravitational radiation*, *Phys. Rev.* **D46** (1992) 4304–4319.
- [810] D. Pollney and C. Reisswig, *Gravitational memory in binary black hole mergers*, *Astrophys. J. Lett.* **732** (2011) L13, [[1004.4209](#)].
- [811] X. Liu, X. He and Z. Cao, *Accurate calculation of gravitational wave memory*, *Phys. Rev.* **D103** (2021) 043005.
- [812] K. Mitman, J. Moxon, M. A. Scheel, S. A. Teukolsky, M. Boyle, N. Deppe et al., *Computation of displacement and spin gravitational memory in numerical relativity*, *Phys. Rev.* **D102** (2020) 104007, [[2007.11562](#)].
- [813] K. Mitman et al., *Adding gravitational memory to waveform catalogs using BMS balance laws*, *Phys. Rev.* **D103** (2021) 024031, [[2011.01309](#)].
- [814] M. Favata, *Nonlinear gravitational-wave memory from binary black hole mergers*, *Astrophys. J. Lett.* **696** (2009) L159–L162, [[0902.3660](#)].
- [815] M. Favata, *Gravitational-wave memory revisited: memory from the merger and recoil of binary black holes*, *J. Phys. Conf. Ser.* **154** (2009) 012043, [[0811.3451](#)].
- [816] M. Favata, *The gravitational-wave memory effect*, *Class. Quant. Grav.* **27** (2010) 084036, [[1003.3486](#)].
- [817] M. Favata, *The Gravitational-wave memory from eccentric binaries*, *Phys. Rev.* **D84** (2011) 124013, [[1108.3121](#)].
- [818] C. Talbot, E. Thrane, P. D. Lasky and F. Lin, *Gravitational-wave memory: waveforms and phenomenology*, *Phys. Rev.* **D98** (2018) 064031, [[1807.00990](#)].
- [819] P. D. Lasky, E. Thrane, Y. Levin, J. Blackman and Y. Chen, *Detecting gravitational-wave memory with LIGO: implications of GW150914*, *Phys. Rev. Lett.* **117** (2016) 061102, [[1605.01415](#)].
- [820] O. M. Boersma, D. A. Nichols and P. Schmidt, *Forecasts for detecting the gravitational-wave memory effect with Advanced LIGO and Virgo*, *Phys. Rev.* **D101** (2020) 083026, [[2002.01821](#)].
- [821] M. Hubner, C. Talbot, P. D. Lasky and E. Thrane, *Measuring gravitational-wave memory in the first LIGO/Virgo gravitational-wave transient catalog*, *Phys. Rev.* **D101** (2020) 023011, [[1911.12496](#)].
- [822] M. Ebersold and S. Tiwari, *Search for nonlinear memory from subsolar mass compact binary mergers*, *Phys. Rev.* **D101** (2020) 104041, [[2005.03306](#)].
- [823] A. Ashtekar, T. De Lorenzo and N. Khera, *Compact binary coalescences: Constraints on waveforms*, *Gen. Rel. Grav.* **52** (2020) 107, [[1906.00913](#)].